University of Minho
School of Engineering

Bruna Filipa Ferreira Martins

Optical Calibration, Alignment and Inspection of OLED Displays

November 2021

Optical Calibration, Alignment and Inspection of OLED Displays

Bruna Filipa Ferreira Martins

Uminho|2021

University of Minho
School of Engineering

Bruna Filipa Ferreira Martins

Optical Calibration, Alignment and Inspection of OLED Displays

Masters dissertation
Integrated Masters in Physics Engineering
Devices, Microsystems and Nanotechnologies

Work carried out under the guidance of
Professor Doctor Eduardo Jorge Nunes Pereira

November 2021

Agradecimentos

Dedico as primeiras palavras aos meus pais, Filipe e Paula, e irmão, Rafael, em forma de agradecimento pelo suporte e carinho ao longo do meu percurso académico e de toda a minha vida. Sem o vosso contributo tudo seria mais difícil.

Ao Sérgio, pelo apoio e carinho de sempre e pelas palavras de conforto e incentivo.

A toda a minha família, especialmente aqueles que me são mais próximos, que sempre me incentivaram a fazer mais e melhor.

Aos meu colegas e amigos Diogo, João Paulo e André, e a toda a equipa com quem trabalhei, um agradecimento pelo acolhimento, ajuda e conselhos que em muito contribuíram para a realização e entrega deste trabalho.

Um agradecimento à Bosch Car Multimedia enquanto empresa, que me permitiu utilizar as suas instalações e recursos para a realização de todo o trabalho apresentado.

Aos meus professores responsáveis pelo meu percurso académico e de certa forma pessoal.

Agradeço também ao Boris Bret e João Paulo Silva pela orientação e acompanhamento ao longo deste percurso.

Finalmente dedico este trabalho, ao professor Eduardo Pereira, que nos deixou cedo demais.

STATEMENT OF INTEGRITY

I hereby declare having conducted this academic work with integrity. I confirm that I have not used plagiarism or any form of undue use of information or falsification of results along the process leading to its elaboration.

I further declare that I have fully acknowledged the Code of Ethical Conduct of the University of Minho.

Resumo

A indústria OLED evoluiu significativamente nos últimos anos, principalmente no que diz respeito ao mercado automóvel. Até então, a maioria dos displays do mercado automóvel utilizavam a tecnologia LCD, baseada em cristais líquidos e os OLED, LEDs de origem orgânica estavam reservados a dispositivos de eletrónica de entretenimento, como telemóveis e televisões. No entanto, o mercado tem evoluído e a possibilidade de utilização de displays curvos com novas formas e contornos, diferentes dos habituais displays retangulares, e de displays transparentes motivaram o estudo e investigação de novas tecnologias nomeadamente OLEDs.

A possibilidade de utilização de novos displays com novos contornos irá permitir uma melhor e mais eficiente utilização da área dos mesmos uma vez que não existirão espaços sem informação, o que acontece nos displays LCD. Esta inovação abre portas a um designe mais eficiente ajustado a cada um dos modelos de automóveis que a utilizem. Para além disso, a ideia de displays transparentes é bastante interessante e estes irão tornar possível a utilização de displays informacionais em espaços pouco usuais como vidro para brisas ou espelhos retrovisores.

Assim, este trabalho, inserido no projeto OCAI (Optical Calibration, Alignment and Inspection) surge da necessidade de investigar e determinar quais os testes necessários para a validação de um display OLED numa linha de produção concebida para testar estes dispositivos.

Palavras chave: Display, OCAI, OLED.

Abstract

The OLED industry has evolved significantly in the last few years, mainly in the automotive market. Until now, most display devices from the automotive market use LCD technology, based on liquid crystal, while OLED technology, which are organic LEDs, was mainly used in entertainment electronics like TVs and mobile phones. Nevertheless, the market has evolved and there is now a possibility of producing curved displays, with new shapes different from the usual rectangles, or even transparent displays. This motivated the study and investigation of new technologies that can be used with that purpose, such as OLED.

New displays with different cutouts and curved contours will allow a better use of the display active area, since there will be no unused space, unlike LCD displays. This innovation opens the door to a more efficient design, adjusted to the car models that use OLEDs. In addition, the idea of a transparent display is quite interesting and has the potential of enabling the use of informational displays in never before seen applications, such as on a car's windshield glass or on its side mirrors.

Thus, this work, inserted in the OCAI (Optical Calibration, Alignment and Inspection) project arises from the need to investigate and determine which are the necessary tests to validate an OLED display in a production line designed especially for testing this type of devices.

Key words: Display, OCAI, OLED.

Table of Contents

Table of Acronyms

AMOLED – Active-matrix OLED

CIE – Comission International de l'Éclairage

HOMO – Highest occupied molecular orbital

IDMS – Informal display measurement standards

LCD – Liquid crystal display

LED – Light emitting diode

LUMO – Lowest unoccupied molecular orbital

OCAI – Optical calibration, alignment and inspection

OLED – Organic light emitting diodes

PMOLED – Passive-matrix OLED

QD-LED – Quantum dots LED

RGB – Red, green and blue

TFT – Thin-film transistor

WPA – White point adjustment

Table of Figures

Table of Tables

Introduction

One of the most important elements to define the success of a company is the quality of its products. This quality factor can be divided in various components, like safety, durability and reliability. All these features are defined mostly on the development of the product and on the production line, where the products are conceived and tested respectively.

Since LCD displays are already well established on the market, there is a well-defined testing line projected for those products, but as we know, the market is always evolving and new products are now being produced and the LCD test line has to be adapted and modified in order to be suitable for these new products.

Therefore, the goal with this work is to define the OLED test chain and to optimize it, while having the LCD test chain as a starting point.

For this reason, and since we are talking about displays, the first step is to know how the human visual system works and how it reacts to a stimulus, Chapter 1.1. Then it is also important to know how to quantify Light and Color, radiometrically and photometrically, as well as review some of the terminology used. This information can be found on 1.2. Finally, and to finalize this first introductory chapter, an exhaustive description of the evolution of both color and light representation models was made, Chapter 1.3. In this subchapter, all the mathematical information that enable us to perform the tests and to calibrate the measure devices is described.

Since the LCD is the foundation for this work and the OLED technology is the one being evaluated, Chapter 2 has a comparison between the two technologies as well as the main reason as to why the LCD displays will probably be replaced by OLED ones in the short/mid-term future.

Chapter 3, OLED Light emission mechanism, is dedicated to the physical mechanism behind the light emission of this technology. Whilst Chapter 4, PMOLED and AMOLED working principle, explains the difference between the passive and active-matrix OLED displays.

The documentation of the practical work starts on Chapter 5, Display characteristics, where there is a description of the OLED samples used to perform the tests.

Test conditions and validation, Chapter 6, presents the conditions in which the tests were performed, according to Booklet 10 [19].

In Chapter 7, Experimental results of OLED optical characteristics testing, there is a description of the tests performed as well as the condition in which they were made and the equipment that was used. In this chapter, one can find the results and analysis of the measurements that were done in terms of Luminance, Color coordinates , Dimming and color difference, White point adjustment, Uniformity, Gamma and Switching Time.

Finally, in OLED characterization as a function of the temperature, Chapter 8, a characterization of the previously mentioned optical features is presented as a function of time and temperature, in order to calculate the time it takes for both temperature and optical properties to stabilize.

In the end, a final chapter summarizes the principal results of this dissertation.

The presented values and conclusions are valid for the measured sample and should not be generalized since the technology is in constant evolution.

1. Human Vision and Color

1.1. The eye

The display industry has evolved significantly, particularly when it comes to Automotive OLED displays. However, regardless of the type of display being evaluated, there are aspects that will be shared between them. When we want to evaluate and make a quality control of a display, properties such as light and color are extremely important. And since the last recipient of the displayed information is the human eye, it is essential that all quality metrics consider human vision and color perception. A display is programmed to emit radiation with different combinations of wavelengths that result in different stimuli that will be also interpreted differently by the user brain. The perception of these stimuli will depend on an infinite set of factors, ranging from the user to the environment involving the display when it is observed. Thus, the conversion between the emitted signal by the display and the one that arrives and is interpreted by the user is quite complex.

It is important to define methodologies and instruments that can turn your measuring equipment's response to a visual stimulus to the same response as the human eye. Radiometry is then the science of radiation measurement, it describes the generation, propagation and detection of optical radiation, that corresponds to a range of wavelengths from 0,01 to 1000 mm and includes regions like UV, visible light and IR. Photometry is the science of measuring the light, which is defined as electromagnetic radiation that is detectable by the human eye. In photometry everything is weighted by the spectral response of the eye [1-3].

The process of identification and formation of an image is extremely complex and evolves multiple systems of the human body. The vision is not limited only to the eye, but also extends to the brain, responsible for processing the information collected in the ocular system.

The human eye, Figure 1, is a complex and sensitive structure that reacts to electromagnetic rays with wavelengths between 380 and 780 nm. The visible light is comprehended in this wavelength range. The eye structure is constituted by several muscles, nerves, skin films and optical

receptors. The retina is the light-sensitive layer in which the cones and rods are located. Cones and rods are photoreceptors responsible for the precession of color and brightness, respectively. [1,7]

One can describe in a simplified way the process of perception and interpretation of light. Firstly, light enters the cornea, which bends the light that will pass through the pupil. The iris controls the pupils size and determines the amount of light that enters the lens. The lens is a clear and flexible structure that works very much like a camera lens and its function is to focus the light rays properly, in order to create a sharp image. From there on, the focused rays pass through the vitreous to the retina. The retina is responsible for capturing all the light rays and converting the light into electrical impulses that travel to the brain through optic nerves. The brain will decode these signals creating neurological patterns that we perceived as visual stimuli.

The absorption, scattering and focusing properties of the cornea, lens and fluids filling the eyeball will strongly influence the quality of the retinal image.

Rods and cones are the two types of photoreceptors present in the retina. They are responsible for the perception of light in different luminance conditions. Their distribution on the retina is very uneven, since there are a lot more rods than cones. Rods are found on the periphery of the retina, and cones are mostly concentrated on the fovea, a depression zone on the retina. Another difference between rods and cones it's their recovery time. Rods have a higher recovery time, which means that when a ray of light activates a rod it takes a while for our eyes to adjust to that illumination, on the other hand, cones have a small recovery time, allowing us to quickly distinguish colors. [1,7,16-17]

Rods are very sensitive to light but not to different colors and that's because they only have one type of photopigment, the light sensitive material in a receptor. That condition results in an achromatic response and we can only see different shades of gray. Rods only send signals to the brain under very low luminance levels, a single photon is enough to generate a signal. This type of vision, under low-light levels, is called scotopic vision and is produced by rod cells. As the light increases, the rods start sending less signals to the brain to a point when they are no longer active. In well illuminated situations, like daytime, these photoreceptors are inactive. [1,16]

On the other hand, cones are very limited in terms of light sensitivity, but they allow us to distinguish very fine details. This type of vision is commonly called foveal vision and we use it in our daily basis for activities like reading or seeing objects at a distance. Outside the fovea, the cones are far apart from each other, and their quantity is very small when compared with the number of rods. [1,17]

They start to send signals to the brain as the luminance increases. Cones, Figure 1, can differentiate color in visible spectrum and therefore are responsible for the color perception, photopic vision. This is the vision under well-lit conditions that provides the capability of color perception to humans. This type of vision is assured by the cone cells. Unlike rods, cones have three types of photopigments that respond differently according to the light wavelength. One can identify the three types of cones as S, M and L, that stands for short, middle and long respectively, which corresponds to the peak sensitivity of each of them in terms of spectral wavelength. [1,7,16-17]

We may think that each cone has an independent connection to the brain, but that is not the case. Between the two structures, cones and brain, there is a complex mesh of interconnected cells connecting them. These cells form the receptive field that is made up of horizontal, bipolar and Amacrine cells, Figure 1. [1]

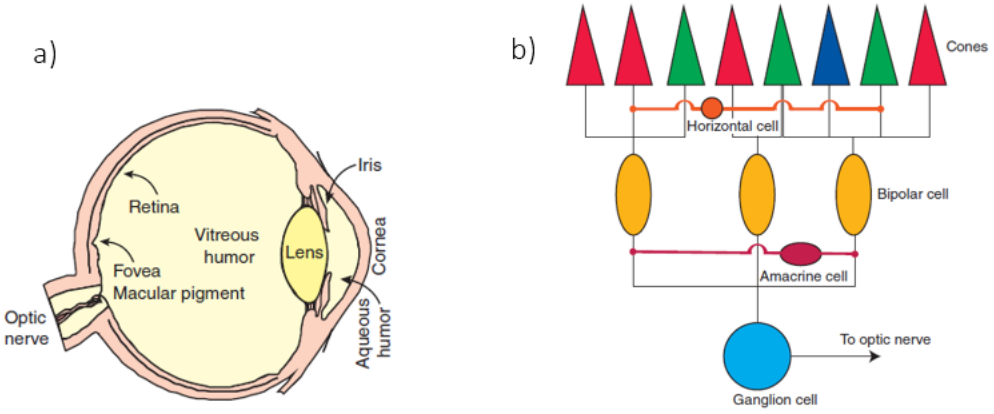

Figure 1-a) Cross section of the human eye; b) Simplified scheme of the retina. Adapted from [1].

1.2. *Light and Color*

There is an international organism responsible for the colorimetric standards definition, the Commision International de l' Éclairage, most commonly referred as CIE. Figure 2 shows the normalized response of each of our cone types, the standardized CIE cone fundamentals. [1,7].

When excited, the three cones integrate all the wavelengths from the incident light and this mechanism results in a theory called trichromacy. [1,7,17] Another important term, when considering color perception, is metamerism. That happens when two or more physical stimuli generate the same LMS response, making them indistinguishable. Different spectra give rise to the same trichromatic response. If we have two different stimuli, they will match in color if the response signal generated by all the cones is equal for both. [1,7]

The eye maximum spectral sensitivity is for green, at 555 nm. [1-2] Figure 2 b) represents the luminous efficiency function also called the 1924 CIE standard photometric observer and denoted by V_λ. This shows that the response of the human visual system is not linear across the spectrum.

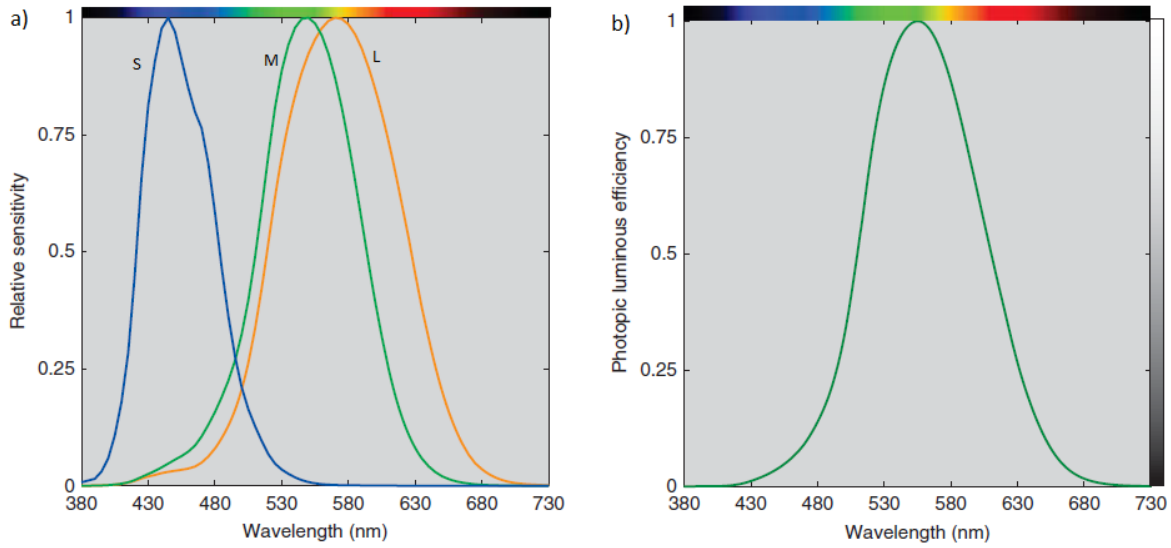

Figure 2-a) Cone fundamentals - Spectral sensitivity of the human visual system. b) Luminous efficiency function- CIE 1924 Adapted from [1].

Since we are interested in making an evaluation of displays that will be used in the automotive industry, it is also important to refer to some terms such as color constancy, light adaptation and chromatic adaptation. Cars are used in different lighting conditions, whether on cloudy or sunny

days or even at night. Thus, it is natural that our visual system has to adapt so that we see an object with the same color whether it is more or less lit. The adaptation that compensates for the intensity of light is named light adaptation, the one that compensates for the color is denominated as chromatic adaptation. These adaptations consist in changes to the pupil diameter, cone sensitivity and number of cones whose signals are pooled, that increase as the intensity of light decreases. Although this compensation happens many times, there are situations where it doesn't work, as we see objects with an approximate hue.[1] This is called incomplete chromatic compensation. Figure 3 shows the practical effects of decreasing the illumination on visual perception, one can see that the colored parts of the image become dimmer and less chromatic, while the blurriness of the image increases.

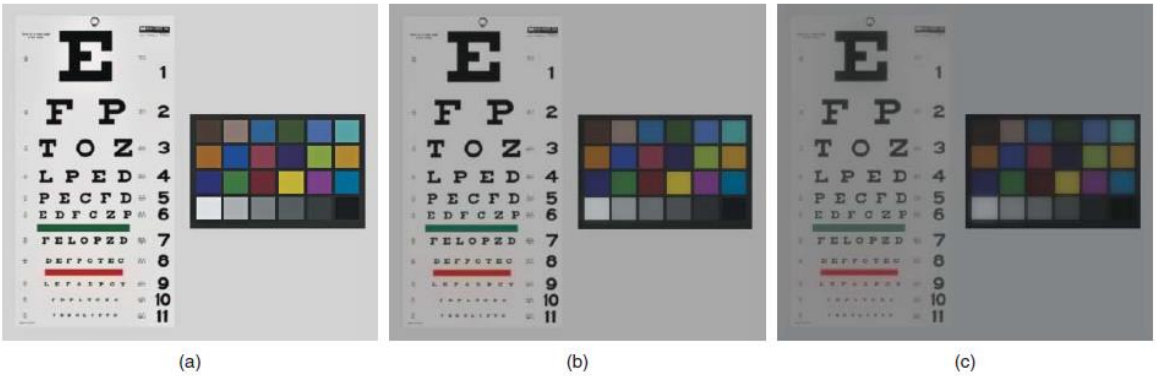

Figure 3-Example of the effect of illumination variation on visual perception: (a) 1000, (b) 100, (c) 10 cd/m2. Adapted from [1].

Besides the nonlinear behavior of the human eye in the spectral response, there is another nonlinear behavior of the eye when it comes to the conversion from the physical stimulus to the psychological response. The human eye's sensitivity to detect and identify small variations decreases with increasing luminosity. This behavior is most evident when trying to evaluate neutral colors. One can verify this by performing an experiment where an observer is shown a couple of images with neutral colors and asked to assign a lightness value from 0 to 100 where 0 is black and 100 is white (Fechner 1860). The result of this experiment is a psychometric function Ψ, plotted in Figure 4. This function is also known as the tone response curve. This nonlinearity give rise to the gamma factor, γ, a nonlinear factor applied to image reproduction. The value of gamma is usually 2.2 but values can go from 2 to 3. [1]

The psychometric function is given by:

$$\Psi = kI^{1/\gamma} \qquad \textit{Equation 1. 1}$$

where k is a normalization constant and I is the stimulus.

Because of this effect, the displayed images are usually gamma compressed so that the human perception can discount this effect.

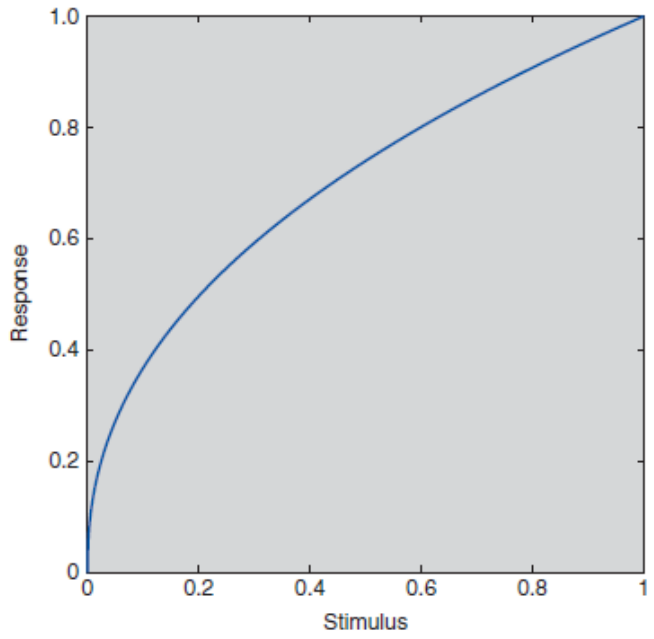

Figure 4- Psychometric function with k=1 and γ=2.3. Adapted from [1].

Another aspect to consider when analyzing a display are the terms which are used. When the assessment is done in objective terms, radiometric quantities are used. However, when trying to qualify the physical and human response to a light stimulus, photometric quantities are used. The conversion from radiometric to photometric quantities is done using the 1924 CIE standard observer plotted in Figure 2 b). This graph represents the photometric weighting function to radiometric quantities. [1-3,7,30] These quantities are summarized in Table 1.

Table 1- Radiometric and photometric quantities.

Radiometry			Photometry		
Quantity	Symbol	Units	Quantity	Symbol	Units
Radiant Energy	Q	J	Luminous Energy	Q	lm s
Radiant Flux	ϕ	W	Luminous Flux	ϕ	lm
Irradiance	E	$\frac{W}{m^2}$	Illuminance	E	$\frac{lm}{m^2}$
Radiant Intensity	I	$\frac{W}{sr}$	Luminous Intensity	I	$\frac{lm}{sr} = cd$
Radiance	L	$\frac{W}{m^2\ sr}$	Luminance	L	$\frac{lm}{m^2\ sr} = \frac{cd}{m^2}$

1.3. Colorimetry

Bearing in mind that color is transversal and measured in a distinct manner by different measuring objects, it is important to establish standards that in some way generalize the numerical values assigned to each color. Colorimetry is then the science that measures and numerically specifies color as perceived by the human eye. Throughout history, several standards emerged [1] that, at the time they were created, were better adapted to the needs of scientists and that at each step added more information to what was already known and documented. Even so, it is very common that nowadays we use information that refers to 1924 standards for example. There are some aspects that determine the validity of a model and the circumstances in which it can be used. First, it is crucial that a linear conversion can be done between models, so that we have equivalent results regardless of the model used. And second, it is important to use each model in the situations for which it was developed, not going out of its scope. Finally, it is important to note that no model is generic or universally preferable, depending on the situation and the parameters to be measured there may be one that is better than another. Considering the scope and application of the work performed, it is crucial that the model used is simple and does not involve additional measurements in order to save time on the production line while not forcing specialized personnel to carry out measurements in line. The 1931 CIE XYZ tristimulus system is the one used in the display industry, regarding color evaluation and quality control, namely calibration, alignment and inspection [7].

We are interested in measuring the human perception of a given light source and not the power distribution of the source itself. Figure 2 a) show us the normalized response of each of the three cone types of our eyes and the wavelength that each of the cones are sensitive to. [1,2] We will use these curves to quantify our human spectral response but first we need to find a standard and objective mathematical way to do it. CIE color-matching functions, Figure 5, provides the basis to perform a quantifiable representation of human spectral response. [7] These curves are also called the CIE 1931 standard colorimetric observer. They represent the color matching prediction for the average population with normal color vision measured with a 2° field of view. It is important to mention that the color-matching functions do not coincide with the cone

fundamentals, they are not the same. The 1931 CIE standard colorimetric observer gives information about human color vision, in fact, the experiment that gave rise to this standard is very simple. Basically, a bipartite field surrounded by dark was illuminated, half with variable amounts of RGB primaries and the other half with a fixed RGB value, and the selected group of people should indicate whether the colors shown match or not. With that information, scientists were capable to establish a relationship between the reference and the variable RGB values. This experiment was the base to the Color-Matching Functions definition, Figure 5, and to the so called tristimulus values that represent the net amount of each primary required to match a color.

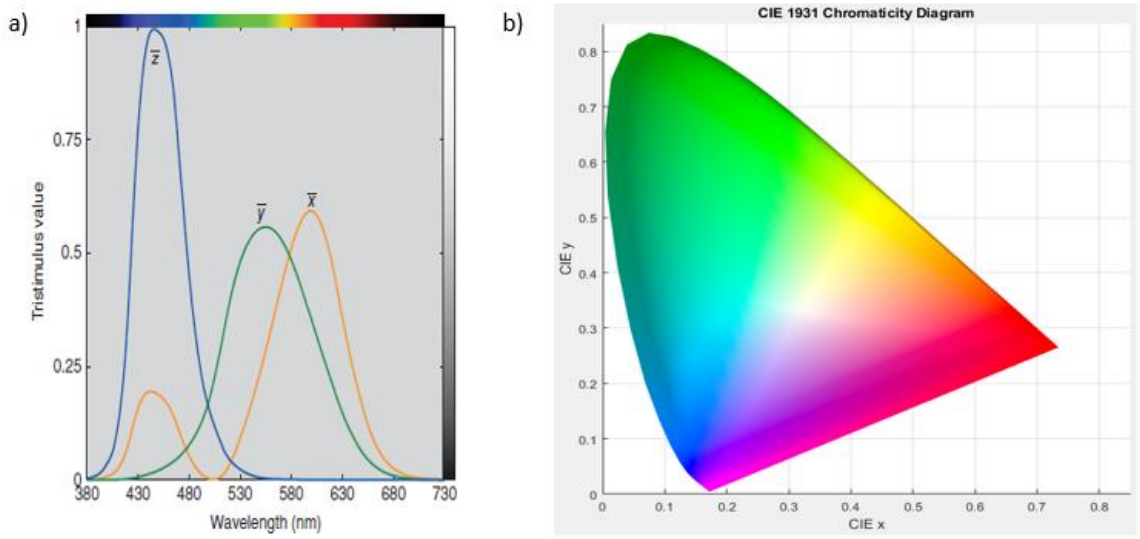

Figure 5-a) CIE 1931 standard colorimetric observer- Color-matching functions. Adapted from [1]. b) CIE 1931 Chromaticity Diagram.

We can obtain the tristimulus X, Y and Z by integrating the spectral power distribution of the light source we want to measure and multiplying that by the CIE color matching functions, Figure 6.

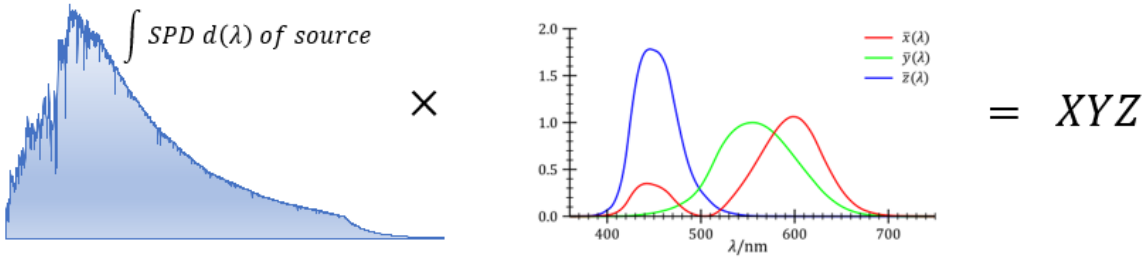

Figure 6-XYZ tristimulus are obtained by multiplying the spectral power distribution integral of the source by the color-matching functions.

Mathematically one can calculate the tristimulus values for displays with the color matching functions [1,7] Equation 1. 2.

$$\begin{cases} X = K_m \int_{\lambda} L_\lambda \bar{x}_\lambda d\lambda \\ Y = K_m \int_{\lambda} L_\lambda \bar{y}_\lambda d\lambda \\ Z = K_m \int_{\lambda} L_\lambda \bar{z}_\lambda d\lambda \end{cases}$$

Equation 1. 2

The $\bar{y}_\lambda$ color matching function was identified as V_λ , the luminous efficiency function or the photopic observer. While Y defines luminance (cd/m^2) and a coordinate in a three-dimension system, X and Z are not photometric quantities. A three-dimensional rectangular color space can be defined with the XYZ tristimulus values each one defining a point in space. However, the XYZ three-dimensional color space can be projected in a two-dimensional one with x and y color coordinates [1,7], Figure 5 b).

$$\begin{cases} x = \dfrac{X}{X+Y+X} \\ y = \dfrac{Y}{X+Y+Z} \\ z = \dfrac{Z}{X+Y+Z} = 1-(x+y) \end{cases}$$

Equation 1. 3

The x and y color coordinates represent color information independent from luminance. Having the luminance value, Y, it is also possible to calculate X and Z from the color coordinates x, y [1,7]:

$$\begin{cases} X = \dfrac{x}{y} Y \\ Y = y \\ Z = \dfrac{z}{y} Y = \dfrac{1-(x+y)}{y} Y \end{cases}$$

Equation 1. 4

In this work, spectroradiometers and colorimeters were used to report both achromatic and chromatic information, in xyY form. This information should not be used to estimate a color appearance, instead, x and y should be used to check if two color stimulus match.

Apart from that, it is also possible to calculate the predicted tristimulus values for any color combination due to the mathematical model provided from the CIE XYZ system, for that we only

need measurements of each primary color (this is possible under scalability and additivity principles). [1,7]

Our starting point is that, under scalability and additivity principles, it is possible to calculate the red, green and blue luminance values for any desirable white point chromaticity coordinates.

If we assume that the radiance does not affect the spectral distribution of each primary emission, a linear relationship between each primary spectral radiance and a scalar can be stablished. [1,7] This relation, Equation 1. 5, describes the modulation of the radiance between zero and a maximum value. This equation represents scalability.

$$\begin{cases} L_{\lambda,r} = RL_{\lambda,r\,\max} \\ L_{\lambda,g} = GL_{\lambda,g\,\max} \\ L_{\lambda,b} = RL_{\lambda,b\,\max} \end{cases} \qquad \textit{Equation 1. 5}$$

Where R, G and B are the scalar values ranging from zero to one.

$L_{\lambda,}$ represents the radiometric spectral radiance value and we can calculate the photometric luminance value, L:

$$L = K_m \int_{\lambda} L_\lambda V_\lambda d\lambda \qquad \textit{Equation 1. 6}$$

The K_m=683 lm/W is the maximum luminous function and it's a normalization constant. V_λ is the luminous efficiency function.

The linear relationship between XYZ tristimulus values and the spectral radiance, Equation 1. 2, enable us to write:

$$\begin{cases} X_r = K_m \int_{\lambda} RL_{\lambda,r\,max}\bar{x}_\lambda d\lambda \\ Y_r = K_m \int_{\lambda} RL_{\lambda,r\,max}\bar{y}_\lambda d\lambda \\ Z_r = K_m \int_{\lambda} RL_{\lambda,r\,max}\bar{z}_\lambda d\lambda \end{cases} \qquad \textit{Equation 1. 7}$$

Equation 1. 7 stands for the red channel, for green and blue the equations are similar.

Additivity is the second important aspect to consider when constructing the model. This property states that the sum of the radiance for each primary when displayed simultaneously obeys this principle:

$$L_\lambda = L_{\lambda,r} + L_{\lambda,g} + L_{\lambda,b} \qquad \textit{Equation 1. 8}$$

When a display is both scalable and additive, one can say that the display has stable primaries. This is a desirable property and enable us to calculate the tristimulus values for any color combination. This is particularly important when we want to calculate the white point adjustment (WPA) test that will be described later on.

While still using the red channel as an example, the maximum tristimulus values that can be realized are:

$$\begin{cases} X_{r\,max} = K_m \int_\lambda L_{\lambda,r\,max} \bar{x}_\lambda d\lambda \\ Y_{r\,max} = K_m \int_\lambda L_{\lambda,r\,max} \bar{y}_\lambda d\lambda \\ Z_{r\,max} = K_m \int_\lambda L_{\lambda,r\,max}\, \bar{z}_\lambda d\lambda \end{cases} \qquad \textit{Equation 1. 9}$$

We can show the CIE XYZ tristimulus in a matrix form, the tristimulus matrix:

$$\begin{pmatrix} X \\ Y \\ Z \end{pmatrix} = \begin{pmatrix} X_{r\,max} & X_{g\,max} & X_{b\,max} \\ Y_{r\,max} & Y_{g\,max} & Y_{b\,max} \\ Z_{r\,max} & Z_{g\,max} & Z_{b\,max} \end{pmatrix} \begin{pmatrix} R \\ G \\ B \end{pmatrix} \qquad \textit{Equation 1. 10}$$

For white, the R, G and B value is 1:

$$\begin{pmatrix} X_w \\ Y_w \\ Z_w \end{pmatrix} = \begin{pmatrix} X_{r\,max} & X_{g\,max} & X_{b\,max} \\ Y_{r\,max} & Y_{g\,max} & Y_{b\,max} \\ Z_{r\,max} & Z_{g\,max} & Z_{b\,max} \end{pmatrix} \begin{pmatrix} 1 \\ 1 \\ 1 \end{pmatrix} \qquad \textit{Equation 1. 11}$$

Using Equation 1. 4 and since Y is equal to the luminance value, one can also write Equation 1. 11 as:

$$\begin{pmatrix} X_w \\ Y_w \\ Z_w \end{pmatrix} = \begin{pmatrix} \frac{x_w}{y_w} \\ 1 \\ \frac{z_w}{y_w} \end{pmatrix} L_w \qquad \textit{Equation 1. 12}$$

Assuming that the display has stable primaries, for different luminance levels the xyz chromaticity values remain constant and the tristimulus matrix, Equation 1. 10, can be reproduced as the product of a chromaticity matrix and a luminance matrix.

$$\begin{pmatrix} X_{r\,max} & X_{g\,max} & X_{b\,max} \\ Y_{r\,max} & Y_{g\,max} & Y_{b\,max} \\ Z_{r\,max} & Z_{g\,max} & Z_{b\,max} \end{pmatrix} = \begin{pmatrix} \frac{x_r}{y_r} & \frac{x_g}{y_g} & \frac{x_b}{y_b} \\ 1 & 1 & 1 \\ \frac{z_r}{y_r} & \frac{z_g}{y_g} & \frac{z_b}{y_b} \end{pmatrix} \begin{pmatrix} L_{r\,max} & 0 & 0 \\ 0 & L_{g\,max} & 0 \\ 0 & 0 & L_{b\,max} \end{pmatrix} \qquad \textit{Equation 1. 13}$$

From Equation 1. 12 for white we have:

$$\begin{pmatrix} \frac{x_w}{y_w} \\ 1 \\ \frac{z_w}{y_w} \end{pmatrix} L_w = \begin{pmatrix} \frac{x_r}{y_r} & \frac{x_g}{y_g} & \frac{x_b}{y_b} \\ 1 & 1 & 1 \\ \frac{z_r}{y_r} & \frac{z_g}{y_g} & \frac{z_b}{y_b} \end{pmatrix} \begin{pmatrix} L_{r\,max} & 0 & 0 \\ 0 & L_{g\,max} & 0 \\ 0 & 0 & L_{b\,max} \end{pmatrix} \begin{pmatrix} 1 \\ 1 \\ 1 \end{pmatrix} \qquad \textit{Equation 1. 14}$$

Using mathematical properties to rearrange this last equation, one obtains Equation 1. 15 for each primary color. As long as the display has stable primaries, with the white chromaticity coordinates and its total luminance value, one can estimate the individual luminance values of each primary.

$$\begin{pmatrix} L_{r\,max} \\ L_{g\,max} \\ L_{b\,max} \end{pmatrix} = \begin{pmatrix} \frac{x_r}{y_r} & \frac{x_g}{y_g} & \frac{x_b}{y_b} \\ 1 & 1 & 1 \\ \frac{z_r}{y_r} & \frac{z_g}{y_g} & \frac{z_b}{y_b} \end{pmatrix}^{-1} \begin{pmatrix} \frac{x_w}{y_w} \\ 1 \\ \frac{z_w}{y_w} \end{pmatrix} L_w \qquad \textit{Equation 1. 15}$$

This result is also very important to calculate the white point adjustment. From the XYZ tristimulus we can obtain the color coordinates used in each of the standards, [1,7] Table 2. The XYZ

tristimulus values can be represented in two-dimensional plane. Converting these values to x and y (lowercase) the colorimetric coordinates are obtained and can be represented in the 1931 CIE color space. This color space represents the full range of colors that the human eye can see. Even though the CIE 1931 2º standard, Figure 5, is the oldest model of the table, it is the most commonly used in imaging applications like display alignment and calibration, because it's basic and easy to understand. [1]

Table 2-Convertion from XYZ to color coordinates.

CIE 1931	$x = \frac{X}{X+Y+Z}$	$y = \frac{Y}{X+Y+Z}$
CIE 1960	$u = \frac{4X}{X+15Y+3Z}$	$v = \frac{6Y}{X+15Y+3Z}$
CIE 1976	$u' = \frac{4X}{X+15Y+3Z}$	$v' = \frac{9Y}{X+15Y+3Z}$

2. OLED vs LCD

The starting point for the characterization of OLED displays was the preexisting tests carried out on LCD displays, so it makes sense to briefly describe these two technologies, their similarities and differences.

The first and one of the most significant differences between these two types of display is the complexity of the LCD structure compared to that of the OLED. An LCD display uses a white-light source, liquid crystals, polarizing filters and color filters. On the other hand, OLEDs are self-emissive devices that do not require backlight or color filters. [4-5,24]

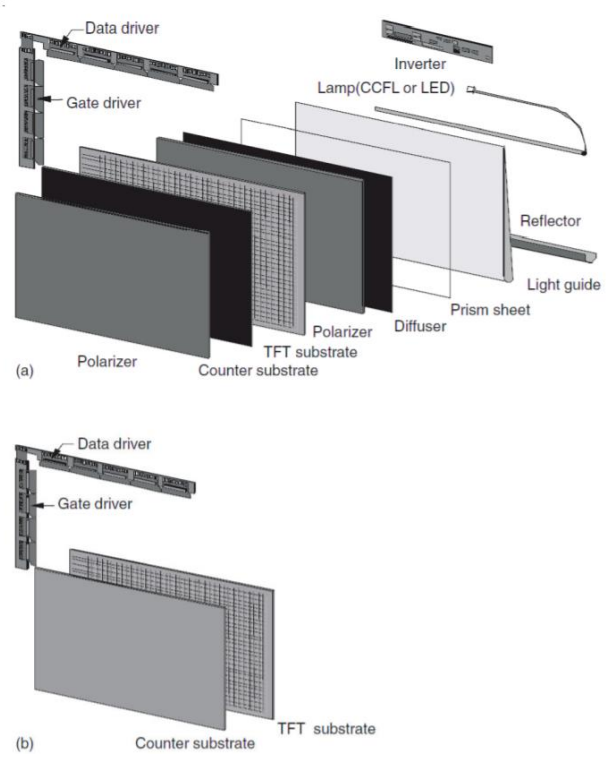

Figure 7- Simplistic LCD (a) and OLED (b) emission representation. The LCD structure is much more complex and needs a white backlight. The OLED is self-emissive and has a simpler structure. Adapted from [4].

This fact give rise to some differences between the two types of display:

- Power consumption: The power consumption of an LCD is much higher than that of an OLED as the LCD backlight is always powered, even if you only want to show part of the

display. On the other hand, in OLEDs there is no need for such since the device is self-emissive and allows pixel-by-pixel control.

- Response time: LCD have higher response times than OLEDs. The alignment of liquid crystal molecules is necessary for the LCD to produce light and OLED self-emissive feature allows it to be extremely fast.
- Color gamut: OLEDs can reproduce a wider range of colors than LCDs.
- Contrast: In LCDs a black image is never completely black because of the white backlight present on the device that cannot be completely blocked. On the other hand, a black pixel in OLED represents a turned off pixel, making it completely black.
- Viewing angle: OLEDs provide much wider viewing angles than LCDs.
- Flexibility/transparency/weight: OLED structure is simpler and therefore lighter than LCD. OLEDs can also be transparent and flexible.
- Lifetime/burn-in: Since OLEDs are made of organic materials, they are sensitive to water and oxygen, which leads to a shorter lifetime of the device and require protection. Other problem of OLED displays is the differential ageing of subpixels, that can be compensated by designing each subpixel, red, green and blue, with different shapes and sizes. Besides this, if only a part of the display is turned on during a considerable amount of time, the pixels will gradually lose their brightness (burn-in) and the aging on that region will be noticeable.
- Sunlight visibility: Another disadvantage of OLEDs is that the materials used in the cathode are commonly reflective. This is particularly difficult under direct sunlight. The use a polarizer can decrease this problem. For LCDs this is also a problem that can be mitigated using a transflective design that consists in applying a reflective layer between the TFT and the backlight of the device structure.
- Cost: Nowadays, LCD devices are cheaper than OLEDs. But that is expected since the LCD technology is older and much well studied and developed. Since OLEDs are simpler to assemble and companies are starting to invest in new manufacturing methods, it is expected that the price will fall drastically in the next few years. Companies like Samsung for instance are investing billions of dollars in production facilities prepared to produce

other technology (like OLED or QD-OLED) based displays and even predict to stop producing LCD displays by the end of 2022 [27-28].

Overall, it is clear that OLEDs have some positive characteristics over LCDs. The negative points of this type of technology can still be improved and mitigated, making it a great substitute for the next generation of automotive displays. [4-6,20-23,34]

3. OLED Light emission mechanism

OLED stands for organic light emitting diode, and its working principal is very similar to a common LED. The main difference between them is that instead of having a p-n junction to create electrons and holes, the OLED generates them using organic layers.

In an OLED, organic layers of semiconductor materials are deposited between two electrodes, a positive one, anode, and a negative one, cathode. When a current is applied to the electrodes, electrons flow from the cathode to the anode. Those electrons flow through the emissive layer of the OLED and photons are released. While the anode is removing electrons from the conductive layer, the cathode is driving them to the emissive layer. The electrons that are now on the emissive layer will recombine with the holes in the conductive layer creating excitons, Figure 8. This recombination process releases photons and therefore emits light. The intensity of light will depend on the current applied. The color of the emitted light can also be controlled and depends on the emissive materials used on the layers of the device. [4-5]

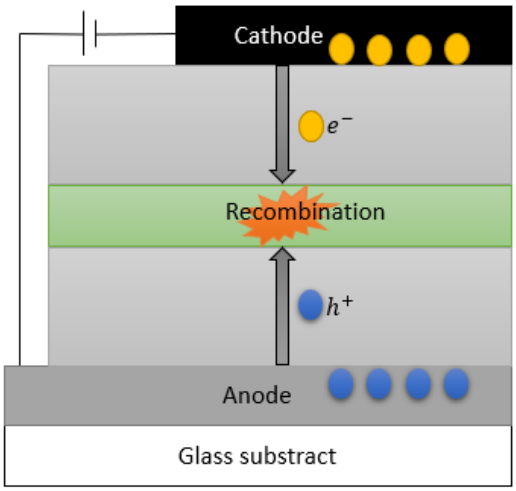

Figure 8-OLED recombination process.

The structure of an OLED can be pictured, in simple terms, by a sandwich of organic material layers between the anode and the cathode. The order of deposition of these layers and the function of each of them is particularly important to enable the device to accomplish a couple of practical requirements in order to promote higher efficiency, longer lifetime and a wider gamut

of colors. The thickness and the type of material of each layer also contribute to those features. The first layer below the cathode is the electron injection layer, the second is the electron transport layer. The middle layer is where the emission occurs, known as the emission layer. Then there's the hole transport layer and finally the hole injection layer followed by the anode. [4-5]

There are three types of OLEDS depending on the type of emission mechanism, fluorescent, phosphorescent and thermally activated delayed fluorescent OLEDS. The first and second ones are the most common and the light emission mechanism depends on the layer's materials [4-5,20-24].

To understand the two main light emission mechanisms, it is important to first have a notion of the meaning of some terms like exciton, triplet and singlet for example.

An exciton is a quasiparticle that results from the union of an electron and a hole. The two particles are attached to each other by the electrostatic Coulomb force. [24]

When the electrons of a molecule are in the ground state, they occupy the lowest energy levels, S0 in Figure 9, the singlet ground state. According to Pauli exclusion principle, only two electrons with opposite spin can occupy an orbital, creating a pair as shown. When enough energy is applied to the molecule, the electron's energy level changes. When this transition is performed without changing the electron spin, the resultant state is S1, the first excited singlet state. Depending on the applied energy the excited states can have higher energy and be called S2, S3…. On the other hand, if the transition does imply a change in the electron spin, the resulting state is called triplet state, T1. [4]

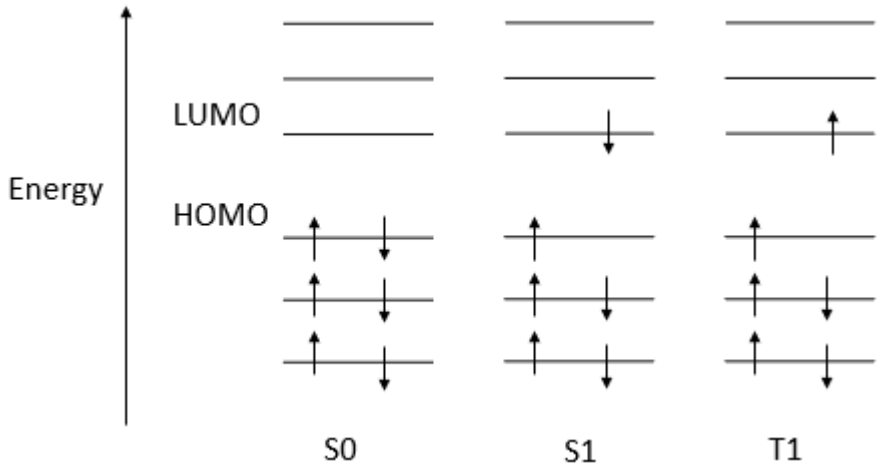

Figure 9-Electron spin configuration in ground and excited state. Adapted from [4].

In the case of fluorescent OLEDs, the electron and hole recombine in an organic layer and the organic molecules in the emission layer are excited generating two type of excitons, singlet and triplet excitons. The ratio between singlet and triplet excitons is 1:3 and only the emission from the singlet state causes fluorescence. The decay from the triplet state to the ground state if non-radiative. For that reason, only 25% of the exciton decay result in light emission, so the maximum quantum efficiency of this type of OLED is 25%.

In phosphorescent materials, the decay both from the singlet and from the triplet excited states are radiative. This means that theoretically, the internal quantum efficiency of a phosphorescent OLED is 100% [4-5,34].

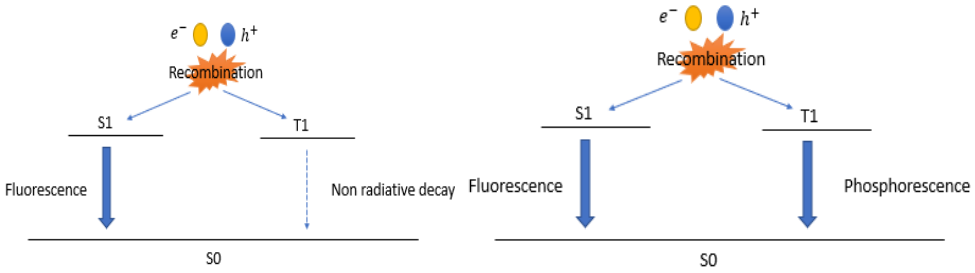

Figure 10-Recombination and light emission process in Fluorescent and phosphorescent materials.

4. PMOLED and AMOLED working principle

There are two types of OLED devices, concerning its matrix, the passive-matrix OLED (PMOLED) and active-matrix OLED (AMOLED). PMOLEDs are usually used in small and low-resolution displays, like mp3 small displays, while AMOLED are used for large and high-resolution screens, like televisions and mobile phones. [4]

In PMOLEDS the control scheme is very simple. Each line and row are controlled sequentially. Turning on a particular line and column will activate the pixel located at their intersection. Every line must have limited current for each diode and depending on the number of diodes that are activated in each row this current can change. Increase the number of rows decreases the available time to derive each pixel. To compensate this, the line or row that is turned on must be brighter. Since the brightness is proportional to the applied current, increasing the line row current will increase the power consumption of the device, affecting its lifetime and making it not efficient. [4,24]

On the other hand, using an active matrix to derive the OLED one can improve the lifetime, brightness, and power consumption of the device. The principle of an active-matrix is to provide the same current over the entire frame. This contributes to a lower power consumption of the display when comparing it with one using PMOLED technology. [4,24]

The major difference from AMOLED and PMOLED, is that for the active-matrix OLED, the pixels are activated by a thin-film transistor, TFT, array. The TFT will control and activate the current that flows to each different pixel, defining if the pixel emits light or not. Each pixel in an active-matrix has 3 components attached to it, a switching transistor, that turns the pixel on and off, a driver transistor, that provides the necessary current to the pixel, and a storage capacitor. The TFT matrix act like a backplane of the display making it less power consuming since TFTs have a very low power consumption. [4,24]

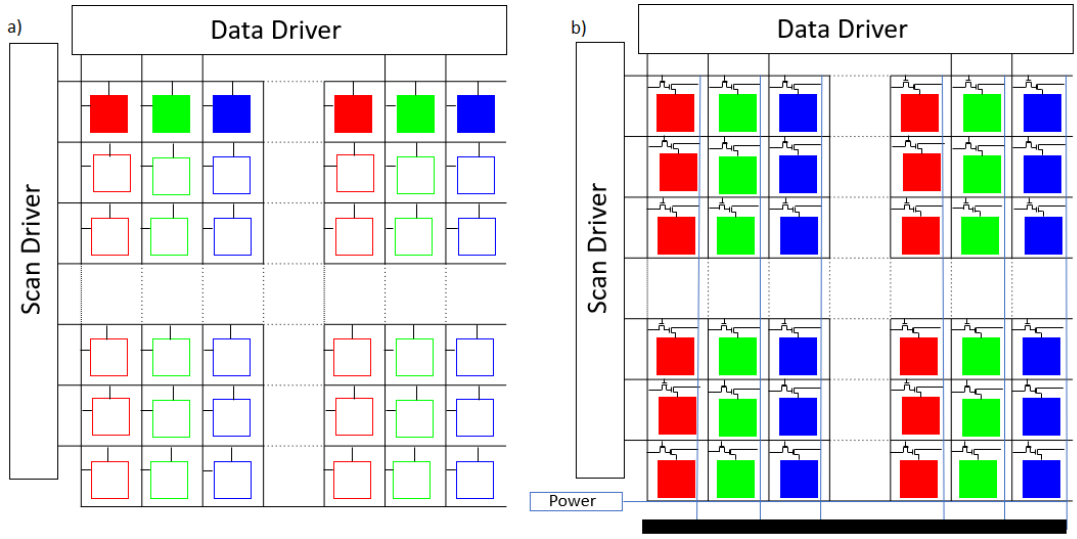

Figure 11-Deriving scheme of a PMOLED (a) and an AMOLED (b) device. Adapted from [4].

5. Display characteristics

The OLED samples used in this work have the following characteristics:

- Display size: 300mm (H) x 110mm (V).
- Display resolution: 2400 x 900 pixels. Theimages below show the display pixel pattern.

5.1. Subpixel structure

Firstly, the size of each of the subpixels is different. This is due to the fact that for the same luminance level the power consumption is different for each of them, causing differential aging, giving origin to potential noticeable different luminance levels between neighboring subpixels. The different sizes of the subpixels compensate the differential aging of each of them, making it imperceptible to the human eye. The blue subpixel has higher dimensions to compensate the lower luminance/power ratio, to minimize the long-term ageing and also to avoid the stress on the subpixel structure. If all subpixels had the same size, they would age differently because the individual input power to achieve the same output luminance is different. The device death is energy driven. [34]

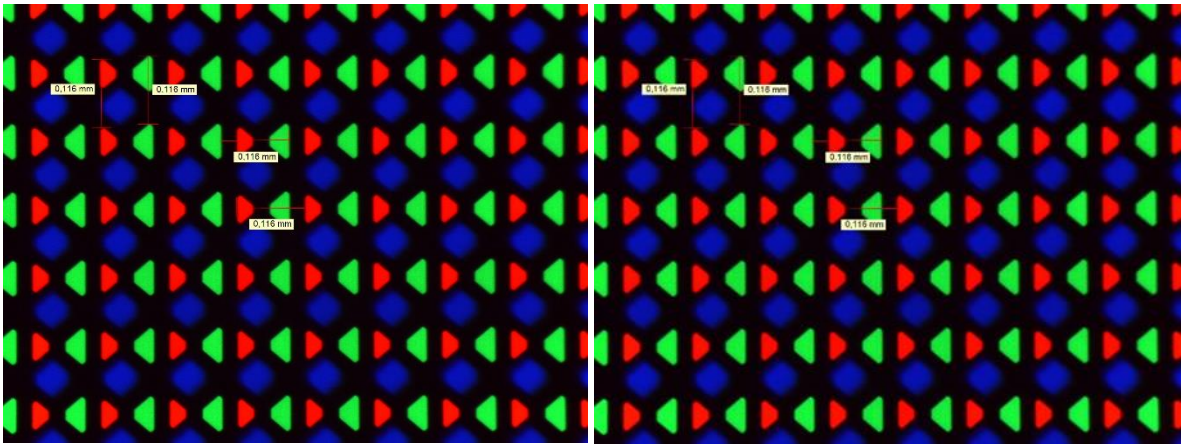

Figure 12-Display pixel pattern.

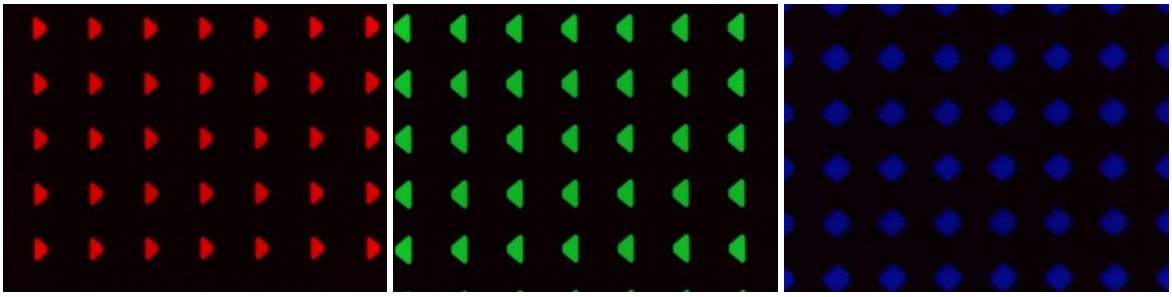

Figure 13-Display subpixel pattern for red, green and blue.

6. Test conditions and validation

In order to obtain good measurement results, some conditions need to be met: first of all, the measurement is performed in a dark room, because there should not be obvious sources of light like equipment lights and reflection of computer screens, walls or people [9].

The workplace temperature should be 24^{o}C±5^{o}C. In this case, the measurements were performed at room temperature [9], that is because the standard [9] was defined for computer monitors, that are typically in places where the temperature is between this range of values. This temperature is controlled and is around 23 degrees.

The display must be warmed for 20 or more minutes before measurements to stabilize its optical characteristics. In OLED, we use a 30 minute warm up time, to meet the required specifications [6,9].

All the settings should be maintained during the measurements, the variations should be only in the parameters we want to evaluate [9].

The measurements should be made perpendicular to the display. By default, 500 pixels of the sample should be considered to perform the measurement. That way, small deviations of the mean value don't have a huge impact on the measured value. The measured point should be at the center of the display [9] unless it's necessary to check the angular dependency of a feature.

Another important thing to consider and to better evaluate the measured values, is the capability. Capability and stability of the measuring process are parameters that guarantee that the measure can be performed without any variations or systematical errors. C_g and C_{gk} are the two capability indexes and should be higher than 1,33. C_g is the potential capability index and is defined as the ratio between precision and tolerance. C_{gk} is the actual capability and represents the ratio between the accuracy and the tolerance [19].

$$C_g = \frac{0{,}2T}{6s} \geq 1{,}33 \qquad \textit{Equation 6. 1}$$

$$C_{gk} = \frac{0{,}1T|\bar{x} - x_m|}{3s} \geq 1{,}33$$ *Equation 6. 2*

Tolerance of characteristic to be measured – T

Standard deviation of measured value – s

Mean of measured values – $\bar{x}$

Reference value of measurement standard – x_m

7. Experimental results of OLED optical characteristics testing

7.1. Luminance

When comparing OLED and LCD one of the major differences found is that the luminance values are much higher for OLED. Even though there is a difference between the two, there is no need to adjust the equipment and the method to determine the luminance of the display, since the device used has a luminance measuring range that comprehends the OLED luminance values.

The device used to perform this test was a spectroradiometer. A spectroradiometer measures light whether it comes from a source, a display or even the one reflected from materials. This device separates polychromatic radiation into its spectral components. For that it is equipped with an input slit, a rotating dispersive element (grating), an output slit and a detector array, and it can also include other optical elements like mirrors, Figure 14. This type of equipment has high sensitivity, captures inappreciable stray light and must be calibrated periodically (every 12 months is the recommended interval). This device provides information of the spectral irradiance and spectral radiance based on the position that visible light hits the detector array, inside the equipment. The acquired data is then processed on the software of the device providing values for luminance, radiance and chromaticity coordinates.

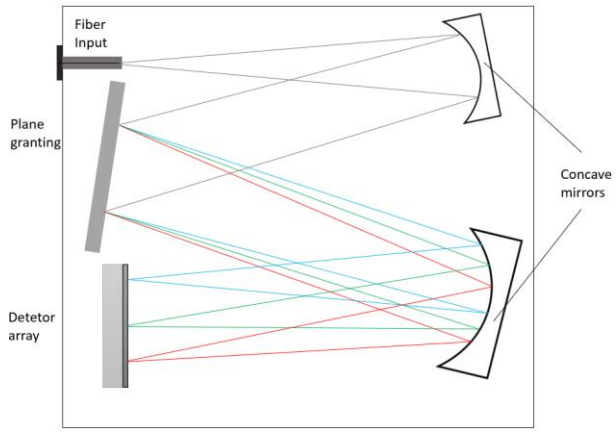

Figure 14-Spectroradiometer set-up.

For this test, we were only interested in the luminance values. The display and the spectroradiometer were 655 mm apart, perpendicular to each other and centered. The values were collected after a 30 minute heating period. As mentioned above, the measurements were performed at room temperature, around 23ºC. A dedicated control software was used, and once the spectroradiometer is plugged to the computer, the program can start the measurements immediately. The integration time is automatically defined for each of the images displayed and the wavelength range is set to the visible part of the spectrum, from 380 nm to 780 nm. This integration time is automatically set according to the light level of the light source before each measurement. For signals with higher values of luminance, the integration time will be smaller since more light is entering the device sensor. For low luminance images, the opposite occurs, and the integration time will be higher.

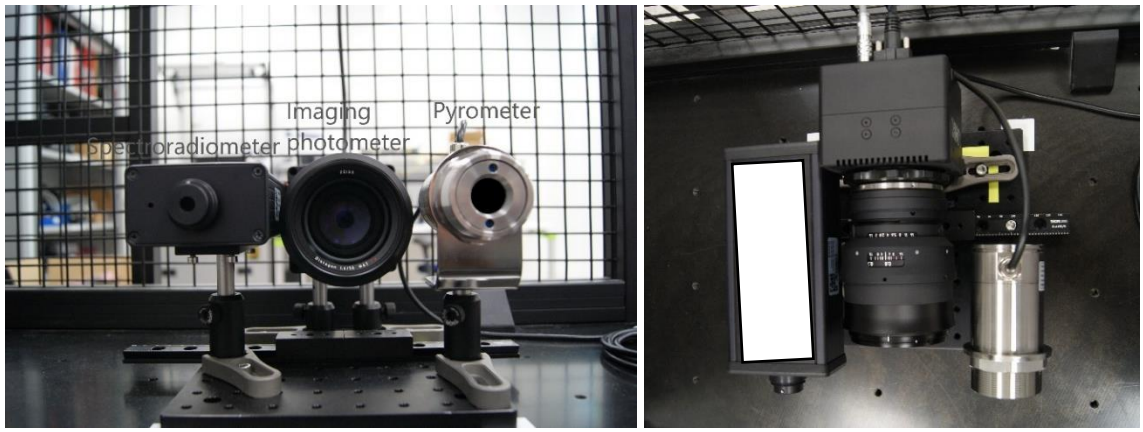

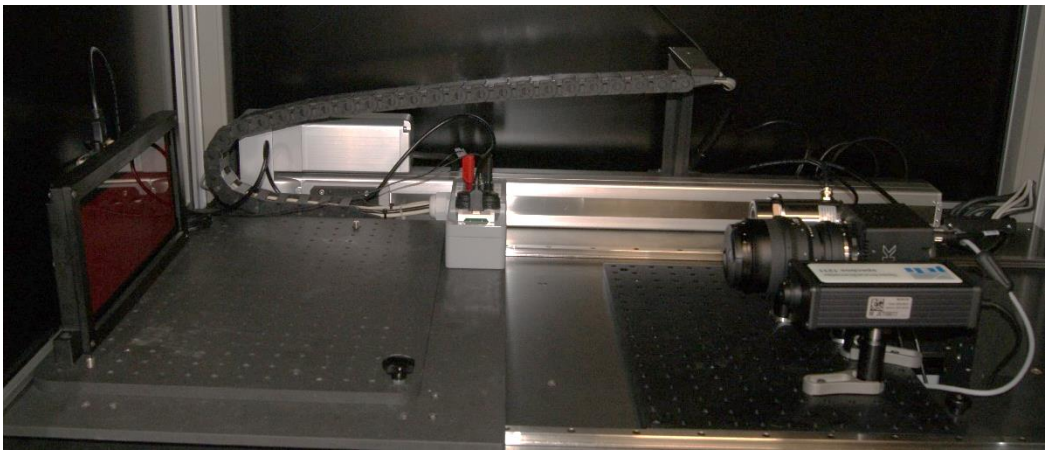

Figure 15-Setup with the OLED, the spectroradiometer, black and white camera and pyrometer (from left to right).

Eight images were compiled and displayed, with digital numbers according to the "Digital number" line of Table 3. The maximum luminance values acquired for both full luminance and low dimming images are also shown in Table 3.

Table 3-Colors tested, the corresponding digital number and the maximum obtained luminance value.

	Full Luminance				**Low Dimming**			
Color	**White**	**Red**	**Green**	**Blue**	**White**	**Red**	**Green**	**Blue**
Digital number	(255,255,255)	(255,0,0)	(0,255,0)	(0,0,255)	(22,22,22)	(48,0,0)	(0,27,0)	(0,0,74)
Luminance (cd/m^2)	911,60	206,90	625,80	78,89	4,97	4,74	5,01	5,28

The requirement for full white luminance is $L = \frac{700^{-0}_{+350} cd}{m^2}$. Figure 16 shows the experimental result of fifty measurements. The measured values are very accurate at around 900cd/m^2, within the tolerance value.

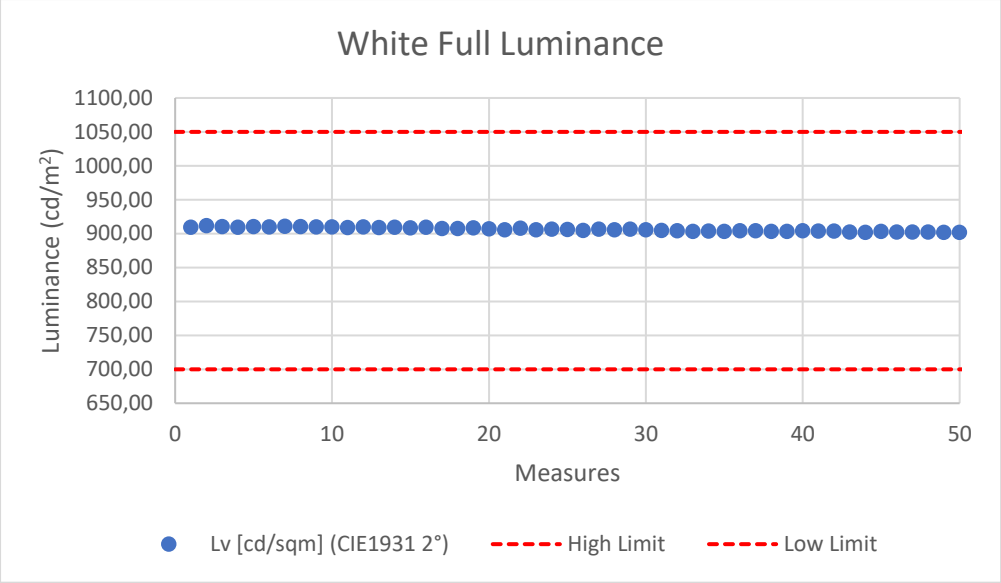

Figure 16- Experimental luminance results and tolerance.

In terms of capability, as already said in Test conditions and validation, Chapter 6, it is important to calculate the potential capability index, C_g. In this case, the measurement was considered reproducible because the C_g value was greater than 1,33. To measure capability, 50 “multipic" captures were taken. This “multipic” mode measures the signal 10 times and gives the mean value as an output.

Table 4- Full white luminance measurement capability.

Mean value	*906,25 cd/m²*
Standard deviation	2,92cd/m²
Tolerance	350 cd/m²
C_g	4,00

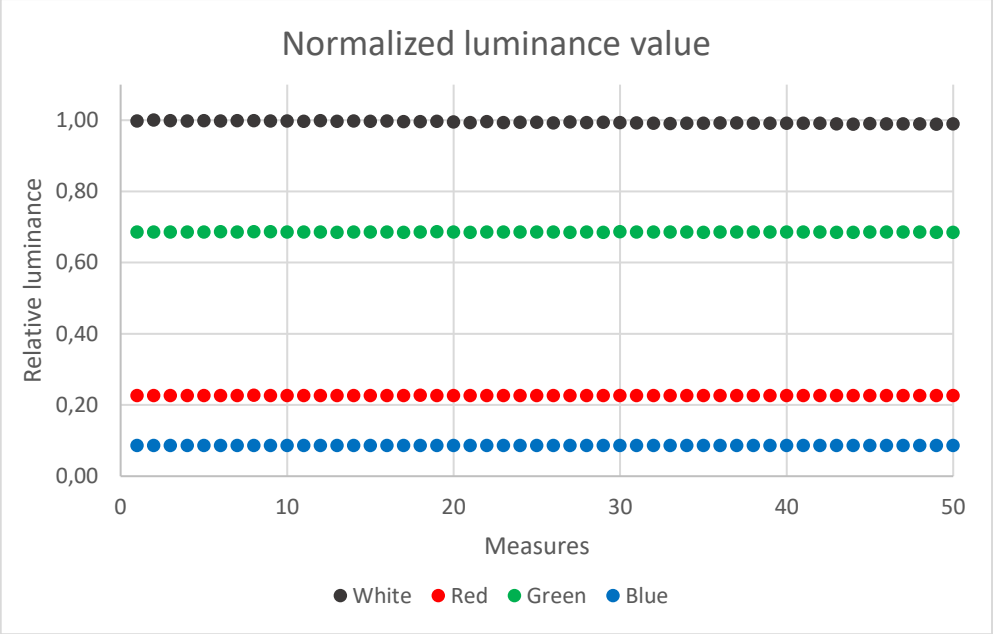

Figure 17-Normalized luminance values for full luminance WRGB images.

Since there were no specified reference and tolerance values for the other images, with full luminance and at approximately 5cd/m^2, one can only evaluate the precision of the measured values. Figure 17 shows the luminance values normalized to the maximum registered luminance value, for full white. There are some minor variations, but overall, the measured values are very precise for all the four full luminance images.

In the case of the low dimming images, the values cannot be normalized to the white luminance value because each of the four images is supposed to have 5cd/m^2 luminance. Once again, some fluctuations were registered, particularly for white and blue, Figure 18.

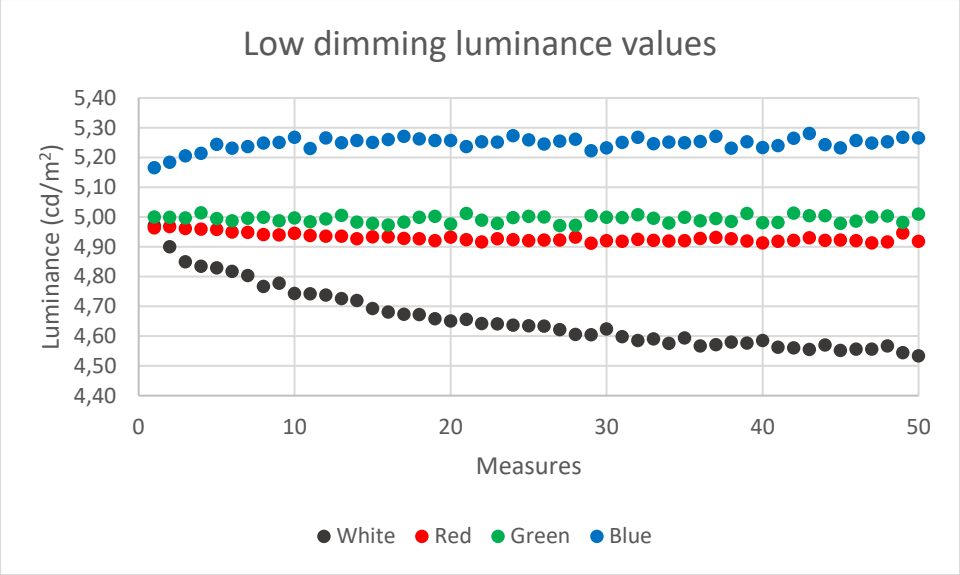

Figure 18-Luminance registered for low diming images.

7.2. Color coordinates

Another reported difference between LCD and OLED technologies is their color gamut. This represents the full range of colors within the spectrum of colors that the display can reproduce. It is known that OLED can reproduce a lot more colors than LCD technology [1,7] Figure 19. The represented information in Figure 19 was acquired and processed in the scope of the OCAI project deliverable [7].

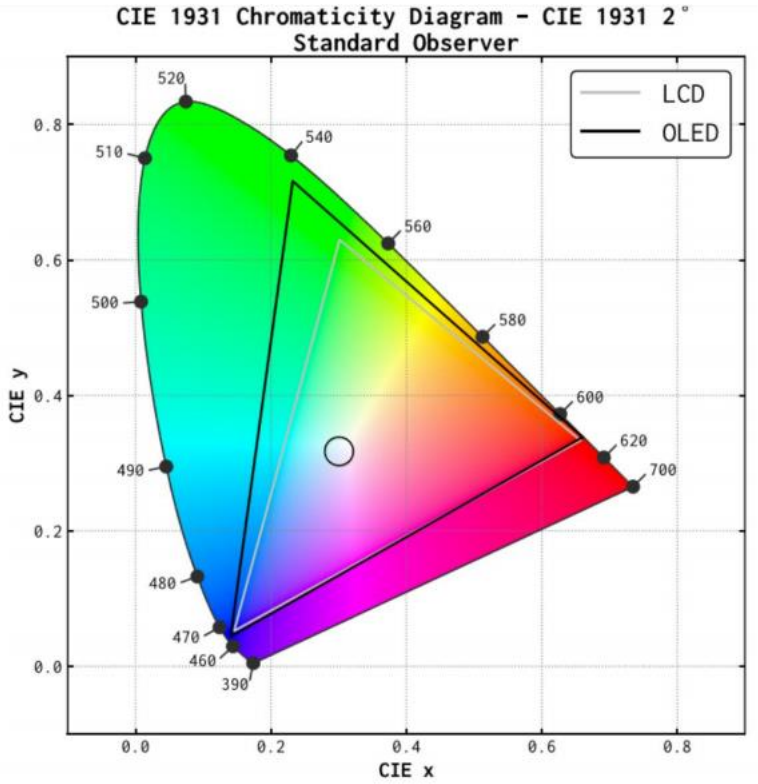

Figure 19-1931 CIE chromaticity diagram for typical LCD and AMOLED consumer electronic product. Adapted from [7].

To evaluate the color coordinates variation, images with different digital numbers were compiled for each of the four colors, white and the three primaries. Then, with a spectroradiometer the x and y values were measured. The test started after a 30 minute heating period and once again the display and the spectroradiometer were 655 mm apart.

Table 5 shows the points and respective digital numbers considered.

Table 5- Points associated with each digital number.

Point	**1**	**2**	**3**	**4**	**5**	**6**	**7**	**8**	**9**	**10**	**11**	**12**	**13**	**14**	**15**	**16**	**17**
DN	255	239	207	159	111	63	223	175	127	79	31	15	191	143	95	47	0

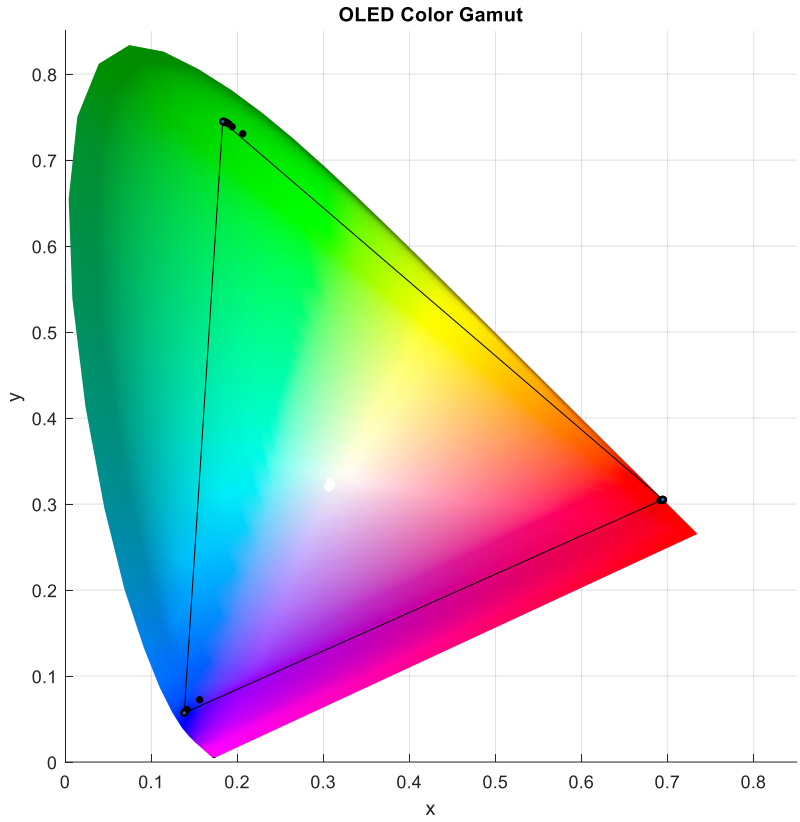

Figure 20-Automotive OLED color gamut.

From the requirements list, [6,29] we can only evaluate the validity of the white coordinates. The experimental obtained values were graphically represented in Figure 20 and can be found in Appendix A-Color coordinates for different DN.

The reference and tolerance values for white were:

$$\begin{cases} x = 0{,}307 \pm 0{,}005 \\ y = 0{,}321 \pm 0{,}005 \end{cases}$$

In Figure 21 one can see that the first five points, from DN 0 to DN 63, are outside the tolerance established by the specification. The rest of the points are within the reference values. We can

also conclude that the OLED is approximately scalable, since the spectral distribution of each primary does not change with the dimming level or digital number.

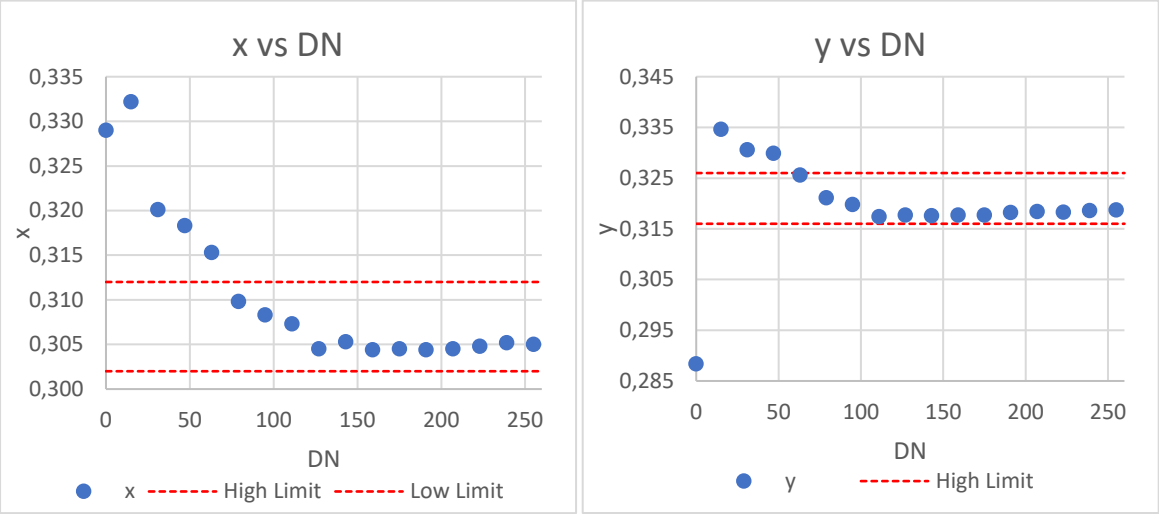

Figure 21-x and y as a function of digital number.

Regarding the accuracy of the color coordinates, from the analysis of the data collected from the 50 tests with a full luminance white image, at digital number 255, one can see that the values are concentrated and there are no major deviations from the mean value, Figure 22. The same analysis was made for the three primary colors and the result was exactly the same (see Appendix B-Color coordinates capability study).

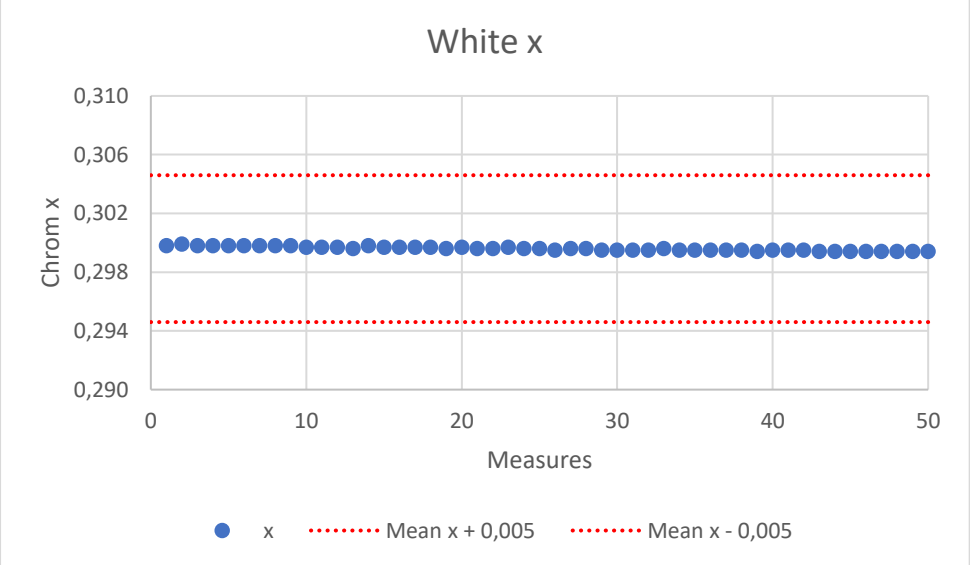

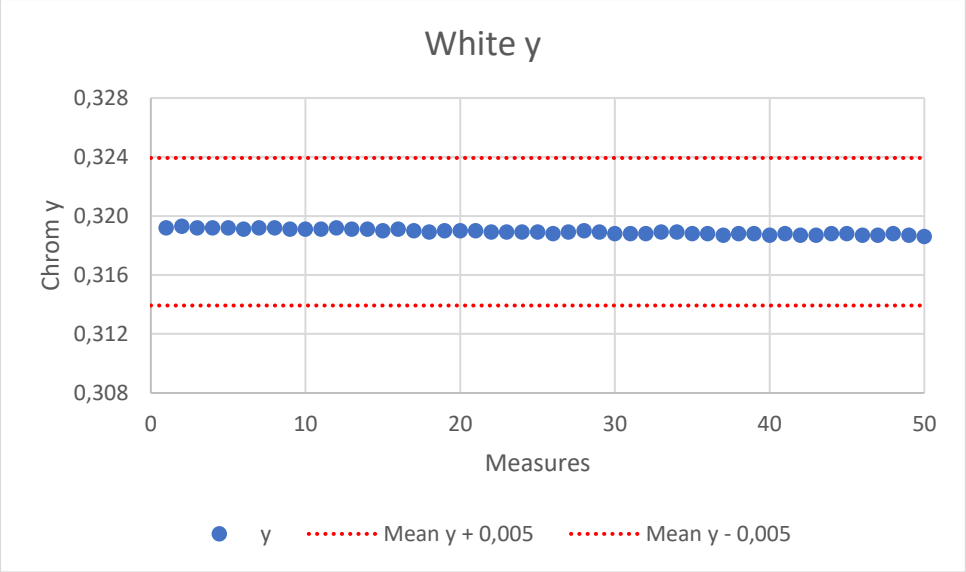

Figure 22-White coordinates measured 50 times.

The C_g value for white color coordinates can be calculated using the requirements list tolerance values -Table 4 from reference [6]. Even though the requirements list used for this work do not provide a specification for color coordinates tolerance values for red, green and blue, the value of 0,03 is commonly used as a reference tolerance. [29] With this, one can calculate a C_g value, that can be used only as a reference.

Table 6-Color coordinate (x) measurement capability.

x	*White*	*Red*	*Green*	*Blue*
Mean value	0,2996	0,6974	0,1996	0,1357
Standard deviation	0,00014	0,00010	0,00006	0,00004
Tolerance	0,0100	0,0300	0,0300	0,0300
C_g	2,3227	10,4054	17,2929	23,5965

Table 7-Color coordinate (x) measurement capability.

y	*White*	*Red*	*Green*	*Blue*
Mean value	0,3189	0,3020	0,7407	0,0609
Standard deviation	0,00018	0,00005	0,00011	0,00006
Tolerance	0,0100	0,0300	0,0300	0,0300
C_g	1,8818	20,0000	8,7895	16,4045

All the evaluated color coordinates show good C_g values, showing that the measured values are stable and reproducible.

7.3. Dimming and color difference

To evaluate the stability of the automotive OLED samples and the dimming effect, several images were compiled, and their radiance and luminance values measured using a spectroradiometer. It was expected that the display would obey the additivity principle, in which the radiance sum of the three primary colors, red, green and blue, is equal to the white radiance value.

The following graphics show the results obtained after a 30 minute warm up.

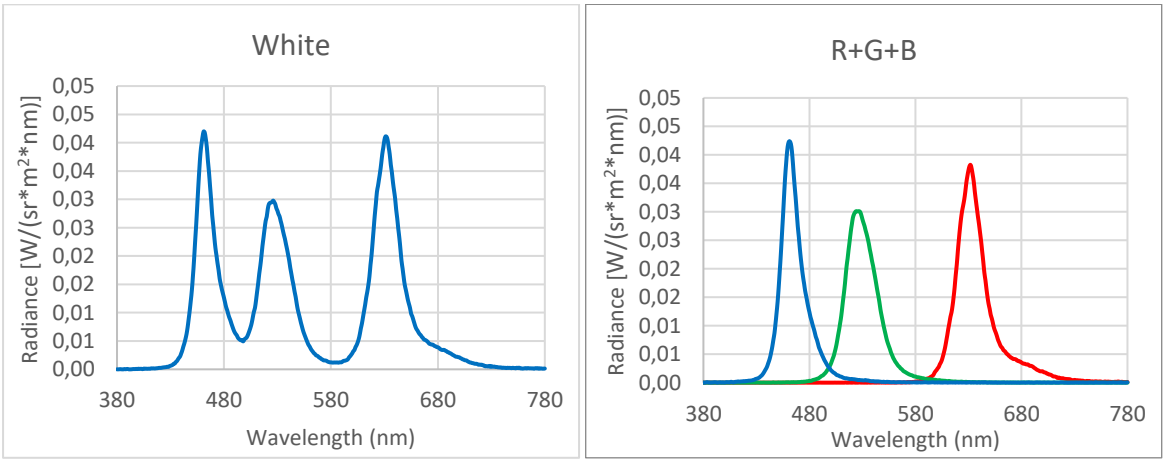

Figure 23-White, red, green and blue spectrum.

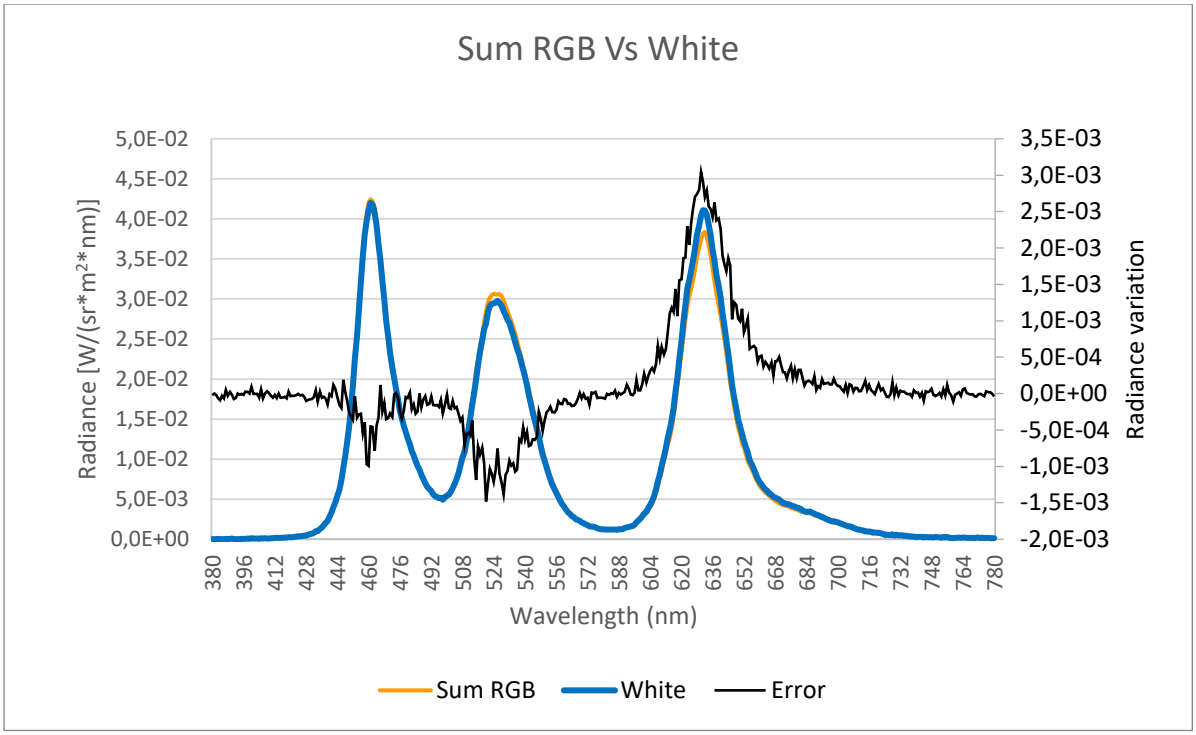

Figure 24-White, sum RGB and the difference between them.

In the "Sum RGB Vs White" graph, Figure 24, one can verify that there are some differences between the values of white and the sum of the primary colors. This variation is due to a Dimming effect in the driving circuit of the sample. This problem is probably related with the power distribution between the three subpixels, red, green and blue. When the display is white, the supplied energy is divided between the three subpixels, and that distribution isn't even. On the other hand, when the image on the sample is red, blue or green, all the available energy can be applied to the corresponding subpixel. For that reason, the sum of luminance of the three primary colors is not equal to the white luminance value. It is possible to overcome this effect by creating a mathematical model that can estimate the non-linear colorimetric output of the displays, as explained below. This can be interpreted as an intrinsic feature of the used OLED samples, if this was a real project, the displays supplier should give us a dimming model that corrects this problem.

The first step to create the Dimming model was to acquire the luminance and chromaticity coordinates (L, x and y) of a group of colors with different combinations of digital numbers. The contribution of each red, green and blue channel is normalized to 1 and then the data is separated

in two “subdivisions”, one with contributions ranging between 0 and 0,5 and one with values equal or higher than 0,5. For each of the two subdivisions, a linear regression model was created as a function of each component in order to output the respective dimming value. The multiple linear regression model respects the following equation.

$$Y = A_1X_1 + A_2X_2 + \cdots . + A_nX_n + K\ , A_1, \dots , A_n, K \in IR \qquad \textit{Equation 7. 1}$$

Since we have three components R, G, B and the output of this model is $Y \in \{Dim_R, Dim_G, Dim_B\}$, for each output components $T \in \{R, G, B\}$, a function f was defined.

$$f = Dim_T = \begin{cases} A_!R + A_2G + A_3B + K_1, & 0 \leq T < 0.5 \\ B_1R + B_2G + B_3B + K_2, & T \geq 0.5 \end{cases} \qquad \textit{Equation 7. 2}$$

To assess the model validity, the multiple R-squared and the correlation values were evaluated. If both are close to 1, we can consider that the model is good and provides a reasonable approximation between the predicted and measured values. Such was the case with this model.

Table 8 shows the resultant coefficients used in the formulated model, that were applied to each of the subsets created.

Table 8-Coeficients used in the calculation of the dimming values.

	COEFFICIENTS	DIM R	DIM G	DIM B
OFFSET (>=0,5)	K	1,052	0,945	0,901
	R	-0,079	-0,003	-0,045
	G	0,159	0,059	0,051
	B	-0,049	-0,035	0,097
OFFSET (<0,5)	K	1,109	0,930	0,793
	R	-0,3572	0,012303	-0,116
	G	0,532	0,121	0,169
	B	-0,123	-0,097	0,290

The observed values, the measured ones, as well as those predicted by the models were recorded for a later analysis.

The following graphs, Figure 25, show the values predicted by the models created for a better and faster perception of the fit quality of the models. In fact, there is a strong correlation between the predicted and observed values.

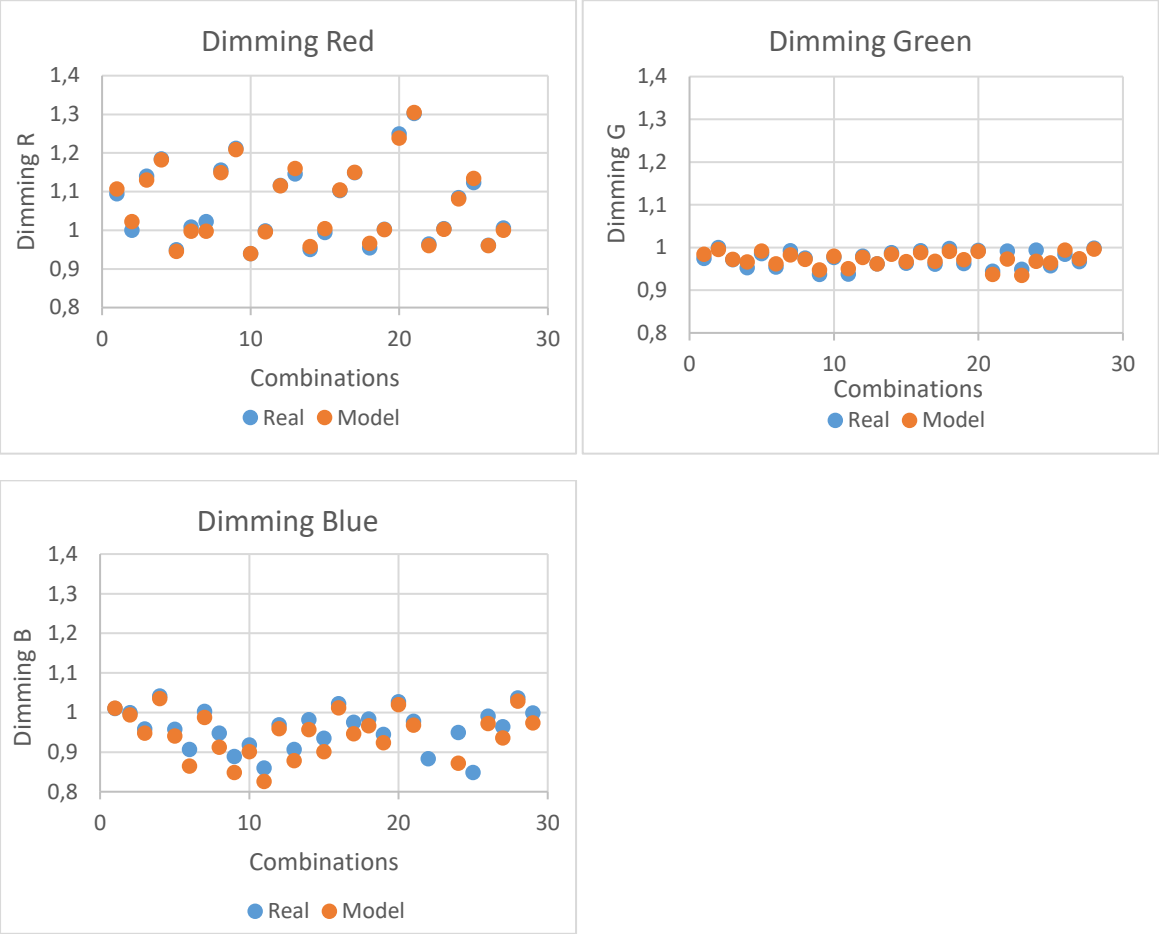

Figure 25-Real and predicted Dimming values.

With this model we were able to predict and calculate the dimming effect on the measured values of luminance and color coordinates. By multiplying each of the dimming components, for red, green and blue, by the correspondent factor, we have a fair mathematical reproduction of the behavior of the display in terms of luminance and color coordinates. Therefore, with the application of the model, smaller color difference values were expected.

Using the Dimming values from the model, the color difference parameter ΔE^*_{uv} is expected to be less than 3. Figure 26 show the ΔE^*_{uv} values for the different RGB combinations tested before and after applying the model.

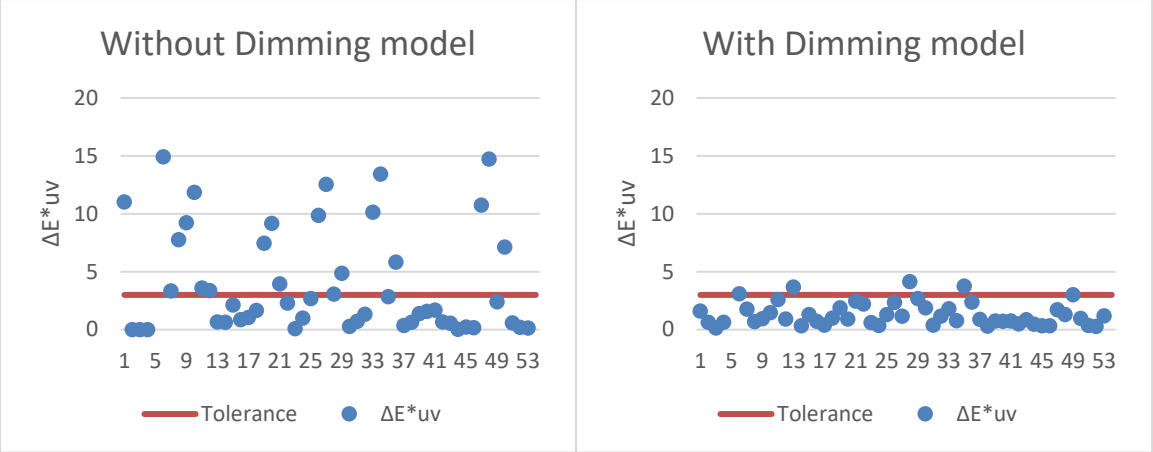

Figure 26-Color difference with and without the dimming correction.

The improvement from one graph in relation to the other is quite evident. Even so, it is possible to see that, even with the Dimming correction, there are some values above or very close to the tolerance (ΔE^*_{uv}=3). This is a very important result; if the correction function is applied to the production line, there is a considerable number of units that will not meet the requirements. Still, it is a good result when compared to those before the correction and those obtained with the non-automotive sample.

7.4. White point adjustment

When evaluating the quality of an OLED display, the white point adjustment is a very important test, it allows us to, for example, evaluate the differential image aging effect. This effect is particularly visible when, for example, a pattern is displayed for a long time and its shape remains noticeable even when other images are displayed. Since white is approximately the sum of the three primary colors, when we want to display a white image, all the three subpixels are on. By measuring the white point of the displayed white image one can verify the white point shift and calculate a way to compensate this shift in order to preserve the quality of the display and increase its lifetime.

To perform the test, the white, red, green and blue full luminance images are evaluated in terms of luminance and chromaticity coordinates. Then the values are applied to the existing excel template that returns the RGB digital numbers of the corrected white image as an output.

Even though this test is straightforward to perform, the used method to calculate the needed adjustment is not. It requires knowledge of some mathematical and colorimetric concepts.

This adjustment takes the measured luminance, chromaticity coordinates, as well as the costumer reference values and tolerances and verifies if the measured values are within these tolerances. This algorithm was computed using Equation 1. 15.

The first step is to measure the initial white point coordinates and luminance values of the display (x_w, y_w and L_w). If these values are within the specification, there is no need to adjust the white point values. From the measured luminance and chromaticity values L_w and $x_w y_w$, and using Equation 1. 15 one can estimate the maximum luminance values for each of the three primary color channels. From Equation 1. 15 one can stablish that the desired maximum luminances for each primary can be written as:

$$\begin{cases} L_{r\,max} = RL_R \\ L_{g\,max} = GL_G \\ L_{b\,max} = RL_B \end{cases} \qquad \textit{Equation 7. 3}$$

Where R, G and B values range from 0 to 1 and L_R, L_G and L_B are the maximum measured luminance value for each of the primaries.

With this information, the RGB values are computed and the digital number is adjusted. This adjustment (WPA) is only achieved for RGB values smaller than 1. If that's not the case, the luminance value for white $L_w$should be decreased.

Then, the image with the new RGB digital numbers is compiled, displayed and measured again. If the white image coordinates are within the target tolerance values the image is considered fixed. If not, a second iteration is needed. Again, the spectroradiometer was used and the display was 655mm apart from it.

In a first approximation, only the target of the specifications was considered. Then, four other targets were selected, based on values from the production samples. Table 9 shows the performed tests.

Table 9-White Point targets and respective tests.

Test		L (cd/m^2)	x	y	Target_x	Target_y	Tolerance
1	Initial	908,80	0,3005	0,3200	0,307	0,321	±0,005
	1st Iter.	890,30	0,3048	0,3203			
	2nd Iter.	-	-	-			
2	Initial	921,90	0,3005	0,3201	0,316	0,336	
	1st Iter.	883,10	0,3145	0,3340			
	2nd Iter.	-	-	-			
3	Initial	914,60	0,3011	0,3202	0,316	0,306	
	1st Iter.	807,00	0,3132	0,3080			
	2nd Iter.	-	-	-			
4	Initial	925,50	0,3009	0,3205	0,296	0,336	
	1st Iter.	891,90	0,2966	0,3342			
	2nd Iter.	-	-	-			
5	Initial	931,00	0,3009	0,3205	0,296	0,306	
	1st Iter.	841,90	9,2959	0,3073			
	2nd Iter.	-	-	-			

Figure 27 represents graphically the tests performed to evaluate if the white point current coordinates correspond to the specified values and if they are within the tolerance values provided by the user. The orange rectangle shows the coordinates set of values accepted by the costumer. If the "white original" point is out of that rectangle, a first iteration is made and the program generates a triplet of RGB digital numbers to correct the image. The five tests show that with only one iteration we can take the white point coordinates to the desired region.

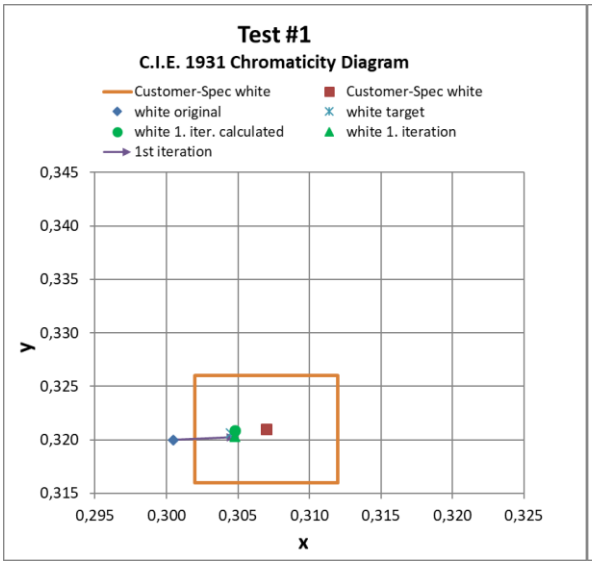
Test #1
C.I.E. 1931 Chromaticity Diagram
Customer-Spec white
Customer-Spec white
white original
white target
white 1. iter. calculated
white 1. iteration
1st iteration
0,345
0,340
0,335
0,330
0,325
0,320
0,315
y
0,295
0,300
0,305
0,310
0,315
0,320
0,325
x

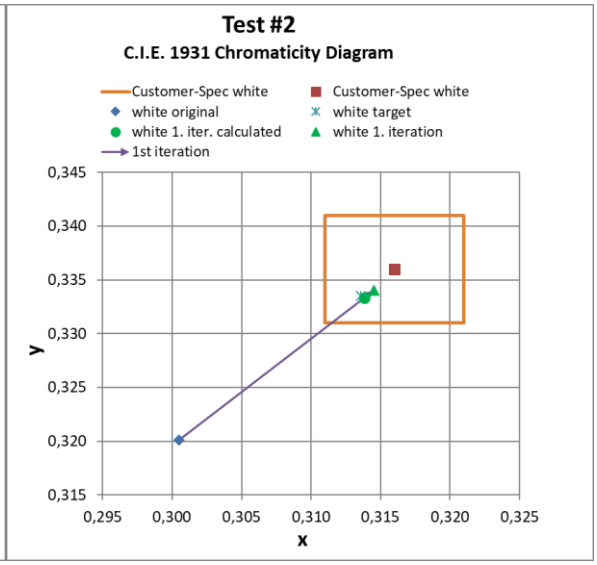
Test #2
C.I.E. 1931 Chromaticity Diagram
Customer-Spec white
Customer-Spec white
white original
white target
white 1. iter. calculated
white 1. iteration
1st iteration
0,345
0,340
0,335
0,330
0,325
0,320
0,315
y
0,295
0,300
0,305
0,310
0,315
0,320
0,325
x

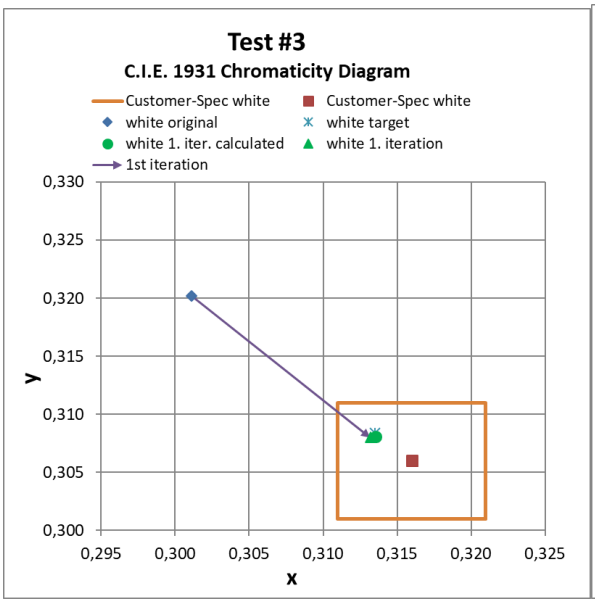
Test #3
C.I.E. 1931 Chromaticity Diagram
Customer-Spec white
Customer-Spec white
white original
white target
white 1. iter. calculated
white 1. iteration
1st iteration
0,330
0,325
0,320
0,315
0,310
0,305
0,300
y
0,295
0,300
0,305
0,310
0,315
0,320
0,325
x

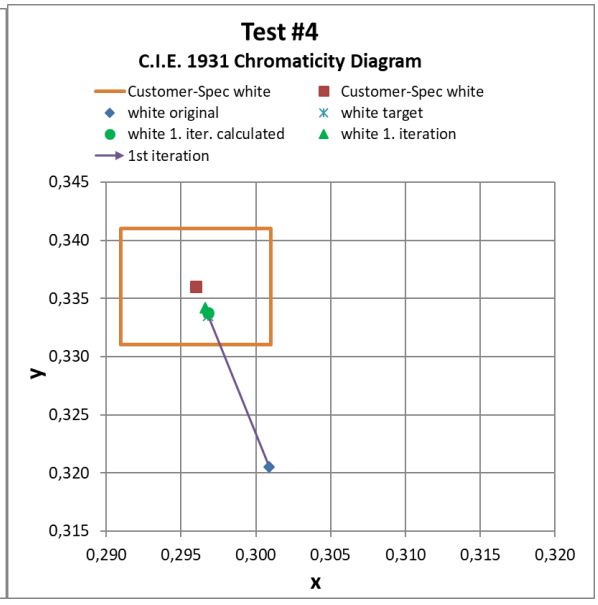
Test #4
C.I.E. 1931 Chromaticity Diagram
Customer-Spec white
Customer-Spec white
white original
white target
white 1. iter. calculated
white 1. iteration
1st iteration
0,345
0,340
0,335
0,330
0,325
0,320
0,315
y
0,290
0,295
0,300
0,305
0,310
0,315
0,320
x

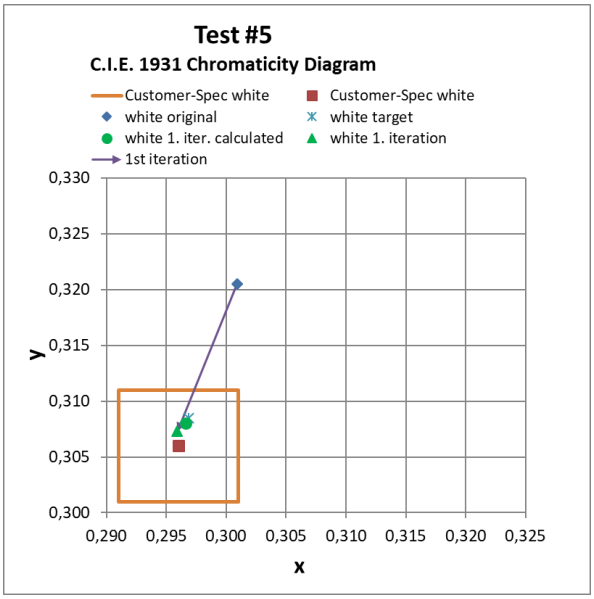

Figure 27-Graphic representation of the results from Table 9.

Overall, from both Table 9 and Figure 27, one can conclude that the sample is easily corrected when needed. It only took one iteration to correct the white point and bring its coordinates to the desired region.

7.5. Uniformity

In OLED displays applications it is important to have both color and luminance uniformity across the display, that is in fact, one of the quality factors when evaluating the performance of the device. When it comes to luminance, the non-uniformity is called Mura, from the Japanese word for inhomogeneity. The non-uniformity of emissive displays such as OLEDs is caused mainly by material non-uniformities or by the TFT driving system.[4] Therefore, for this type of displays, the non-uniformity and Mura are subpixel level, and require subpixel uniformity correction.

The uniformity test is very important in terms of quality and safety. We can say that a display is uniform when it is capable of displaying the content as expected, with no variations from the original image and with no missing information. It is particularly noticeable in cases where the displayed image has only one color. When the displays have a non-uniformity, it is important to correct it. Our OLED requirements list states that uniformity values must be above 80% for full luminance white, red, green and blue (DN 255) and above 60% for low dimming cases, with luminance close to 5cd/m^2.

7.5.1. Imaging photometer

For this test a calibrated imaging photometer was used. A photometer is a simple device conceived to simulate the human eye response to light. The relative response of the human eye to monochromatic light is defined as the photopic luminous efficiency function, Figure 2. Questions like alignment, focus and the Moiré effect were taken into account.

Moiré is a phenomenon that occurs when displaying repetitive structures, like line-gratings or dot-screens. This results in a superposition of the patterns, creating a new pattern that is observed in the display but not in the original image. [25-26]

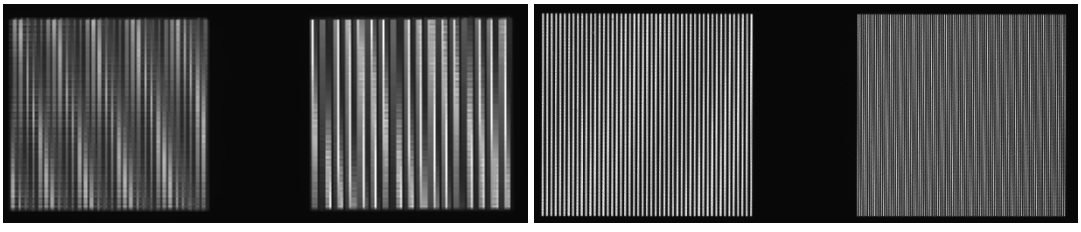

Figure 28-Before and after Moiré correction.

Several tests were performed in order to find the correct set up for this data acquisition.

On the first attempt to perform this test we used a 25 mm lens and a 12 megapixels camera. The camera effective number of pixels was 2453x2055, the display effective number of pixels was 2400x900 so the reproduction scale was very close to one and effects like Moiré were visible on the collected image. To eliminate this problem, the size of the image projected on the display was reduced in a way to increase the pixel ratio between the camera and the display. The displayed image was half the size of the display horizontally, and the pixel ratio went from 1,02 to 2,04 horizontally and stayed at 2,28 vertically. Besides that, we replaced the 25mm lens with a 50 mm one in order to reduce possible image distortions and to reduce the influence of light angular distribution.

Finally, a 30 megapixels camera with a 50mm lens was used and the problems related to the Moiré effect and reproduction scale were easily eliminated. The working distance was defined as 655mm and the display was turned on for 30 minutes before performing the measurements.

This test was performed according to the Uniformity Measurement Standard for Displays V1.30 norm. [25] This norm proposes a method to measure the uniformity of a display and gives instructions on how to align it and how to remove the Moiré effect using the focus of the camera, the setup and the available test patterns.

The software used was Labsoft, Figure 29.

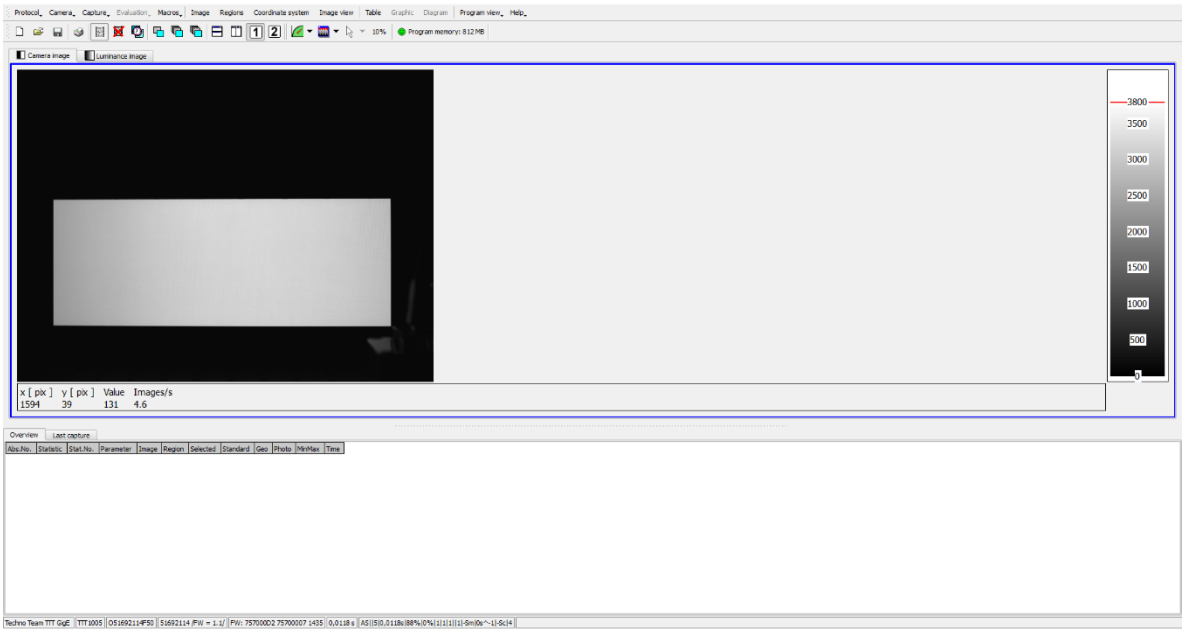

Figure 29-White image displayed on the OLED display and evaluated with the imaging photometer software.

7.5.1.1. Alignment and focus

The first step when preparing the setup for this test was to align the camera and the display, using an alignment pattern, that is shown on the display, and specialized algorithms to estimate the relative position. The already mentioned norm says that the display orientation has to be aligned, either by using the before mentioned pattern to a deviation of less than one pixel or by any other means that ensure that each tilt angle is less than 0,5°. In our case, we choose to generate an alignment image, as shown in Figure 30.

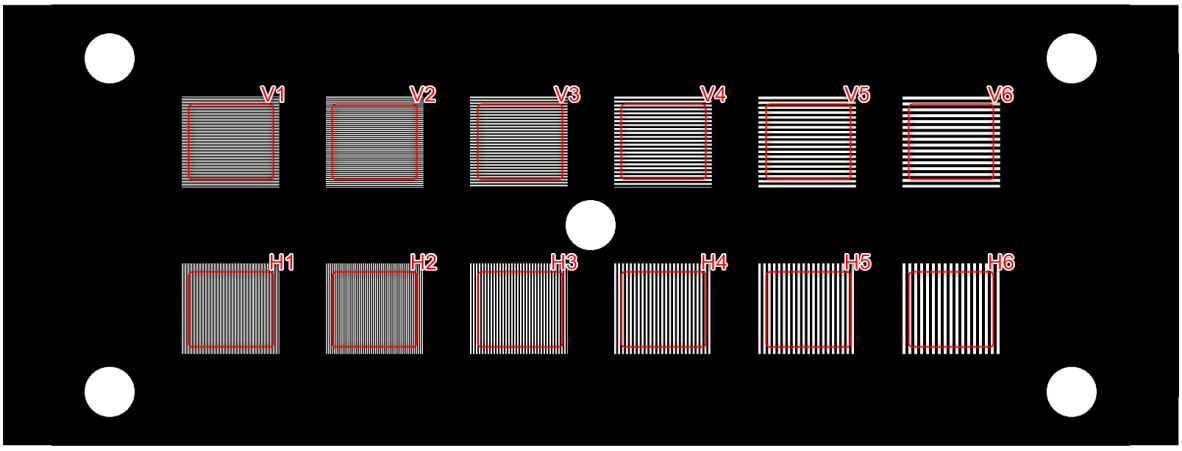

Figure 30-Alignment image generated to adjust the display position.

This image is generated in the imaging photometer software and after that, the generated image should be displayed. To align the display and the camera, the dialog page “Orientation” shows the geometric parameters between the two objects. After starting the measurement, the geometric values like x and y orientation will change according to the relative position of the display and the camera. In order to get good results, all the yellow marked parameters should turn green, indicating that the setup is according expectation. The next step is to focus the camera. Here we are interested in the Modulation value of H4. According to the above-mentioned norm, the image should be slightly defocused and the modulation should be between 50% and 90% in order to avoid Moiré effect while maintaining a good resolution. Then the lens is fixed. Finally, it is important to set the focus factor into Labsoft [25] to the current physical setting of the lens. The align and focus steps will determine the working distance for the setup.

The following flowchart, Figure 31, describes the steps from the generation of Figure 30 to the focus factor correction.

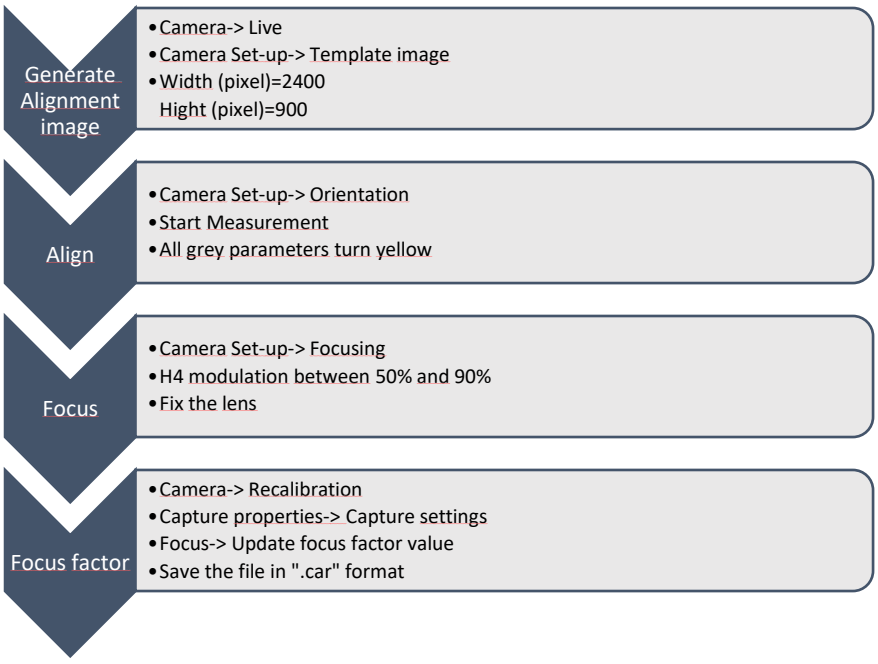

Figure 31-Software steps to alignment and focus definition.

7.5.1.2. Statistics

The next step is to define the type of statistics that we want to apply to our measurement. For that, the procedure presented in Figure 32 was followed. The border and filter sizes were calculated according to the norm V1.30. [25]

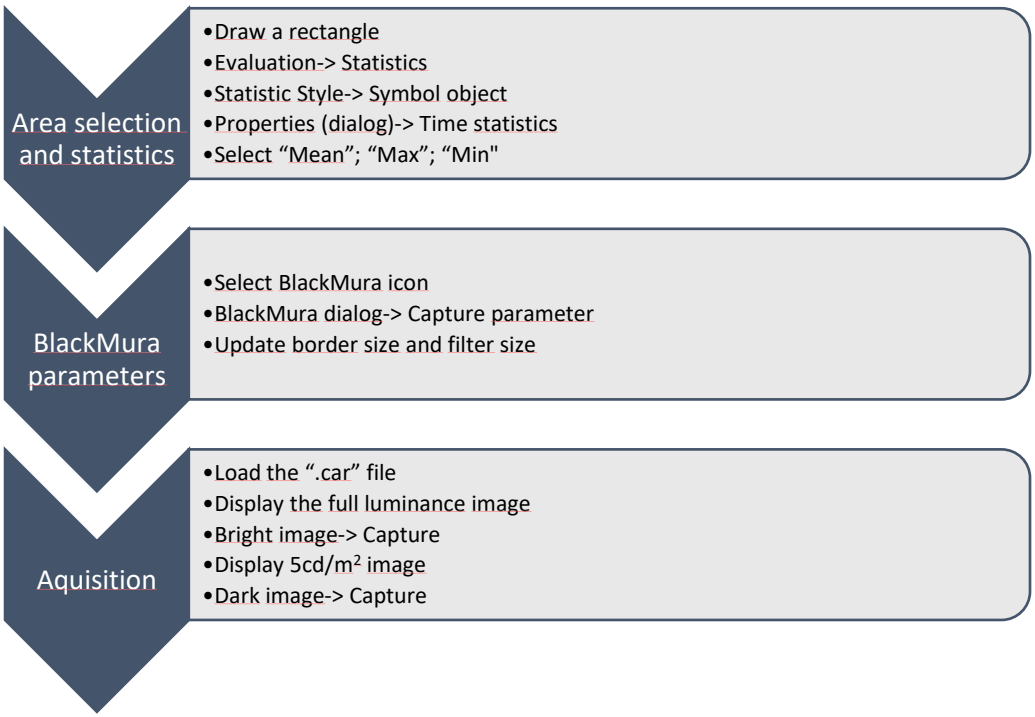

Figure 32-Software steps to define the applied statistics to the acquired images.

$$Display\ pixels\ for\ averaging = \frac{Ndel * Pl}{Pixel\ Pitch} \qquad \textit{Equation 7. 4}$$

$$Border\ size = Filter\ size = Reproduction\ scale \times Display\ pixel\ for\ averaging \qquad \textit{Equation 7. 5}$$

Where N_{del} is the legacy display pixels for averaging, which is 11, Pl is 0,204 and represents the legacy pixel pitch. In the Focus step from Figure 31 the reproduction scale and the modulation values were defined. The obtained value for reproduction scale was 2,58 and the modulation was set at 84% for H4. The pixel pitch is defined by the manufacturer of the display and is 0,1218. This number represents the distance between the center of two adjacent pixels.

The border and filter size values must be the next odd number from the calculated value.

$$Display\ pixels\ for\ averaging = \frac{Ndel * Pl}{Pixel\ Pitch} = \frac{(11 * 0{,}204)}{0{,}1218} = 18{,}4236 \qquad \textit{Equation 7. 6}$$

$$\begin{aligned} Border\ size &= Filter\ size \\ &= Reproduction\ scale \times Display\ pixel\ for\ averaging \\ &= 2{,}58 * 18{,}4236 = 47{,}53 \rightarrow 49\ (Next\ odd\ number) \end{aligned} \qquad \textit{Equation 7. 7}$$

Since we were interested in measuring the uniformity for full luminance and low dimming images, we used both full luminance white, red, green and blue images as well as ones with approximately 5cd/m^2 luminance. For white, the full luminance image, with digital number (255,255,255) was causing the saturation of the measurement equipment due to the need of having a minimum integration time higher than the period defined by the 60Hz refresh rate, which without a neutral density filter could compromise the experiment. Therefore, a reduction of the digital number was performed and a new white image, with digital number (200,200,200) was compiled and displayed, solving the saturation problem. The other images had digital numbers according to the information on Table 3.

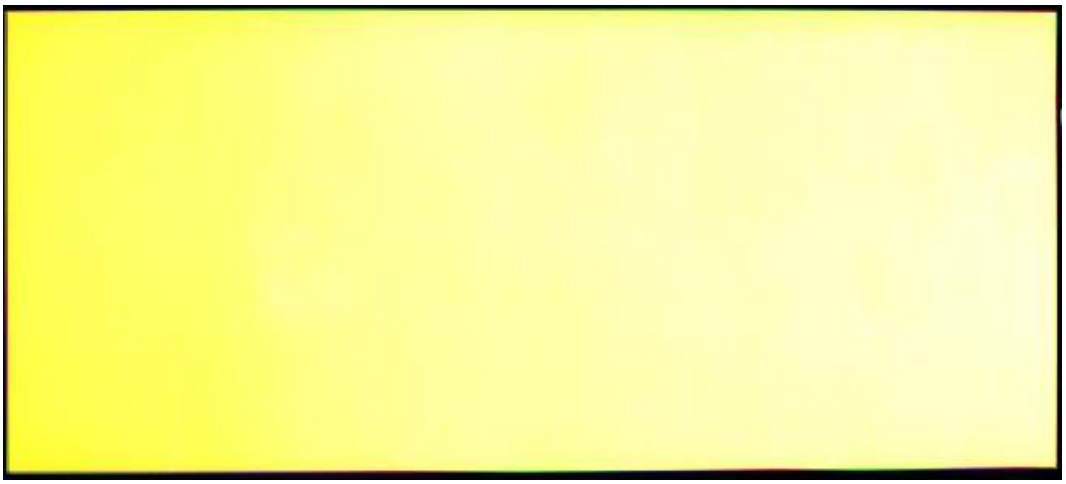

Figure 33 -Captured white image from which the uniformity value is calculated.

Table 10 shows the results from the uniformity evaluation with the photometer. The presented values were acquired after a 30 minute heating period of the display. The overall results were very good. The required values for uniformity were higher than 80% for full luminance images and higher than 60% for low dimming images. These values were achieved for white, red and

green, but one can see that for full luminance blue the uniformity value is smaller when compared with the other colors. The uniformity value in this case stays just under the limit of acceptance.

Table 10-Uniformity values measured with the imaging photometer with a 30 Megapixel resolution and a 50mm lens.

		UNIFORMITY (%)
FULL LUMINANCE	White	85,85
	Red	85,81
	Green	84,47
	Blue	79,88
GREY	White	83,57
	Red	89,23
	Green	87,11
	Blue	81,90

Regarding capability, as was already mentioned, the tolerance values for full luminance images was 20% since the minimum required uniformity value is 80%. In the case of low dimming images, a 40% tolerance value was established since the minimum admitted uniformity value is 60%. With this information, the capability factor C_g was calculated and from the tables below, one can conclude that the measured values were good and stable since all C_gs are greater than 1,33 (except for full luminance Green).

Table 11-Full luminance uniformity measurement capability.

Full luminance	*White*	*Red*	*Green*	*Blue*
Mean value	82,776	86,186	81,979	76,896
Standard deviation	0,334	0,107	0,580	0,048
Tolerance	20	20	20	20
C_g	1,996	6,221	1,150	14,022

Table 12-Low luminance uniformity measurement capability.

Low dimming	*White*	*Red*	*Green*	*Blue*
Mean value	82,593	91,482	85,400	79,872
Standard deviation	0,209	0,085	0,160	0,100
Tolerance	40	40	40	40
C_g	6,371	15,668	8,317	13,307

7.6. Gamma

The CIE 1924 luminous efficiency function, Figure 2 b), describes the spectral sensibility of the human eye to light with different wavelengths. It is a standard function used to convert radiant energy into luminous energy, visible light. [1] From the curve one can see that the red and blue parts of the spectrum are particularly difficult for the human eye to convert and that the sensibility peak occurs at 555nm. It is also known that the human perception of light (brightness) follows an approximate power function, the so-called psychometric function or tone response curve, Figure 4. It is more difficult for humans to perceive changes in higher light levels. This non-linearity of the human eye when converting radiant energy to luminous energy give raise to the gamma factor γ. [1,11,15] If this effect is not considered and somehow corrected, images will have a bandwidth distribution that is not efficient. We would have too much bandwidth for highlights that the human eye can't differentiate and too little bandwidth to shadows that we are sensitive to, effecting the image visual quality. Therefore, it is necessary to correct this effect. The practice of reproducing images gamma compressed is performed so that human perception discounts that effect.

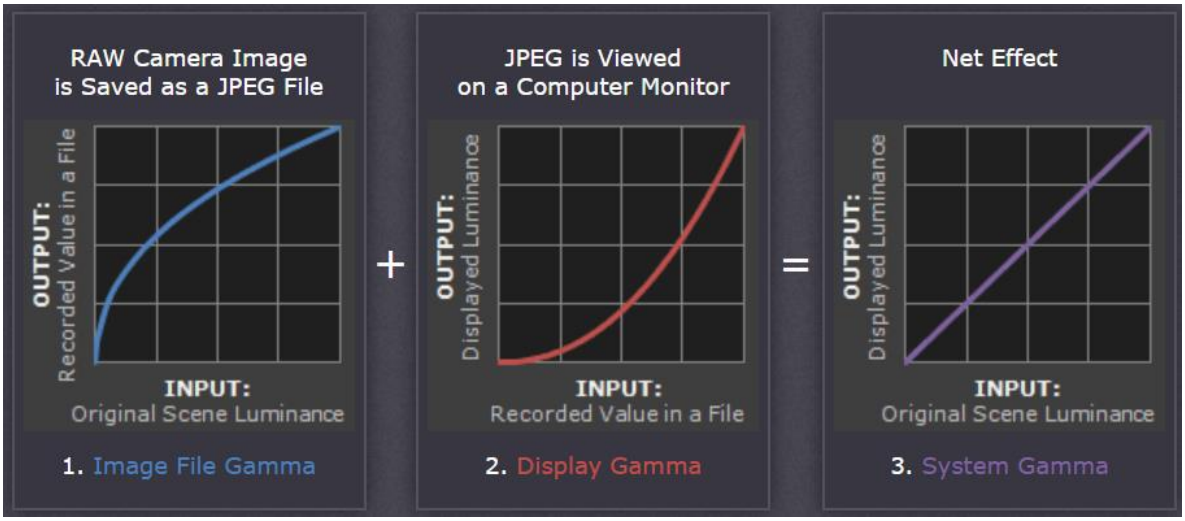

Figure 34-Gamma encoding and decoding of a digital image. Adapted from [11].

Figure 34 shows a representation of the gamma workflow, encoding and correction of a captured image. The first image (from left to right) shows a gamma encoded image in sRGB color space with a gamma factor of approximately 2,2. The second graph represent the image being reproduced in a display with a gamma value of 1/2,2. The purpose of the display gamma is to

compensate for the gamma value of the original file. The last image shows the net effect of all gamma values combined from the original image to the one that we see. This is also called the "viewing gamma".

The usual and reference value for gamma is 2,2. [1] It was already said that for OLEDs the non-uniformity is subpixel level due to material non-uniformity or TFT driving circuit. Since TFT are thin film transistors, the TFT driving current depend on the threshold voltage. The current-voltage variation (I-V curve) results on different gamma for each subpixel. For that reason, four values of gamma were calculated on this test, one for each of the primary colors and one for white.

This test was performed following the procedure described in [9]. An imaging photometer with 30 megapixels resolution and a 50mm lens was used in this test. Once again, the test was performed after a 30 minute heating period. The working distance was kept at 655mm and the same precautions with alignment, Moiré effect, and resolution were taken into account.

It is possible to calculate the gamma value showing one image at the time, with a certain digital number, but with the Manhattan Gamma images it is possible to calculate this value with only three images, the two shown in Figure 36, and other completely black. This is an optimized way to perform the test. Equation 7.8 is a standard commonly used in industry to calculate the local gamma value for several digital numbers. One can see that three images are necessary to calculate the gamma value with this method instead of 36 if we evaluated each digital number individually.

However, since OLED is a self-emissive device, when the digital number of the image is 0, the luminance value is also 0, so here, and contrasting with LCD technology, instead of using an image with digital number equal to 0, we use an image with a low luminance value and digital number 8. Besides the two already mentioned images, the white one and the low luminance one, another is necessary, the one with the gradient pattern with 36 different digital numbers, Figure 35. The displayed images for this test are shown in Figure 36.

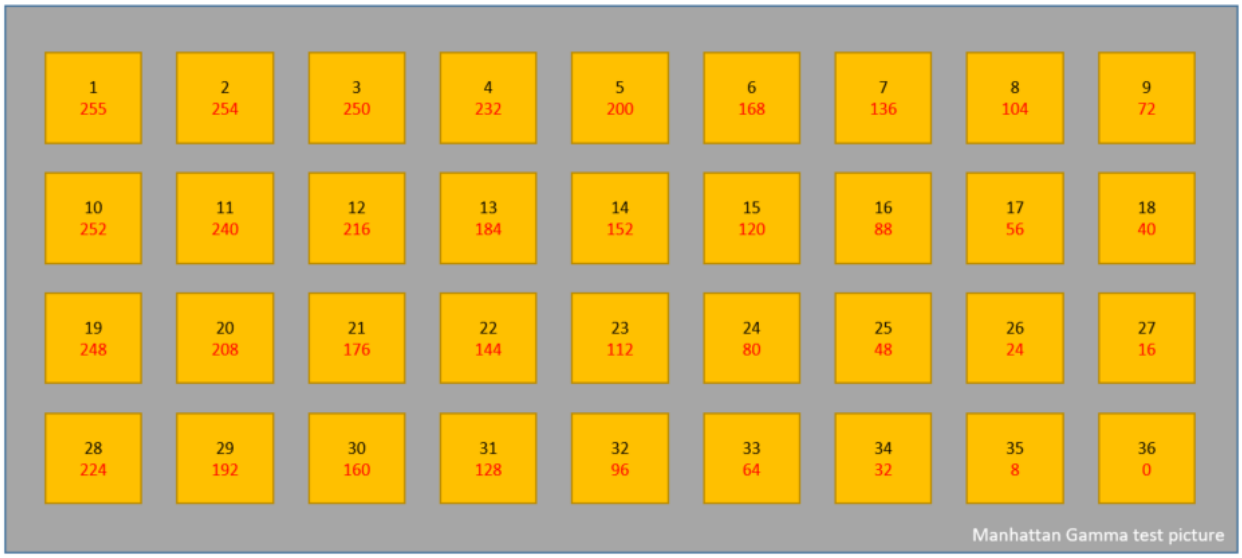

Figure 35-Manhattan Gamma gradient test picture.

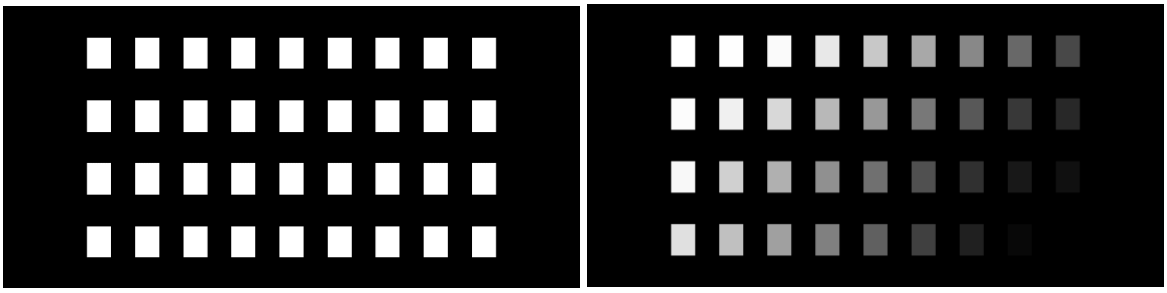

Figure 36-Manhattan gamma reference images for White.

To calculate the gamma value for each of the digital numbers we use the following equation, Equation 7.8. $Grey_n$ is the luminance value of the square with digital number n from the gradient image and $GreyLevel_n$ is the digital number we are considering. The $Black_n$ and $White_n$ values usually stand for the minimum and maximum luminance values from the White and Black images respectively. In the OLED case, as already mentioned, the black luminance is 0 since the device is self-emissive.

$$Gamma_n = \frac{Log\left(\frac{Grey_n - Black_n}{White_n - Black_n}\right)}{Log\left(\frac{GreyLevel_n}{255}\right)} \qquad \textit{Equation 7.8}$$

When measuring the three images for each of the four colors, the three primaries and white, we notice a couple of curious facts. The sum of the red, green and blue luminance values from the gradient image matched the luminance value for the white gradient image. Until now, the tests performed showed that the additivity principle was not verified. Besides that, we noticed that the

sum of the RGB luminance values when the image has all the squares at digital number 255 is higher than the maximum luminance registered for the white image. If we look at the two situations independently, one can say that the first one validates the additivity principle and that the second one does not.

In a first instance, we replace the $Black_n$ luminance value with the one with digital number 8 and the $White_n$ value was the maximum registered luminance value from the image with all squares with digital number 255. Using these values, the gamma values increased significantly as the digital number increased, reaching values close to 6 for example. Since the maximum and minimum reference values are 2 and 2,4, respectively, using this method, our results cannot be considered, Figure 37.

Then, instead of considering the image with DN8, we considered a black image, with digital number 0 and luminance value 0 cd/m^2. Besides that, we also considered the maximum luminance value of the gradient image as the $White_n$ value. Using this method, the gamma values for each DN are mostly within tolerances and the values that are not, are very close, Figure 38. In fact, the white and black images were displayed only to correct possible effects like vignetting. Our system is already calibrated and adjusted in a way to cancel these effects, so it is not critical if we do not use the reference images.

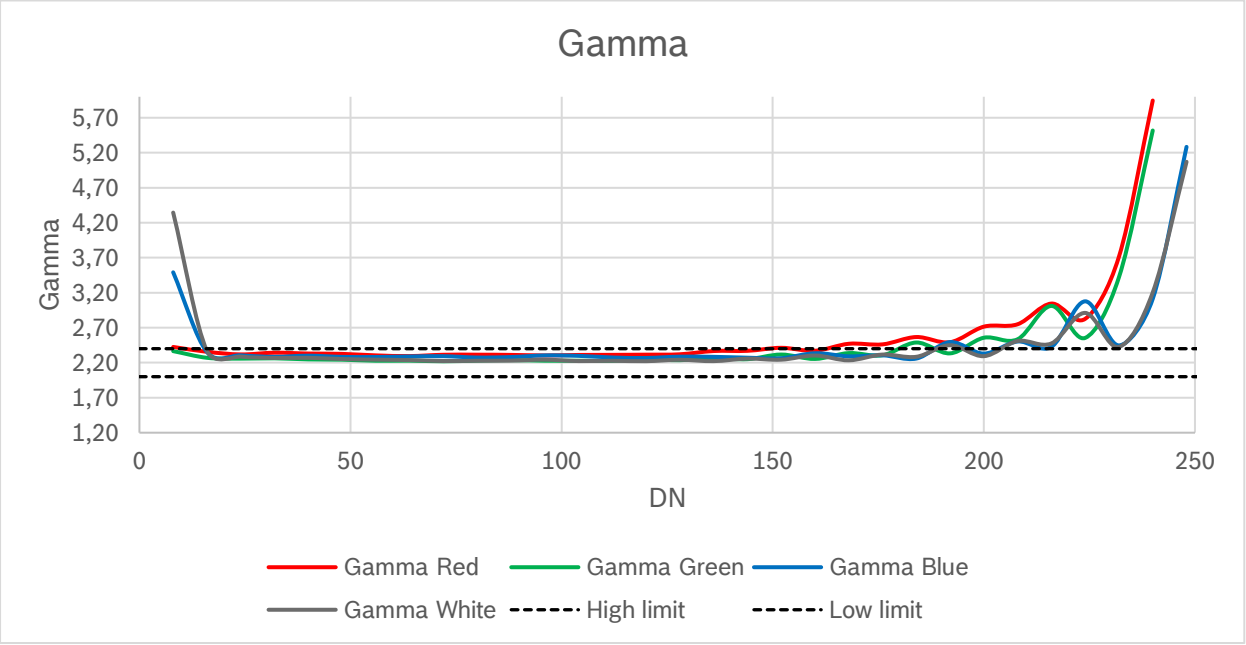

Figure 37-Gamma evolution with DN using the previous method.

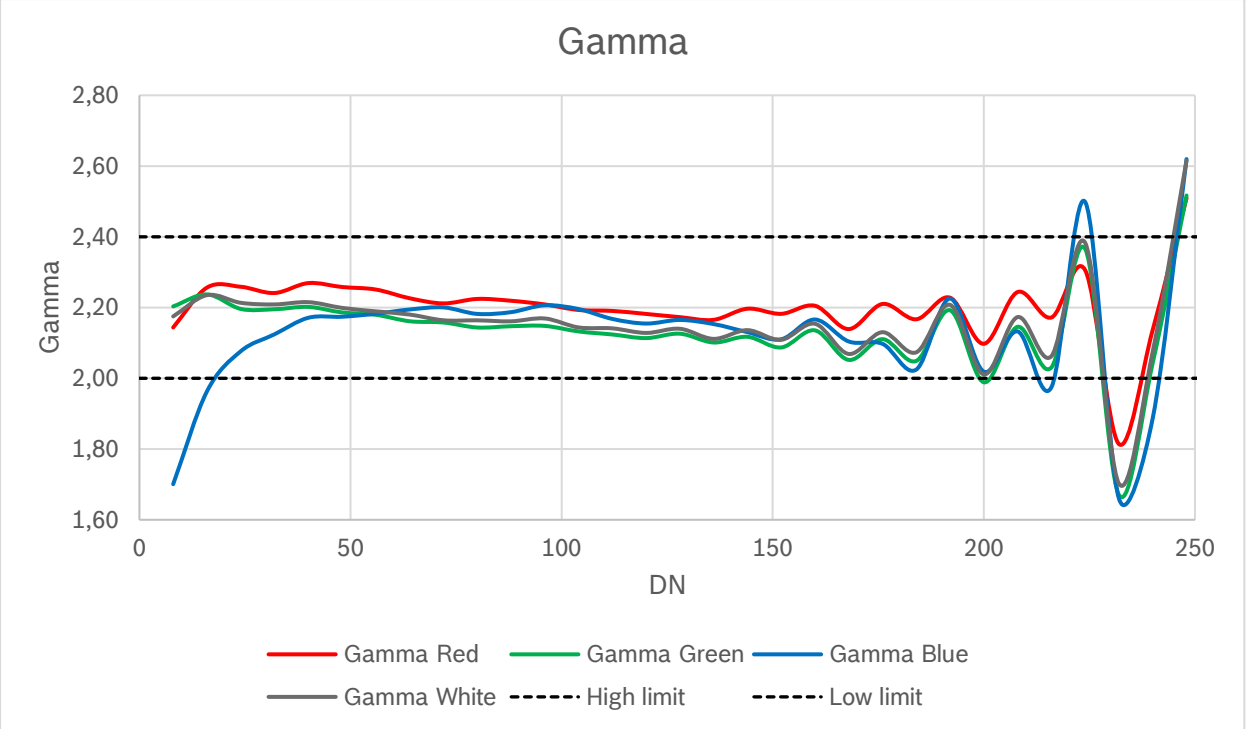

Figure 38- Gamma evolution with DN using the new method.

When comparing the two graphs, Figure 37 and Figure 38 the difference between using the old and the new method to calculate gamma becomes obvious. Although the result has improved, we can still see that for higher digital numbers the gamma values tend to be more dispersed. This problem is probably related with the area of the squares we are considering for our test. Those with higher digital numbers will have an influence on the luminance value of the "direct neighbors". If this happens, the measured values are not the individual luminance value for each square but a sum of it and the contributions of the neighboring ones. One can mitigate this problem reducing the squares size, increasing the distance between them or reducing the number of squares per image.

In addition to the local gamma value for each of the digital numbers, we are also interested in calculating the overall gamma value for each of the four colors. For that, we use the following equation that gives us the slope between the $Grey_n$ luminance value and the normalized luminance value.

$$IDMS_{33} = Slope\left[x() = Log(GreyLevel_n); y() = Log\left(\frac{Grey_n - Black_n}{White_n - Black_n}\right)\right] \quad n = 2, \dots, 33 \qquad \textit{Equation 7. 9}$$

Table 13 show the results for white, red, green and blue. One can see that all values are within the specification except for blue.

Table 13-IDMS33 and mean value for white, red, green and blue.

	IDMS33	MEAN GAMMA
WHITE	2,209	2,156
RED	2,219	2,203
GREEN	2,216	2,137
BLUE	1,930	2,124

7.7. Switching Time

The goal of this test is to determine the amount of time it takes for the display to switch from black to white. In fact, the measured time is the time between 10% and 90% of the signal when switching from one image to the other. This test was performed with two XYZ colorimeters. The only factor that weighed in the choice of the equipment used in the measurement of switching time was the number of samples that the device was able to show per second. Colorimeter 1 can sample 2000 samples per second. Since the response time specification is 10 ms and the device can measure 2000 samples/second it complies with the minimum of 10 samples/second rule, so Colorimeter 1 is expected to be sufficient to perform this measurement. Colorimeter 2 can also sample 22 000 samples per second, following the previous reasoning this is expected to be more than enough to measure our switching time. We used both and compared the results.

This test is totally performed with a dedicated software (RTMS), that synchronizes the image displaying with the measurement. This is achieved by showing a black image followed by a white one, while sampling, and detecting the point in time when the signal reaches 10% and 90% of the steady state level. Afterwards, switching time is calculated as the time difference between 10% and 90% of the signal. The setup for this test is constituted by the colorimeters that were placed a couple of centimeters from the display.

The standard conditions of the dedicated software were adjusted for Colorimeter 2 but not for Colorimeter 1, so some adaptations had to be made in order to avoid over-saturation of the measurements. The “Autorange” was disabled and gain was set on 3.

Figure 39 shows the switching time curves, both for Colorimeter 1 and Colorimeter 2.

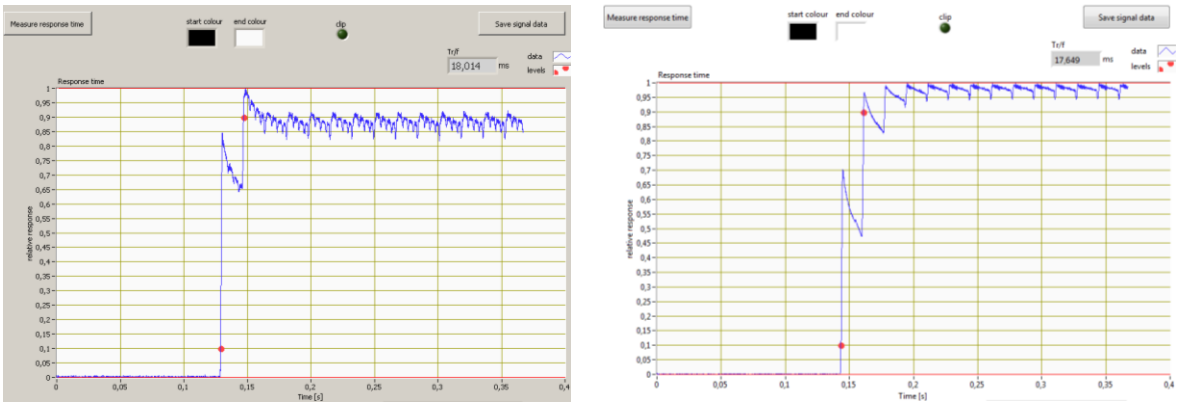

Figure 39-Response Time measurement with Colorimeter 1 (left) and Colorimeter 2 (right).

Both instruments gave us similar results, around 18ms, which was expected since there is no difference between them, apart from accuracy. Something we were not expecting was the 60 Hz sawtooth signal. Since this is the refresh rate of the display, this is most probably a product characteristic related to the deriving scheme. Our sample is an AMOLED and as referred in PMOLED and AMOLED working principle, each pixel is individually excited and the TFT responsible for that has a storage capacitor that conserves the excited state of the OLED. When another pixel is excited, the previous one stays on due to the capacitor. The current leakage of the capacitor originates the sawtooth wave shape.

Lastly, we confirmed the switching time by measuring it with a photodiode and an oscilloscope, Figure 40. The result was quite different, but the Colorimeter 2 and Colorimeter 1 measurements are more accurate and those devices were specially designed and projected to perform this kind of test. Therefore, the test with the photodiode was important to confirm the order of magnitude of the result and not to accurately measure the switching time.

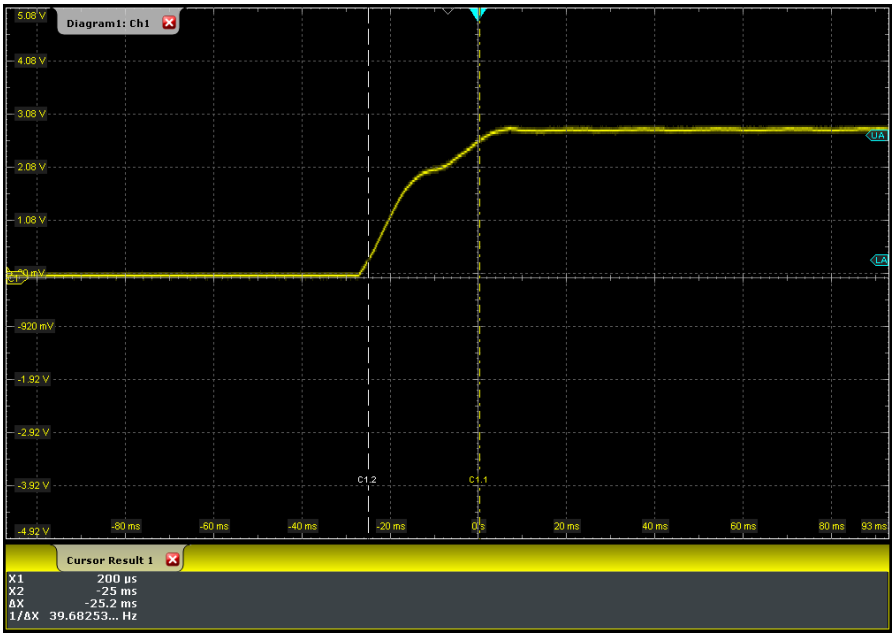

Figure 40-Switching time measurement using an oscilloscope and a photodiode.

In order to compare the two technologies, LCD and OLED, the same test was performed for a LCD. For the same test and conditions, the obtained value was smaller for the LCD. The conclusion is that LCDs are faster in the black to white transition. The response time for LCD was 14,36ms with Colorimeter 1 and 16,74ms with Colorimeter 2.

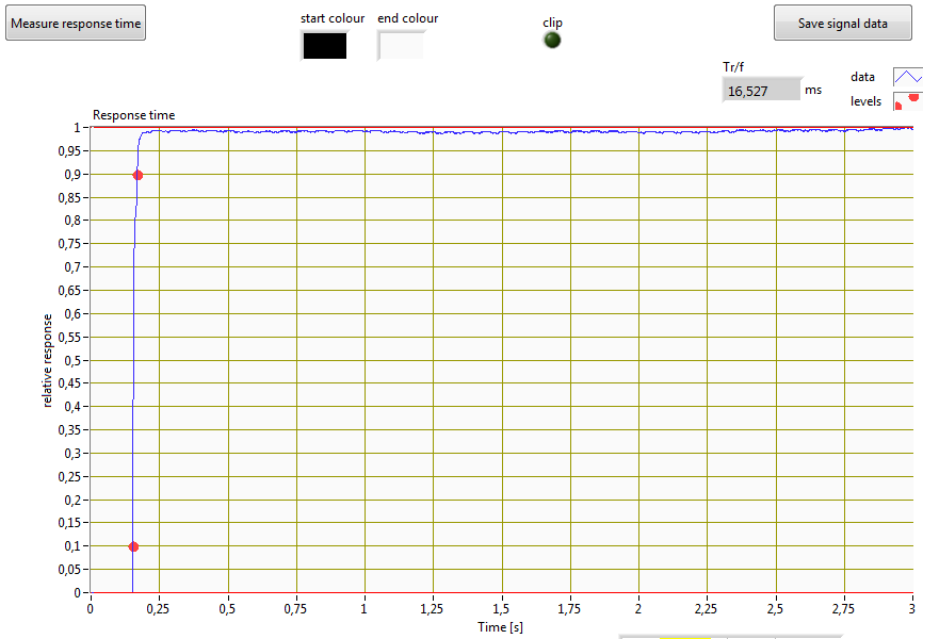

Figure 41- Response Time measurement for LCD with Colorimeter1.

Even though the switching time curves look different for the two technologies, the resultant switching time is very similar, 18 ms for OLED and 17 ms for LCD.

In terms of capability, the accomplished C_g value for this measurement is 86,93.

8. OLED characterization as a function of the temperature

This characterization was performed to assess the necessary heating time for the OLED display to stabilize its temperature dependent optical characteristics and the temperature itself.

Physical characteristics like luminance, color coordinates, uniformity, switching time and gamma will dictate the time that is necessary for the sample to heat before performing any test.

8.1. Luminance

In this test, the major goal was to see the evolution of the luminance values both for the three primary colors and for white as well as the thermal evolution of the display as a function of time and of the displayed color. Besides the previously mentioned spectroradiometer, a pyrometer was also used, Figure 15. A pyrometer is a thermometer used to measure temperature of distant objects. The working distance for this test was 665mm.

Again, eight images with digital numbers according to Table 3 were compiled and displayed, except for full white. Since this test was performed along with other tests using the imaging photometer, the full white digital number was (200,200,200) to avoid the saturation of the camera.

The spectroradiometer was set to acquire the luminance value every 30 seconds for 30 minutes. The pyrometer, on the other hand, acquired values every 2 seconds for 30 minutes.

Here we are going to present the results for white, the other results can be found in Appendix C- Luminance and temperature evolution over time.

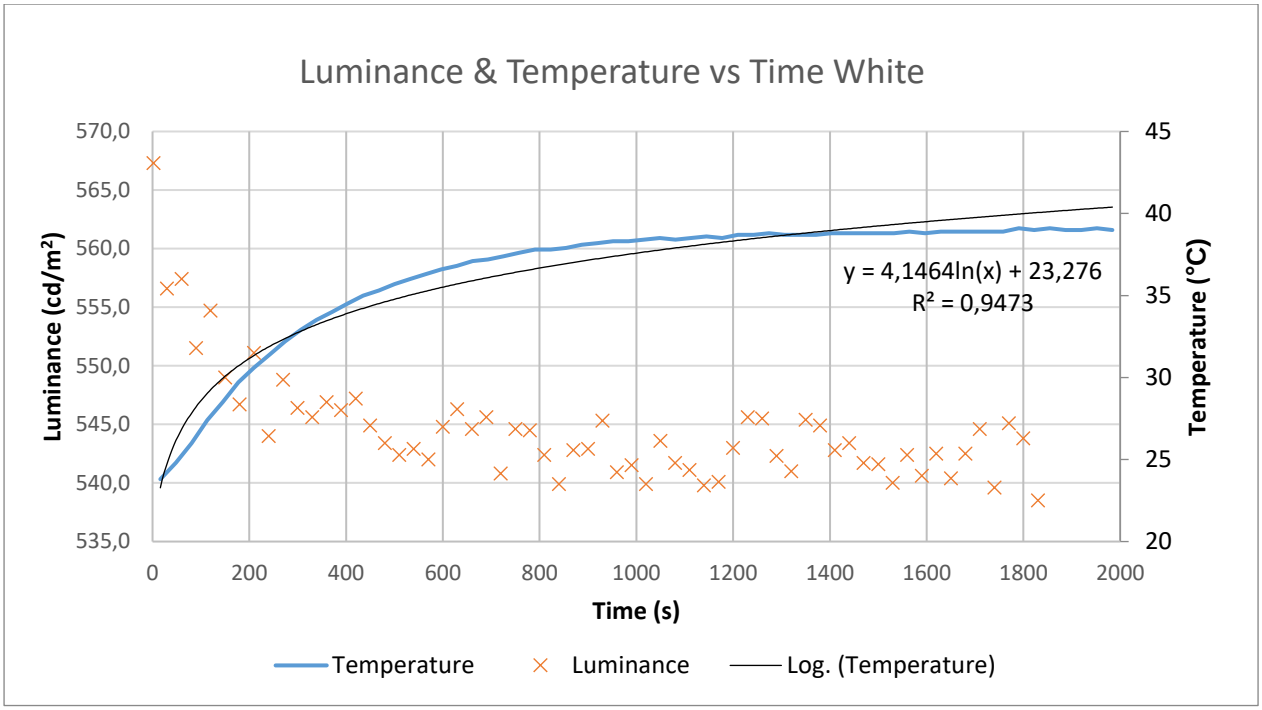

Figure 42-Lumiance and Temperature variation over 30 minutes for a high dimming image.

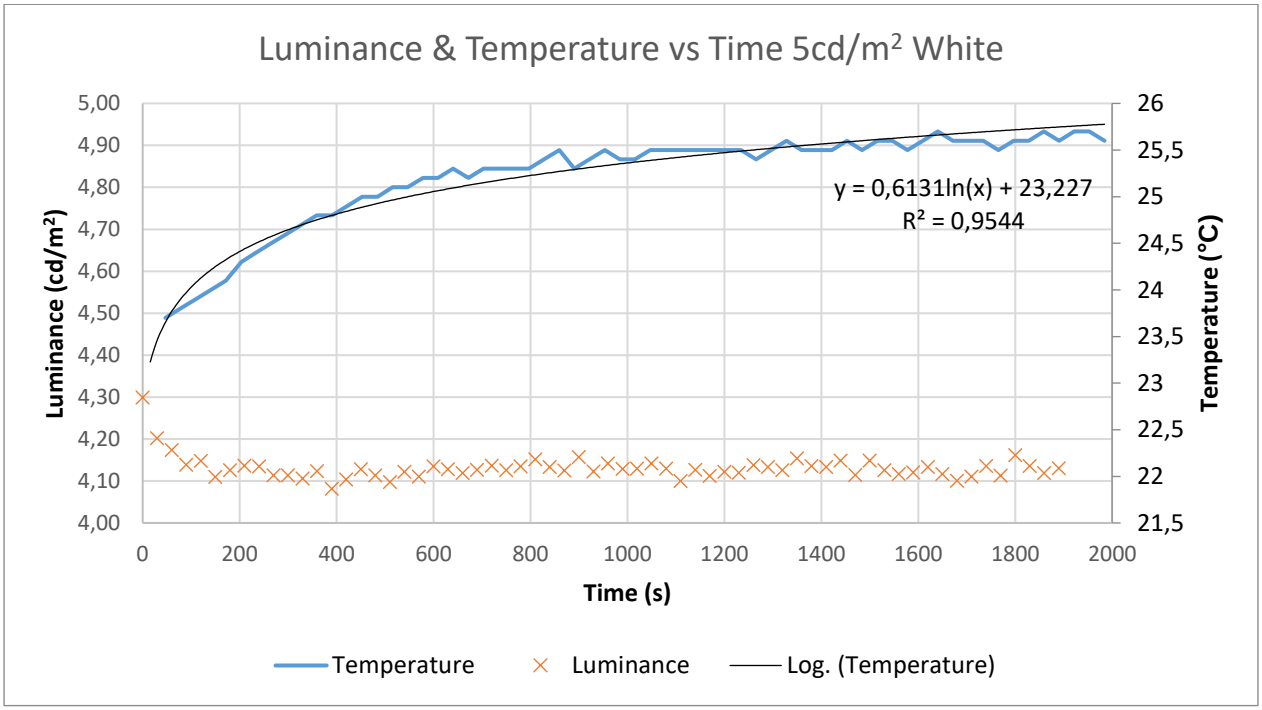

Figure 43-Lumiance and Temperature variation over 30 minutes for a low dimming image.

When evaluating the results for high luminance values, one can see from Table 14 that the major luminance variation was for white and green, they have variations in the order of 5% and 4%

respectively. The red and blue had lost about 3% of their initial luminance. From Figure 42 and Figure 43 one can see that in the first few minutes luminance tends to decrease its value. After approximately 10 minutes, for full luminance white, the luminance stabilizes. This stabilization time is smaller for the low dimming white. This test will determine the necessary time to preheat the display before performing any measurement.

Table 14-Experimental luminance values for full luminance images.

LUMINANCE (cd/m^2)	MAX	MIN	DELTA	MEAN	% LOSS
WHITE	567,30	539,60	27,70	544,71	4,89
RED	217,00	211,00	6,00	213,31	2,76
GREEN	660,60	633,00	27,60	640,68	4,18
BLUE	79,75	77,68	2,07	78,73	2,60

When it comes to the temperature variation, as expected, due to the driving system and due to the fact that, for white, all the three subpixels are on, the white color was the one that when displayed caused the major temperature variation corresponding to a higher steady state temperature, Table 15. This test also showed that blue and white are the most power consuming colors, followed by green and red. This test, that showed that the blue color was the one with higher power consumption, is justified by the fact that the blue subpixel is bigger than the others. The higher driven energy will stress the subpixel decreasing its lifetime, and to compensate this, the blue subpixel is bigger. Due to this fact, the power consumption is also higher. The temperature monitorization also showed that the temperature stabilizes after a certain time both for high and low dimming images.

Table 15-Experimental temperature value for full luminance images.

TEMPERATURE (°C)	MAX	MIN	DELTA	MEAN
WHITE	39,10	23,80	15,30	36,31
RED	30,10	22,70	7,40	28,56
GREEN	33,70	22,80	10,90	31,55
BLUE	35,60	23,20	12,40	33,32

For the low dimming images, there were no major variations in the luminance values, Table 16, or temperature, Table 17. As expected, the steady state temperature (maximum) is smaller when compared to the one registered when displaying the full luminance images, due to less power

consumption. On the other hand, the percentual loss of luminance is greater for lower luminance values.

Table 16-Experimental luminance values for low dimming images.

LUMINANCE (cd/m^2)	MAX	MIN	DELTA	MEAN	% LOSS
WHITE	4,30	4,08	0,22	4,13	5,12
RED	5,08	4,69	0,39	4,72	7,68
GREEN	4,80	4,63	0,17	4,66	3,54
BLUE	5,29	5,02	0,27	5,12	5,10

Table 17-Experimental temperature value for low dimming images.

TEMPERATURE (°C)	MAX	MIN	DELTA	MEAN
WHITE	25,70	23,70	2,00	25,18
RED	25,00	22,70	2,30	24,39
GREEN	25,20	23,10	2,10	24,61
BLUE	26,00	22,90	3,10	25,26

8.2. Color coordinates

After checking the luminance variation over time, we are now interested in evaluating the color coordinates variation as a function of time and temperature. For that we use the above-mentioned spectroradiometer, that also provides information about color coordinates, x and y. Here the same method and setup used to assess luminance was used.

The x and y chromaticities represent color information, independent of the overall luminance, and therefore should correlate with the stimulus hue and chromatic intensity. If the display is stable, no major variations are expected.

In regard to temperature, the variations are those already described in Table 15. As for the coordinates, we can see that there are some fluctuations for both x and y, Figure 44. However, we cannot say that this variation has a linearity relationship with the temperature variation. In addition, these variations can be accepted if the coordinate's values fall within the limits imposed by the specification's tolerances.

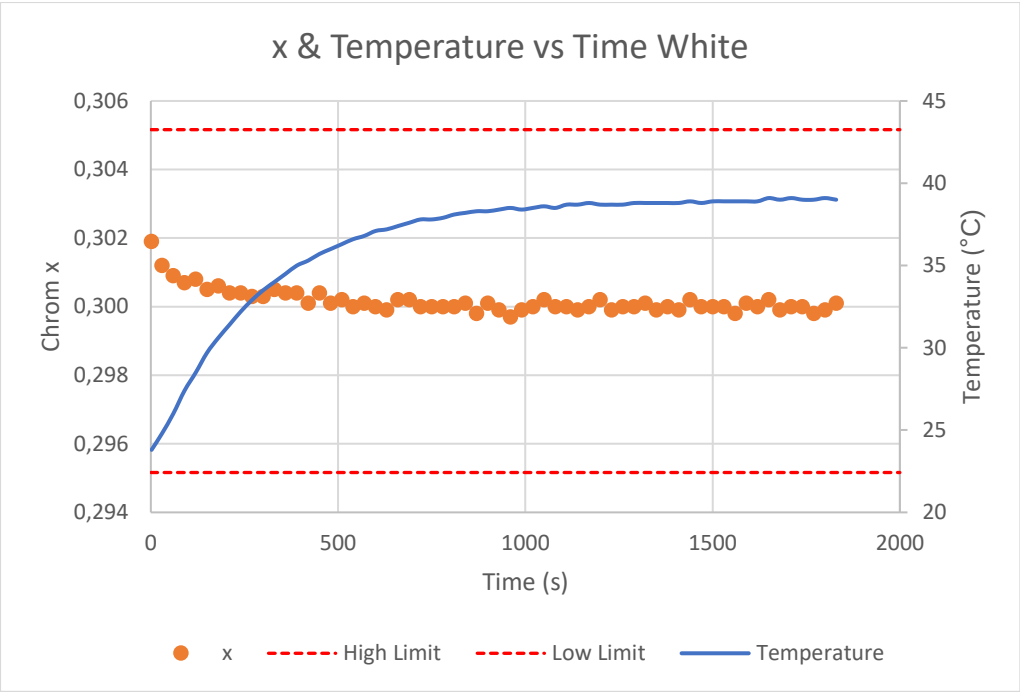

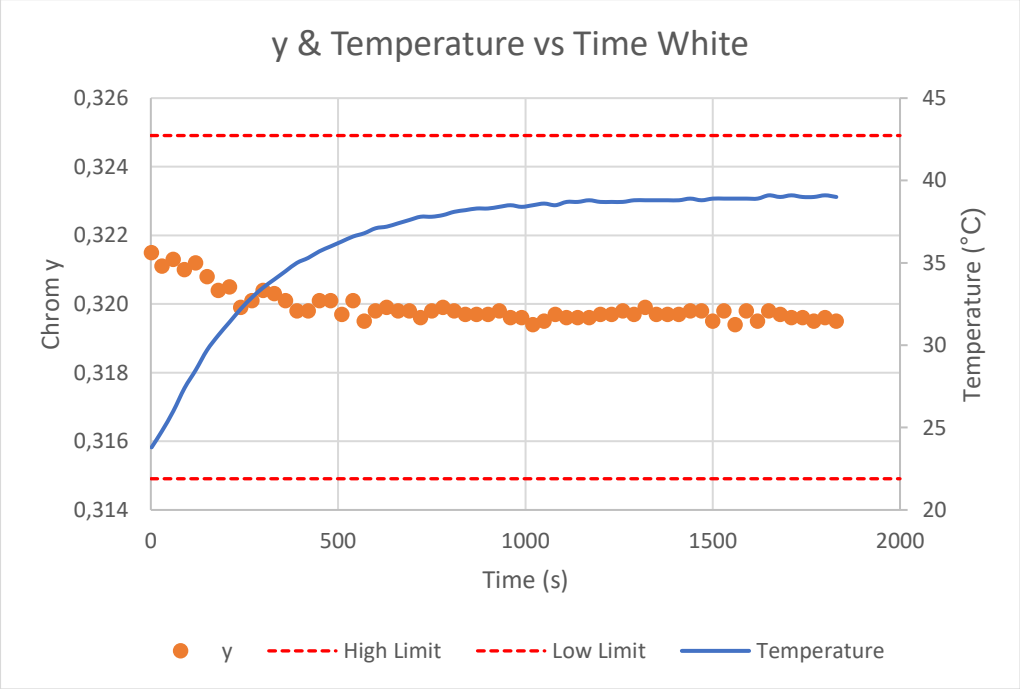

Figure 44- x and y coordinates over 30 minutes.

The behavior of the x and y coordinates is not linear or equal for the four colors. The values can be very dispersed, the data on Appendix D- Color coordinates and temperature evolution over time, shows that behavior.

8.3. *Uniformity*

To trace the uniformity evolution over time, the same steps performed in Chapter 7.5 were followed. This time, we only use the photometer. The results were very stable over time and no major variations were detected. Once again, the uniformity value for full luminance blue were the only ones a little bit smaller than what was expected.

Figure 45 shows the result for both full luminance and low dimming white. As expected, the temperature variation was much higher for full luminance white. On the other hand, the uniformity value for low dimming white varies more. This was also expected since it is more difficult to control the luminance values across the display when its value is smaller, and this originates more fluctuations over uniformity values.

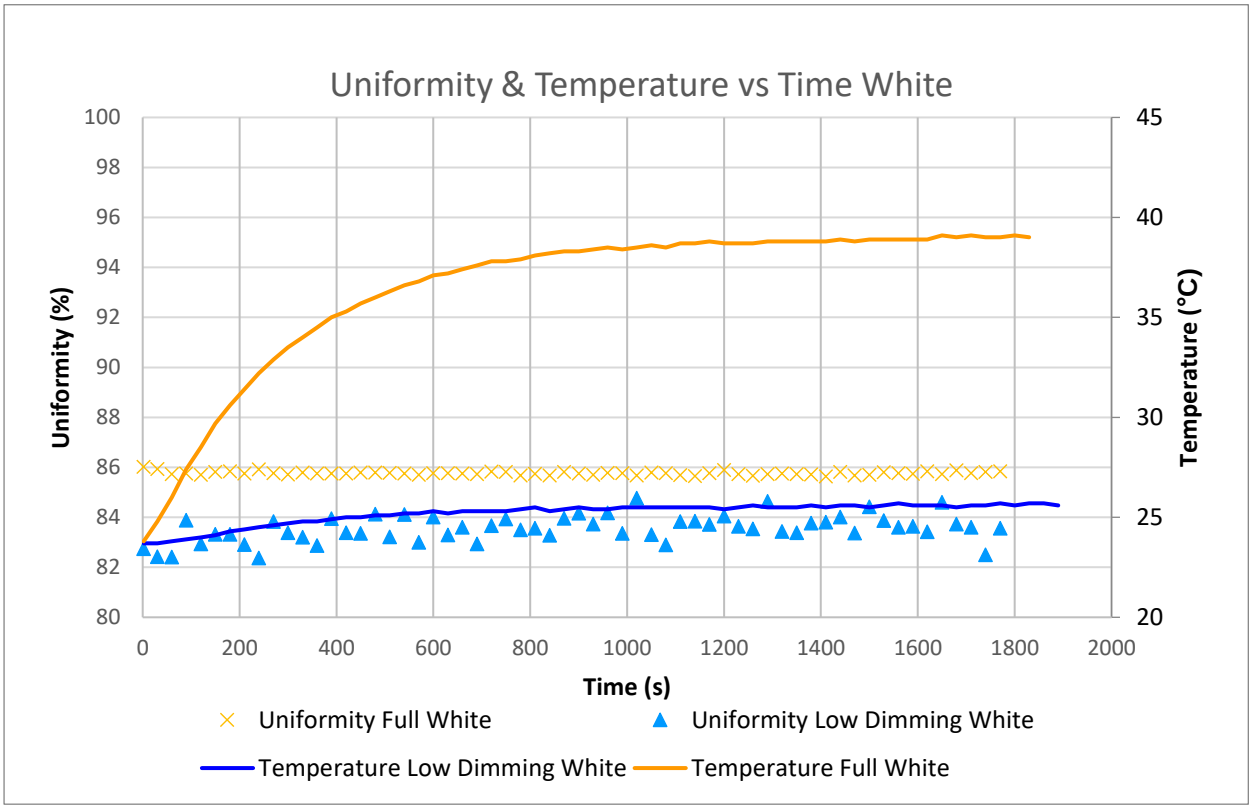

Figure 45-Uniformity and temperature evolution over time for full luminance white and for low dimming white.

8.4. Gamma

The Manhattan Gamma and IDMS behavior over time and temperature were evaluated with an imaging photometer and a pyrometer. In both cases, the registered values were stable over time, and therefore one can conclude that this display feature has no dependence on temperature. Figure 46 shows the graphical representation of the Manhattan Gamma measured 60 times over 30 minutes. One can see that the graphs overlap each other, showing that there are no major differences between them. On the other hand, Figure 47 represents the IDMS value, that is calculated considering the gamma value for each of the 255 digital numbers (Equation 7. 9), over time. One can identify some fluctuations over time that are not related to the temperature increase. For the three primary colors the results were pretty similar.

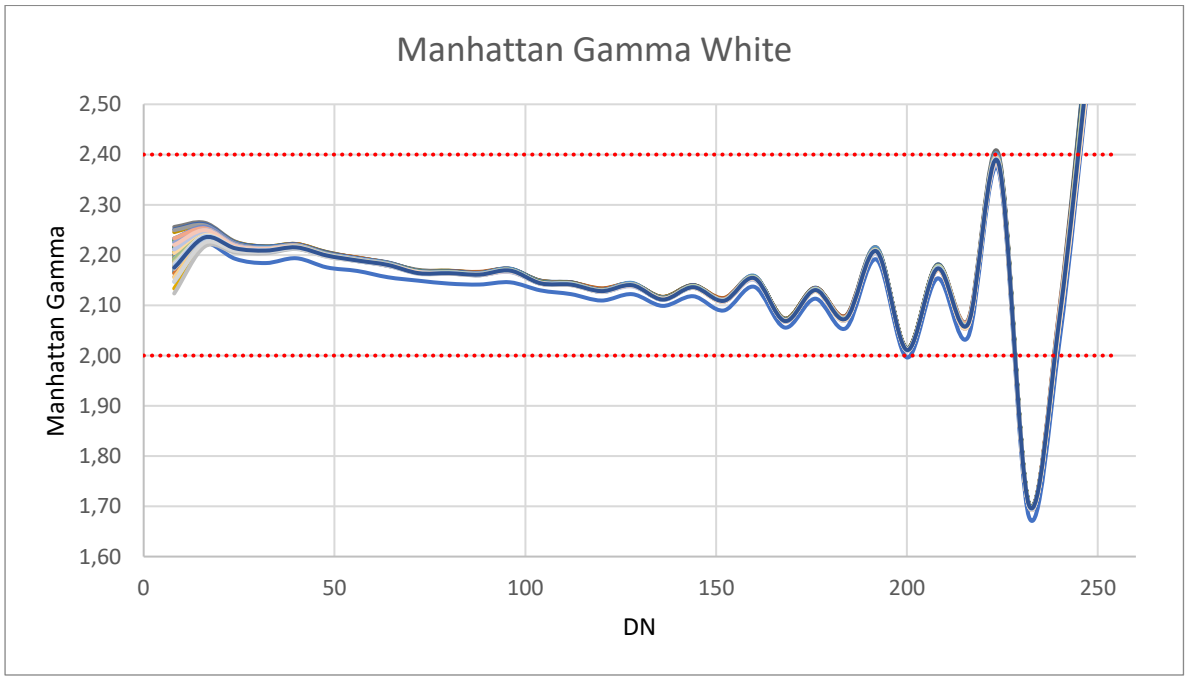

Figure 46-Manhattan Gamma evaluation over time.

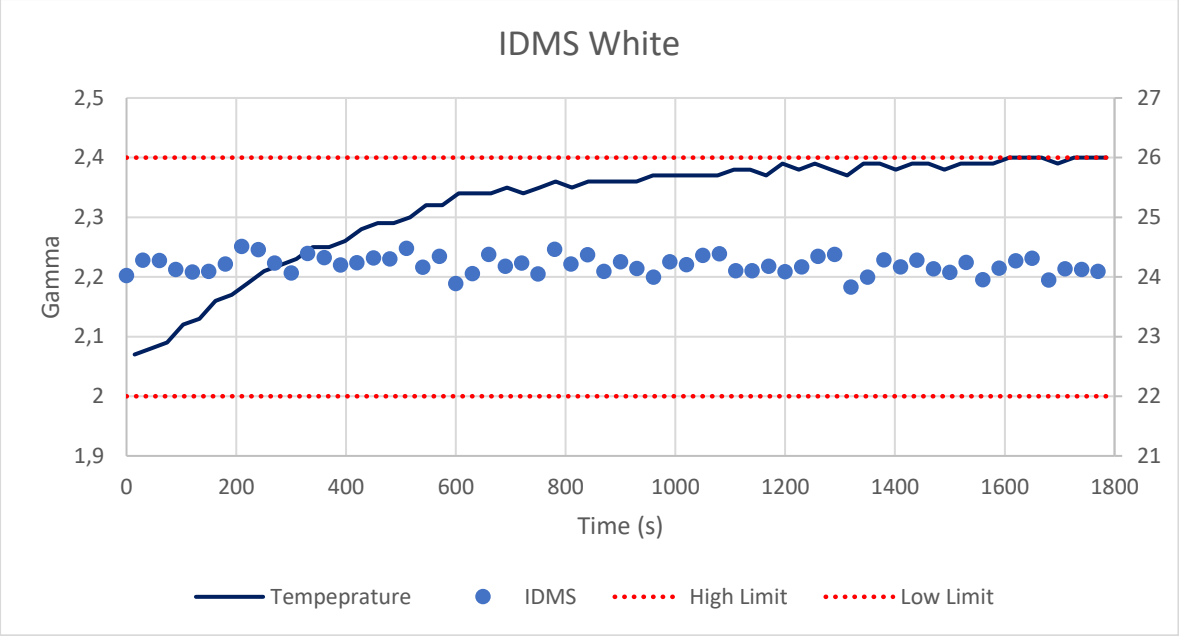

Figure 47-IDMS and temperature evaluation over time.

8.5. Switching Time

The evaluation of temperature and transition time as a function of time was performed using the pyrometer, to trace the temperature over time, and the Colorimeter1, to measure the switching time of the device. The measurement of the switching time was performed manually, by activating the RTMS software each 30 seconds for 30 minutes. The temperature was automatically acquired every 2 seconds for 30 minutes.

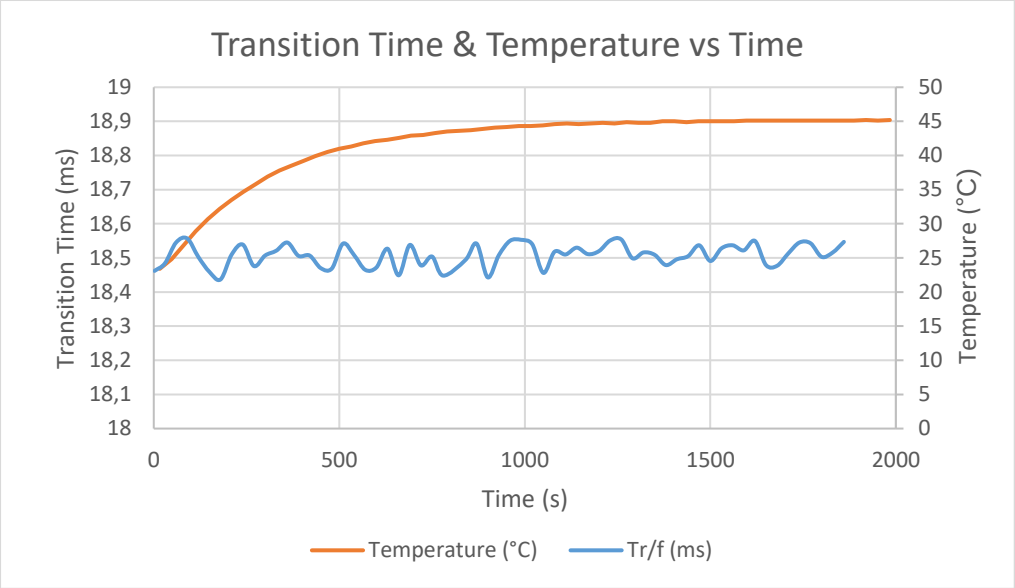

Figure 48-Transition time and temperature evolution over 30 minutes.

Figure 48 shows that there were no major variations of the display switching time over the 30 minutes test. This also means that there is no relation between the heating period of the device and its transition time.

8.6. Run-In

Run-In is defined as the time it takes for the properties of the display to stabilize. Previously, in OLED characterization as a function of the temperature, those properties were analyzed and documented. Physical characteristics like luminance, color coordinates, uniformity and switching time will dictate the time that is necessary for the sample to heat before performing any test. If the tests are performed before that time, the measured values should not be considered.

From Figure 45 and Figure 48 one can see that the uniformity and switching time values do not fluctuate considerably over time. On the other hand, Figure 42, Figure 43 and Figure 44 show that for luminance and color coordinates the heating time is important. It took approximately ten minutes for these features to stabilize and reach a stationary value over time.

When evaluating temperature over time it was also clear that after ten minutes the temperatures of the display was stable.

Therefore, one can say that the run-in time to perform the mentioned tests in the mentioned sample is ten minutes.

9. Conclusion

The main objective of this work was to determine and optimize a suitable test chain for the new automotive OLED displays market based on the preexisting one for LCDs, as well as define the conditions and the adjustments needed to perform the alignment and calibration of the device. The starting point of this work was the human eye and its response to luminous stimulus and also the mathematical basis of colorimetry and light that are behind the working principle of the measurement devices used.

It was also important to refer the main reasons why the transition from LCD to OLED will occur in a medium/short period. Lower power consumptions and response time, larger color gamut and higher contrast as well as the possibility of transparency and flexibility are some of the points that differentiate the two technologies, boosting the transition.

The core part of this work were the experimental tests that were performed. From the first test, in which the luminance values of the display were acquired for different colors with different dimming levels, one can conclude that the luminance for full luminance white is within specifications, and is reproducible, since the C_g value is greater than 1,33. One can also conclude that the display is not “perfectly” additive and this fact can be mitigated using a dimming model that corrects the fact that the sum of the luminance values from red, green and blue is not equal to the luminance value of white.

In terms of color coordinates the registered values are also within tolerance and both x and y capability values are greater than 1,33, which means that the measurement is reproducible.

When measuring the white point adjustment, the display also showed good results. With only one iteration the five tested targets were met.

Regarding uniformity, the results were also very satisfactory, and the specification values were achieved for both full luminance and low luminance values. In terms of capability, only the full green uniformity showed a smaller C_g value than expected.

For Gamma, even with the proposed optimization, the values for each point fluctuated a lot, this means that the test can still be improved in the future.

The switching time test also went as expected and the collected values are according to the specification. The capability factor showed that the measurement is reproducible.

Finally, the dependence of optical features on the temperature was evaluated. From those tests the main conclusion is that after 10 minutes, all the characteristics were stable, including the temperature. This result is very important since it means that in a production line, the device heating time is smaller when compared with the LCD technology.

Overall, the main objectives of this thesis were accomplished and the results of this work can be used in real cases, where it will be necessary to elaborate an OLED dedicated test chain for a production line. There are some aspects yet to be improved, namely ones regarding the Gamma factor and some other tests in order to improve C_g values. Since this is a preliminary study of the automotive OLED devices, there is not a reference value of measurement standard, x_m, and therefore it is not possible to calculate C_{gk}. In the future, with more OLED devices and a golden sample, this value can be properly calculated.

Appendix A-Color coordinates for different DN

	White		Red		Green		Blue	
DN	**x**	**y**	**x**	**y**	**x**	**y**	**x**	**y**
255	0,3050	0,3187	0,6964	0,3032	0,1971	0,7399	0,1364	0,0605
239	0,3052	0,3186	0,6964	0,3033	0,1973	0,7398	0,1365	0,0606
223	0,3048	0,3183	0,6964	0,3034	0,1974	0,7396	0,1366	0,0609
207	0,3045	0,3184	0,6964	0,3033	0,1976	0,7397	0,1362	0,0603
191	0,3044	0,3182	0,6965	0,3033	0,1978	0,7397	0,1363	0,0603
175	0,3045	0,3177	0,6965	0,3032	0,1978	0,7400	0,1365	0,0606
159	0,3044	0,3177	0,6966	0,3032	0,1981	0,7399	0,1365	0,0606
143	0,3053	0,3176	0,6966	0,3031	0,1978	0,7395	0,1364	0,0605
127	0,3045	0,3177	0,6968	0,3030	0,1987	0,7398	0,1366	0,0609
111	0,3073	0,3174	0,6968	0,3030	0,1990	0,7396	0,1365	0,0606
95	0,3083	0,3198	0,6967	0,3030	0,1997	0,7395	0,1366	0,0607
79	0,3098	0,3211	0,6967	0,3030	0,2009	0,7388	0,1370	0,0608
63	0,3153	0,3256	0,6970	0,3027	0,2015	0,7383	0,1373	0,0616
47	0,3183	0,3299	0,697	0,3027	0,2033	0,7372	0,1379	0,0617
31	0,3201	0,3306	0,6961	0,3023	0,2062	0,7353	0,1405	0,0643
15	0,3322	0,3346	0,6912	0,3014	0,2165	0,7278	0,1564	0,0766
0	0,3290	0,2884	0,3709	0,3108	0,3823	0,3236	0,4822	0,3493

Appendix B-Color coordinates capability study

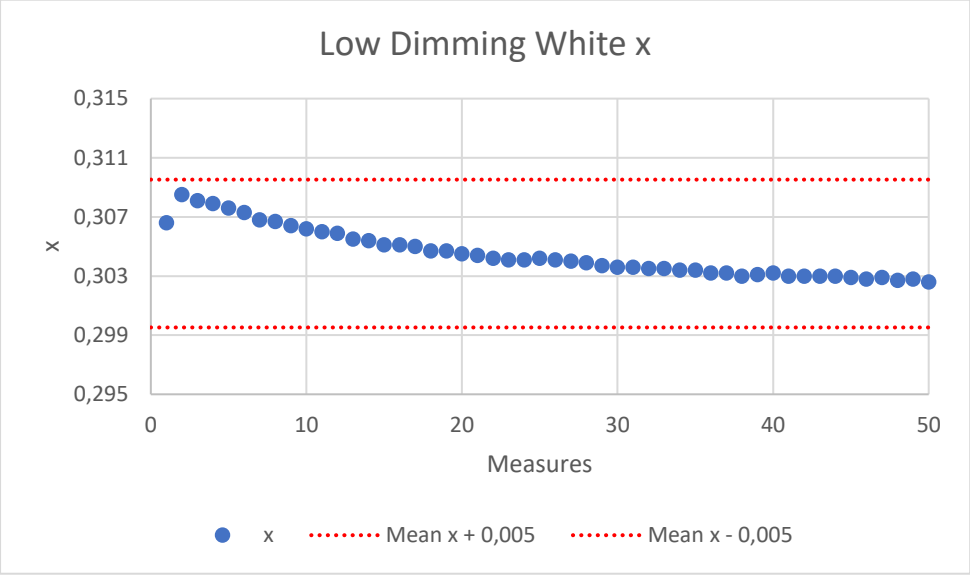

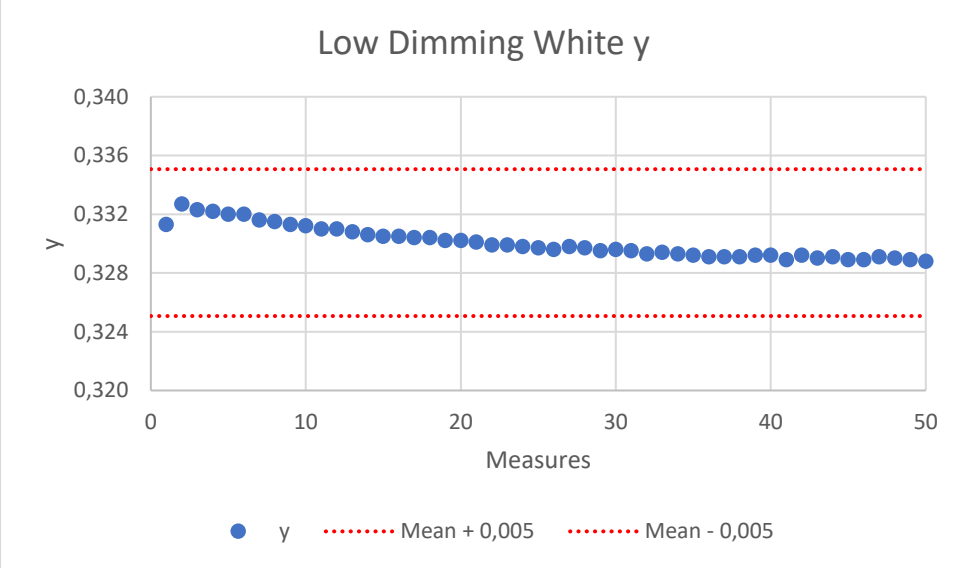

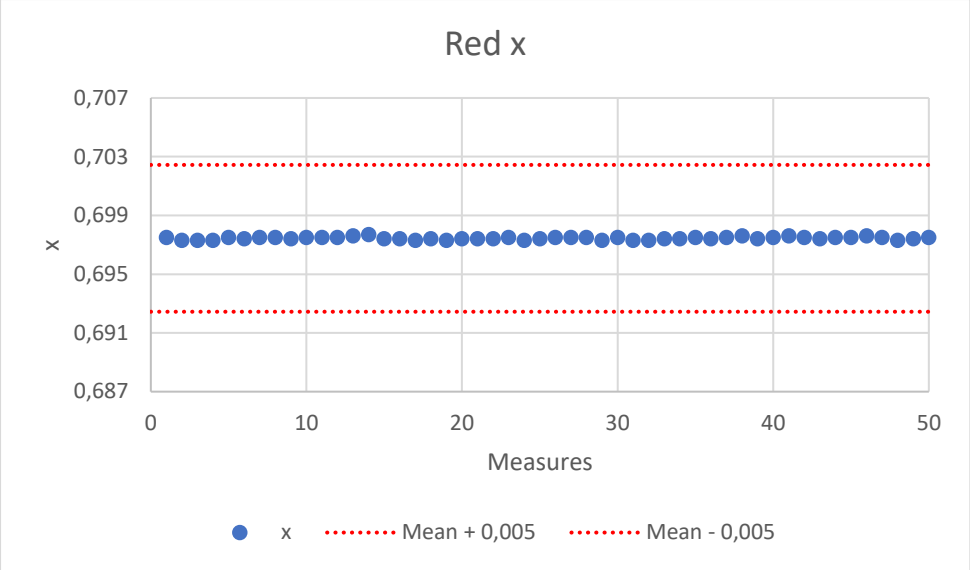
Red x
0,707
0,703
0,699
0,695
0,691
0,687
x
0
10
20
30
40
50
Measures
x
Mean + 0,005
Mean - 0,005

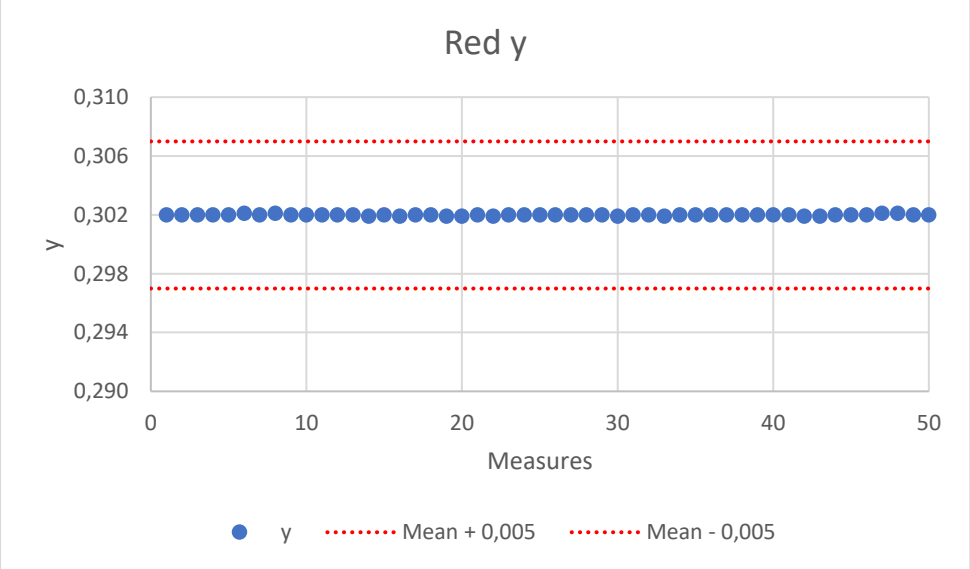
Red y
0,310
0,306
0,302
0,298
0,294
0,290
y
0
10
20
30
40
50
Measures
y
Mean + 0,005
Mean - 0,005

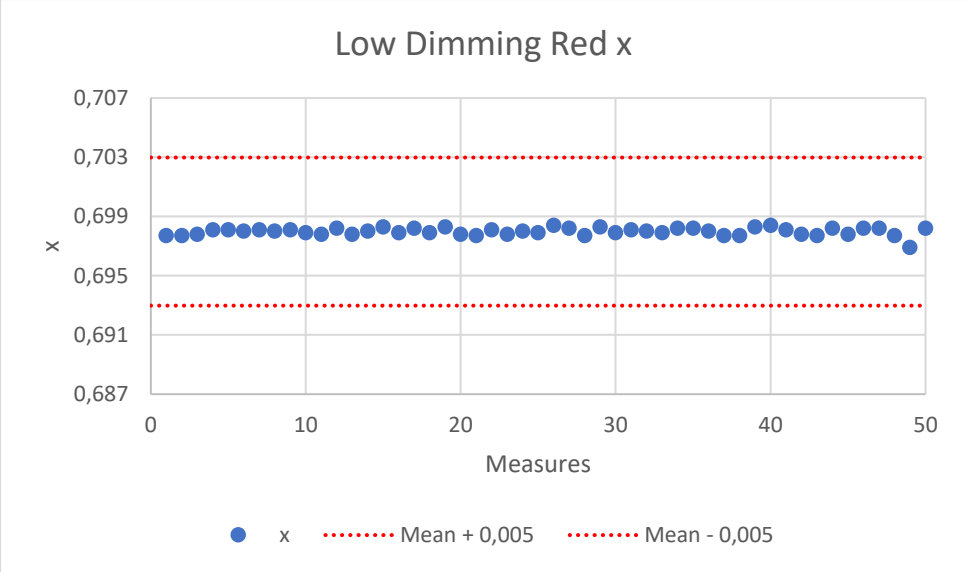
Low Dimming Red x
0,707
0,703
0,699
0,695
0,691
0,687
x
0
10
20
30
40
50
Measures
x
Mean + 0,005
Mean - 0,005

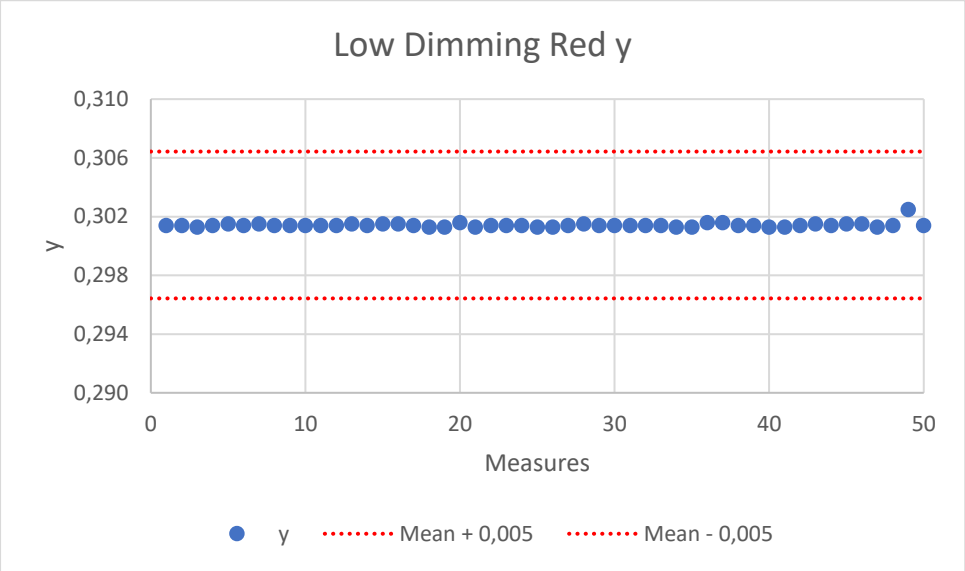
Low Dimming Red y
0,310
0,306
0,302
0,298
0,294
0,290
y
0
10
20
30
40
50
Measures
y
Mean + 0,005
Mean - 0,005

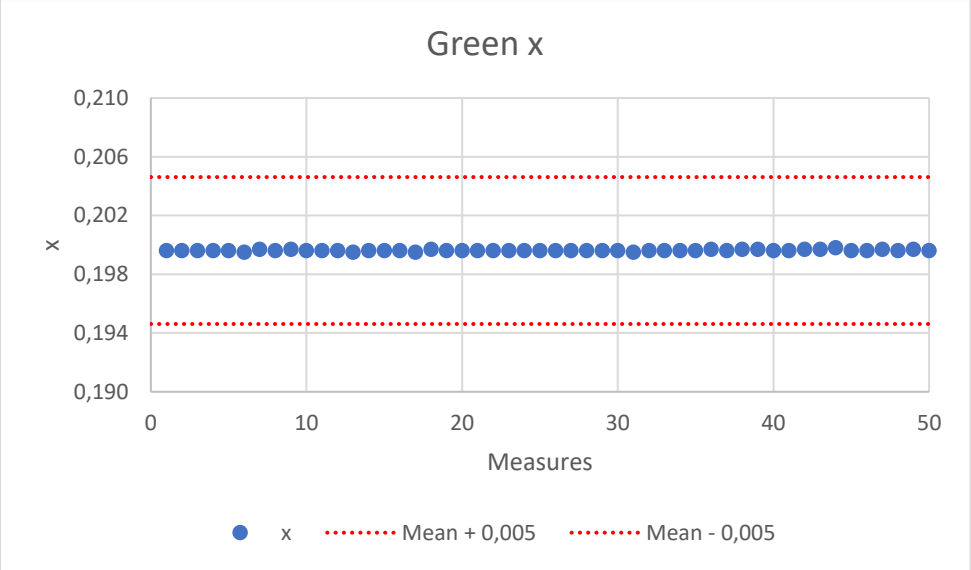
Green x
0,210
0,206
0,202
0,198
0,194
0,190
x
0
10
20
30
40
50
Measures
x
Mean + 0,005
Mean - 0,005

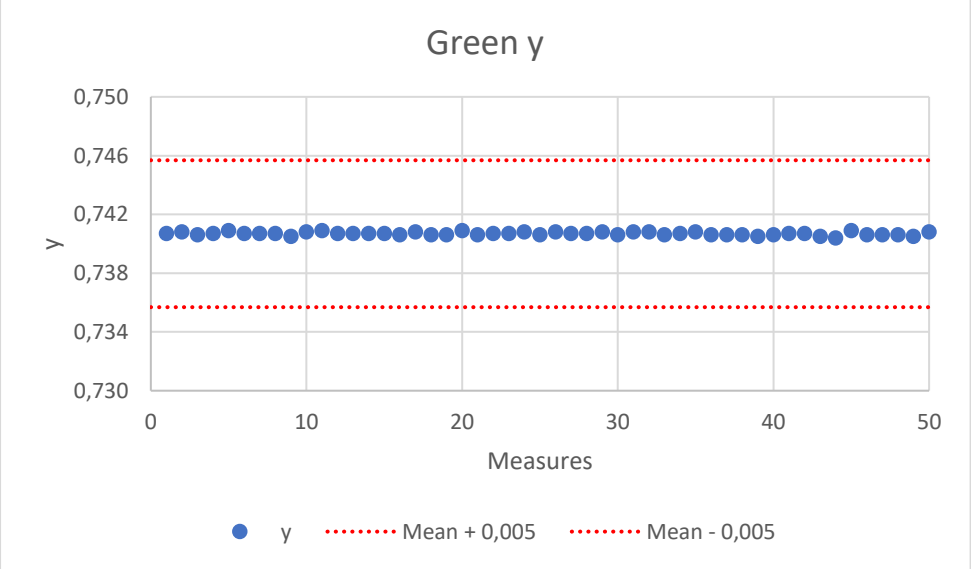
Green y
0,750
0,746
0,742
0,738
0,734
0,730
y
0
10
20
30
40
50
Measures
y
Mean + 0,005
Mean - 0,005

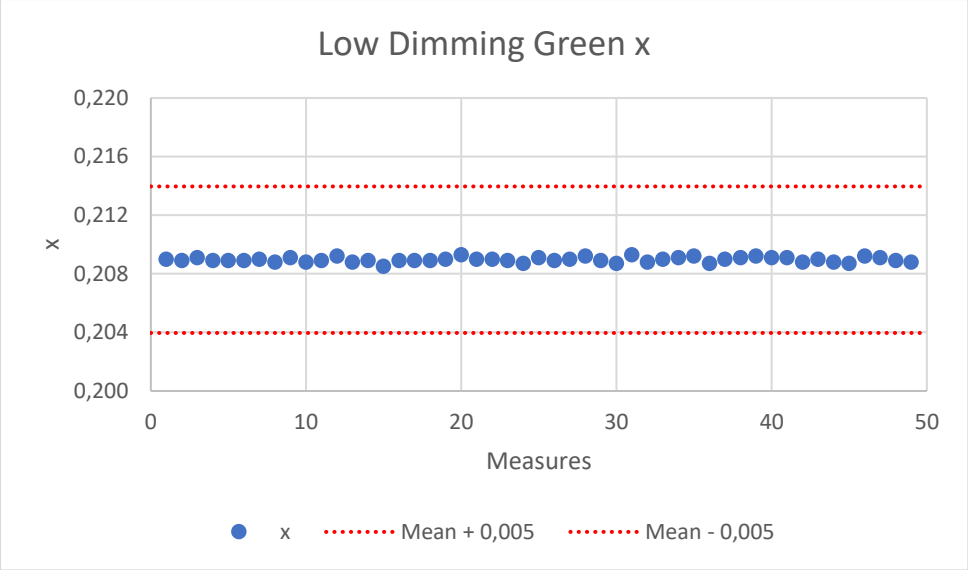
Low Dimming Green x
0,220
0,216
0,212
0,208
0,204
0,200
x
0
10
20
30
40
50
Measures
x
Mean + 0,005
Mean - 0,005

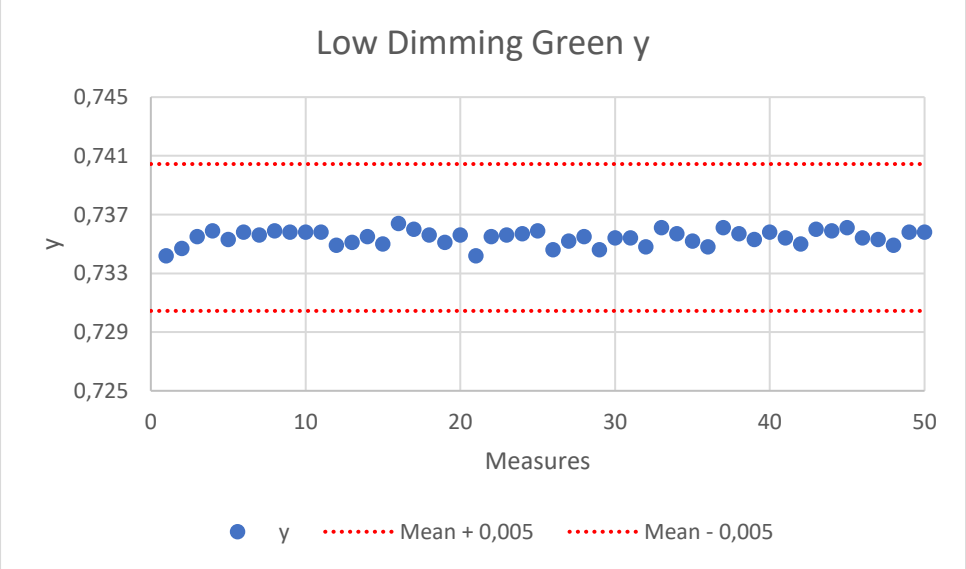
Low Dimming Green y
0,745
0,741
0,737
0,733
0,729
0,725
y
0
10
20
30
40
50
Measures
y
Mean + 0,005
Mean - 0,005

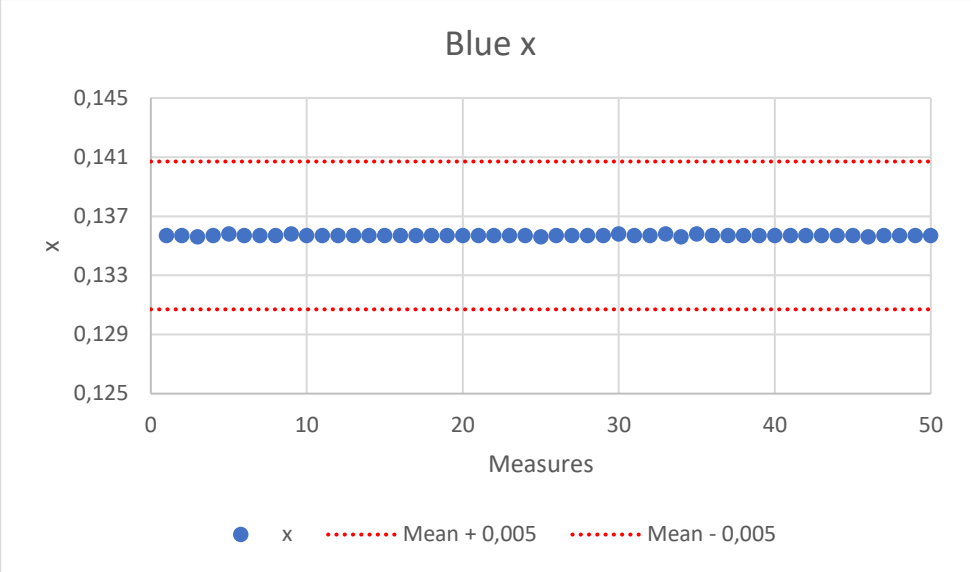
Blue x
0,145
0,141
0,137
0,133
0,129
0,125
x
0
10
20
30
40
50
Measures
x
Mean + 0,005
Mean - 0,005

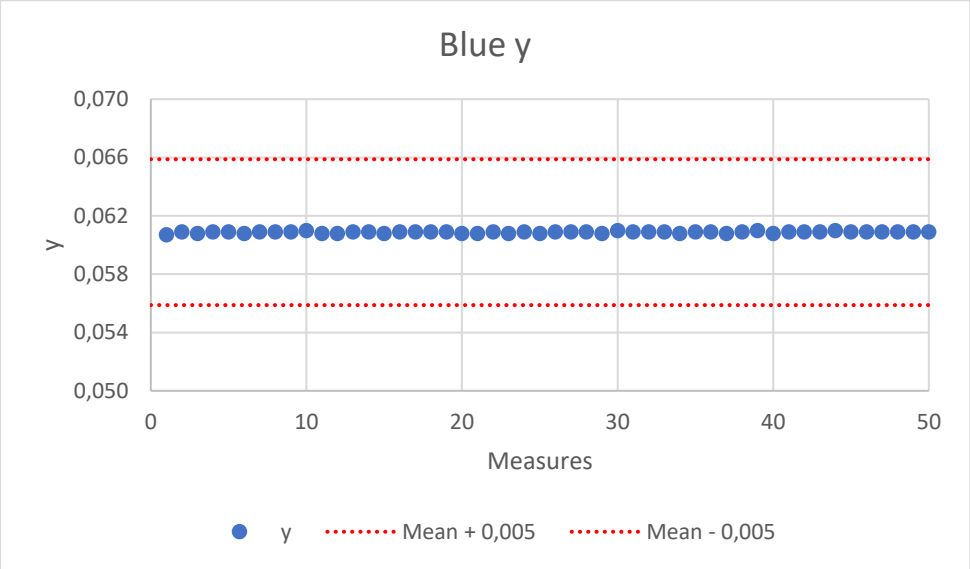
Blue y
0,070
0,066
0,062
0,058
0,054
0,050
y
0
10
20
30
40
50
Measures
y
Mean + 0,005
Mean - 0,005

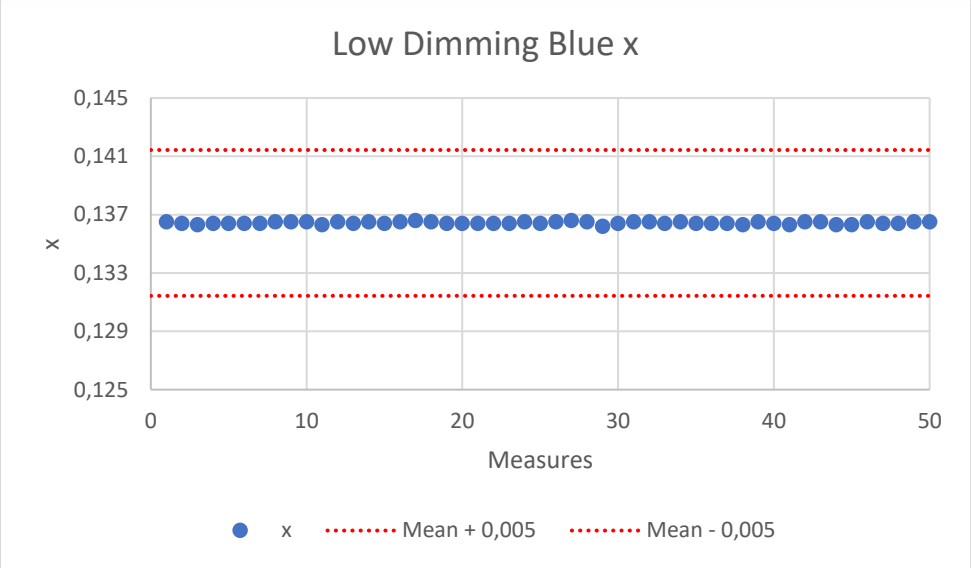
Low Dimming Blue x
0,145
0,141
0,137
0,133
0,129
0,125
x
0
10
20
30
40
50
Measures
x
Mean + 0,005
Mean - 0,005

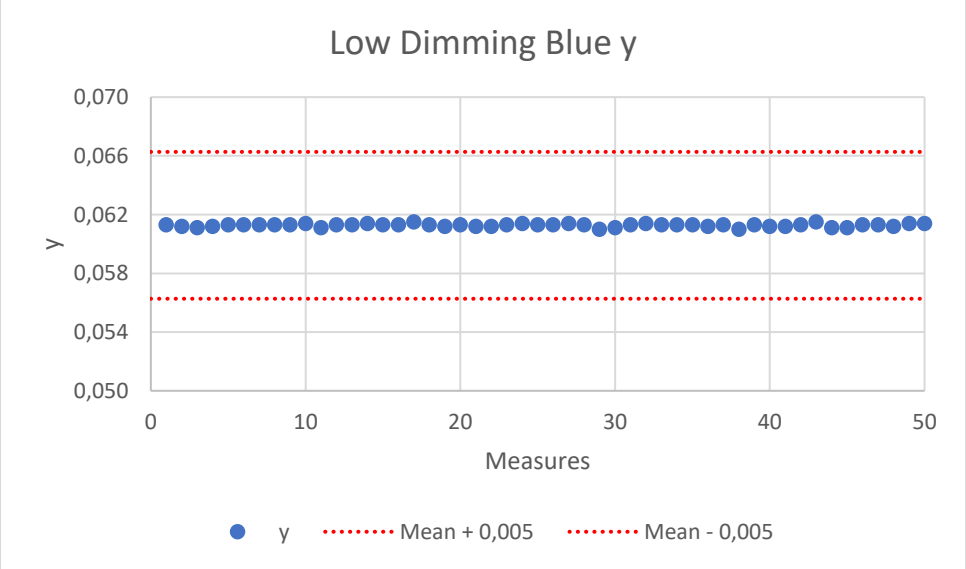
Low Dimming Blue y
0,070
0,066
0,062
0,058
0,054
0,050
y
0
10
20
30
40
50
Measures
y
Mean + 0,005
Mean - 0,005

Appendix C- Luminance and temperature evolution over time

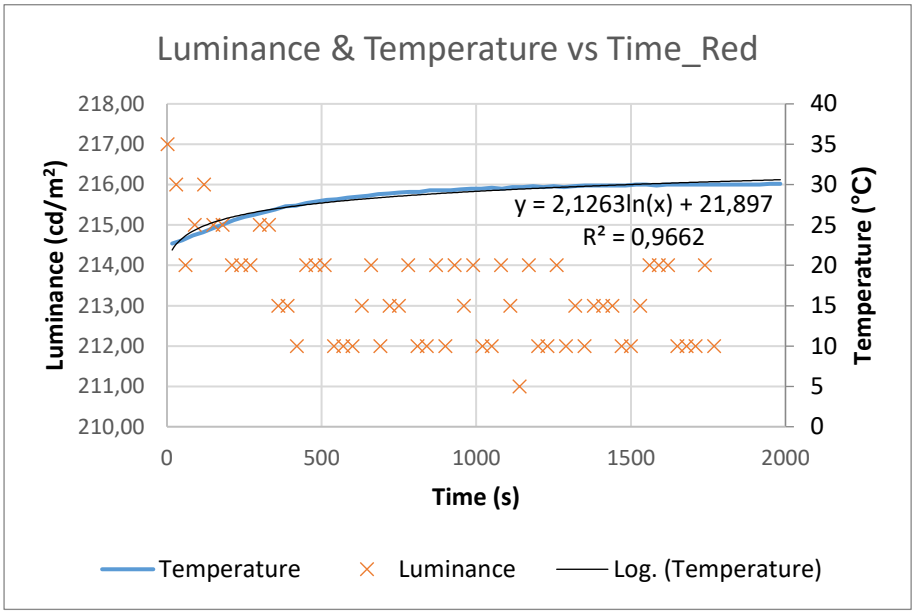

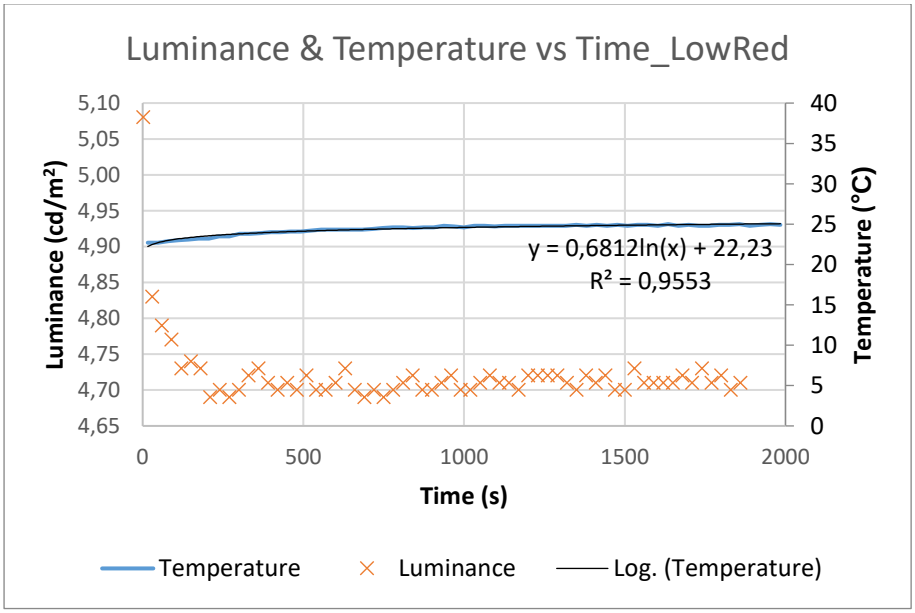

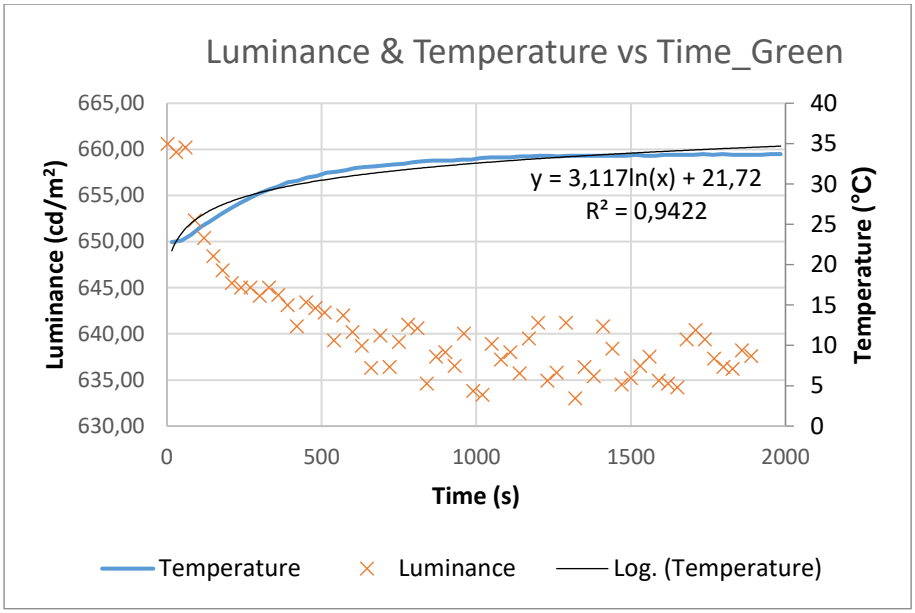
Luminance & Temperature vs Time_Green
665,00
660,00
655,00
650,00
645,00
640,00
635,00
630,00
Luminance (cd/m²)
40
35
30
25
20
15
10
5
0
Temperature (°C)
y = 3,117ln(x) + 21,72
R² = 0,9422
0
500
1000
1500
2000
Time (s)
Temperature
Luminance
Log. (Temperature)

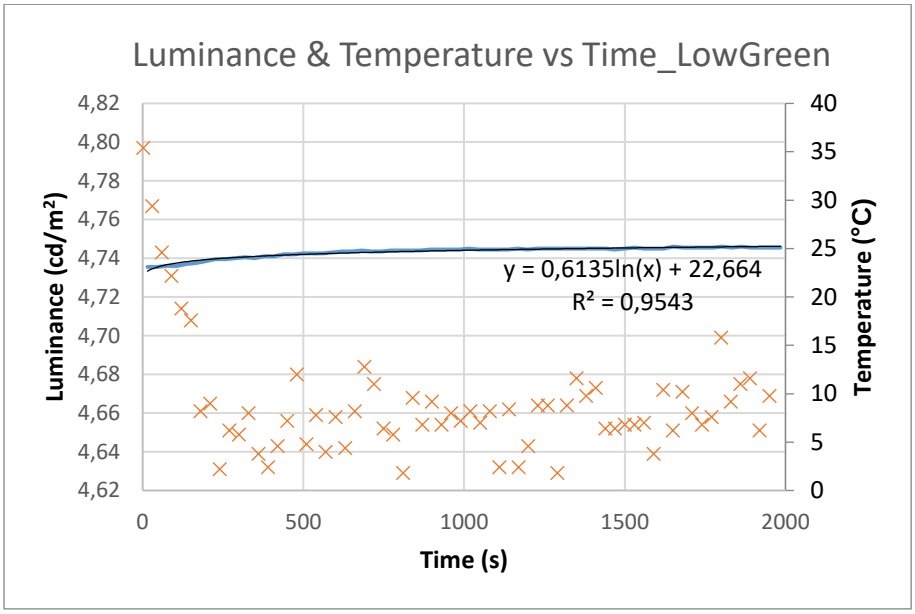
Luminance & Temperature vs Time_LowGreen
4,82
4,80
4,78
4,76
4,74
4,72
4,70
4,68
4,66
4,64
4,62
Luminance (cd/m²)
40
35
30
25
20
15
10
5
0
Temperature (°C)
y = 0,6135ln(x) + 22,664
R² = 0,9543
0
500
1000
1500
2000
Time (s)

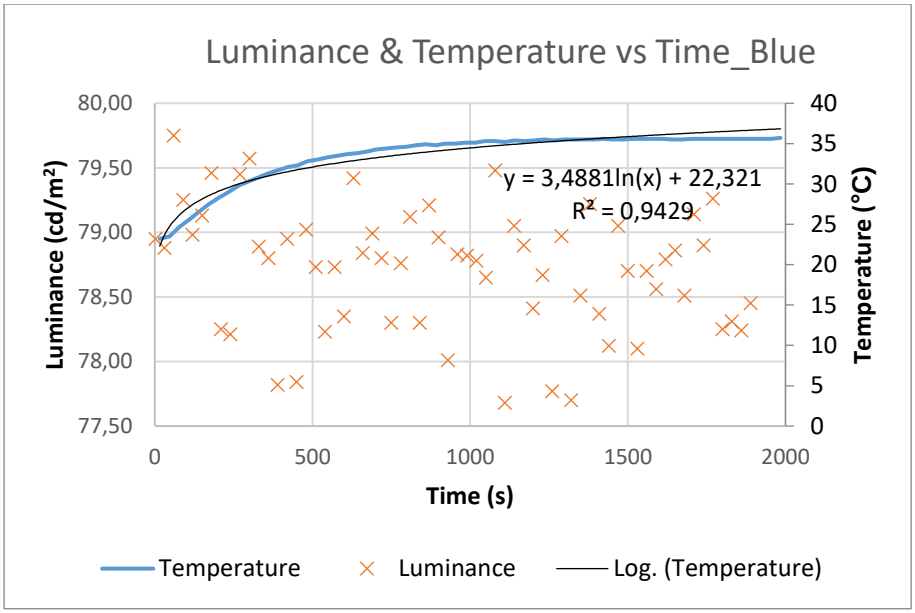
Luminance & Temperature vs Time_Blue
80,00
79,50
79,00
78,50
78,00
77,50
Luminance (cd/m²)
40
35
30
25
20
15
10
5
0
Temperature (°C)
y = 3,4881ln(x) + 22,321
R² = 0,9429
0
500
1000
1500
2000
Time (s)
Temperature
Luminance
Log. (Temperature)

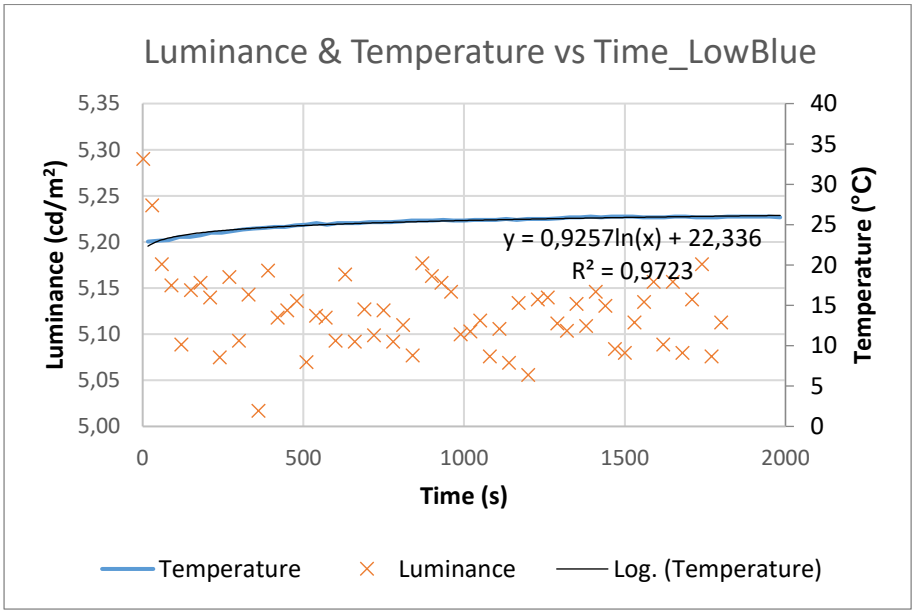
Luminance & Temperature vs Time_LowBlue
5,35
5,30
5,25
5,20
5,15
5,10
5,05
5,00
Luminance (cd/m²)
40
35
30
25
20
15
10
5
0
Temperature (°C)
y = 0,9257ln(x) + 22,336
R² = 0,9723
0
500
1000
1500
2000
Time (s)
Temperature
Luminance
Log. (Temperature)

Appendix D- Color coordinates and temperature evolution over time

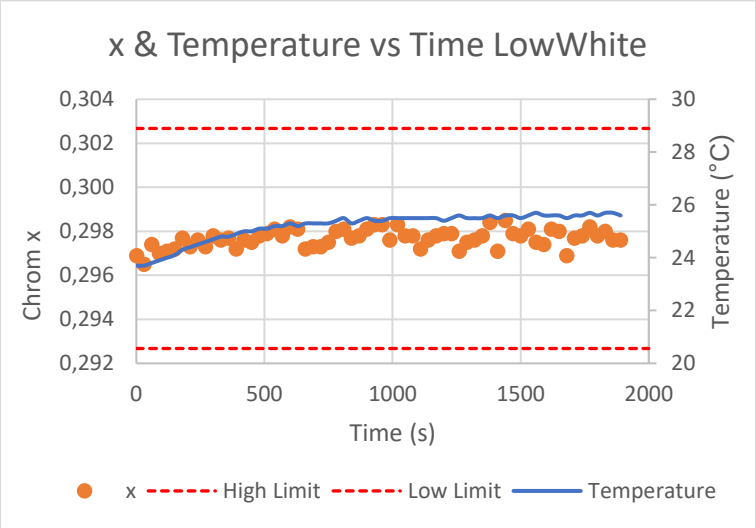

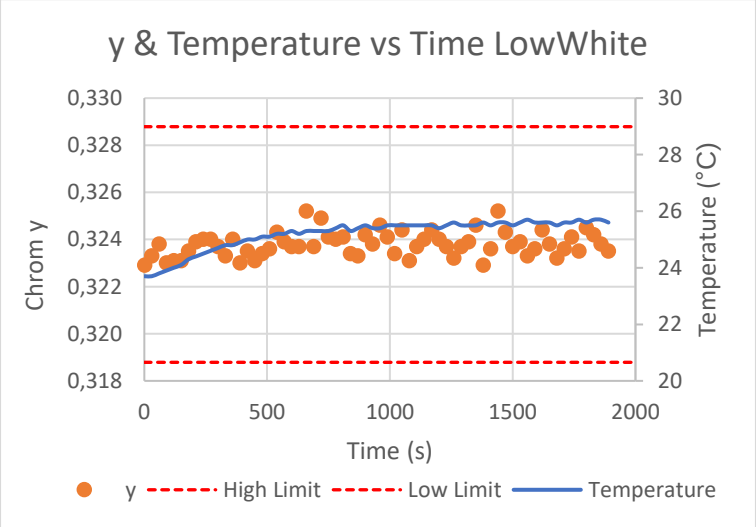

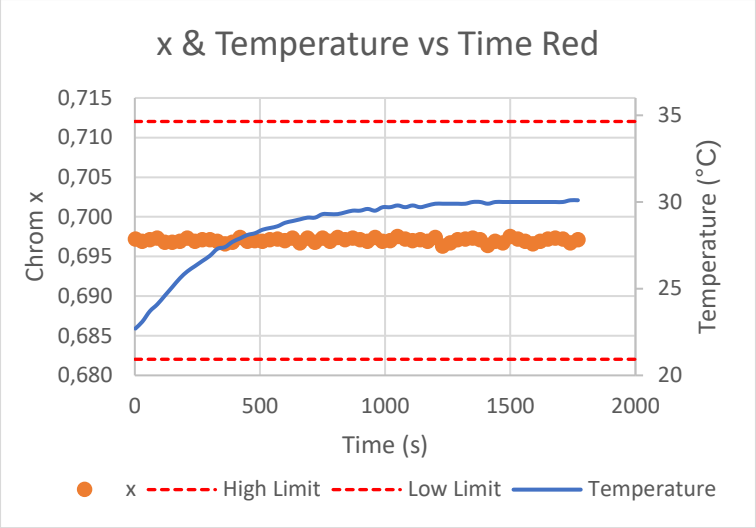
x & Temperature vs Time Red
Chrom x
0,715
0,710
0,705
0,700
0,695
0,690
0,685
0,680
Temperature (°C)
35
30
25
20
0
500
1000
1500
2000
Time (s)
x
High Limit
Low Limit
Temperature

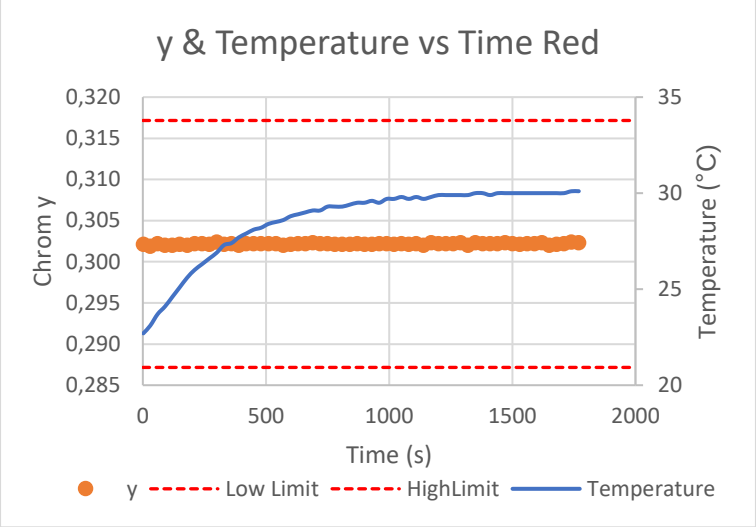
y & Temperature vs Time Red
Chrom y
0,320
0,315
0,310
0,305
0,300
0,295
0,290
0,285
Temperature (°C)
35
30
25
20
0
500
1000
1500
2000
Time (s)
y
Low Limit
HighLimit
Temperature

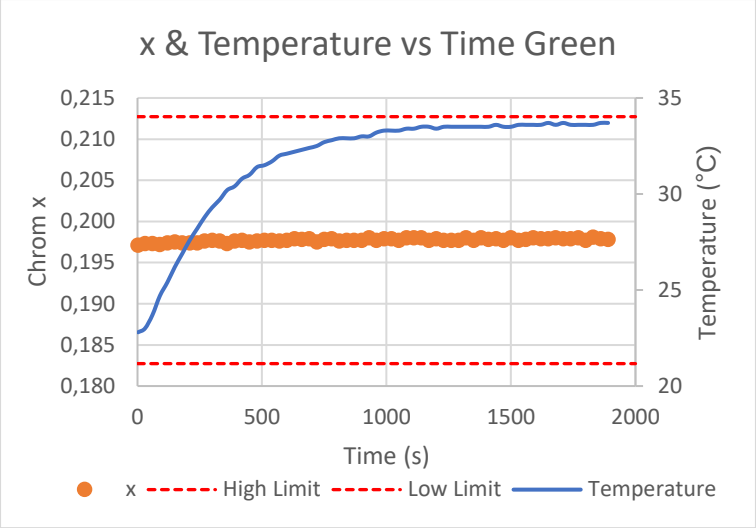
x & Temperature vs Time Green
0,215
0,210
0,205
0,200
0,195
0,190
0,185
0,180
Chrom x
35
30
25
20
Temperature (°C)
0
500
1000
1500
2000
Time (s)
x
High Limit
Low Limit
Temperature

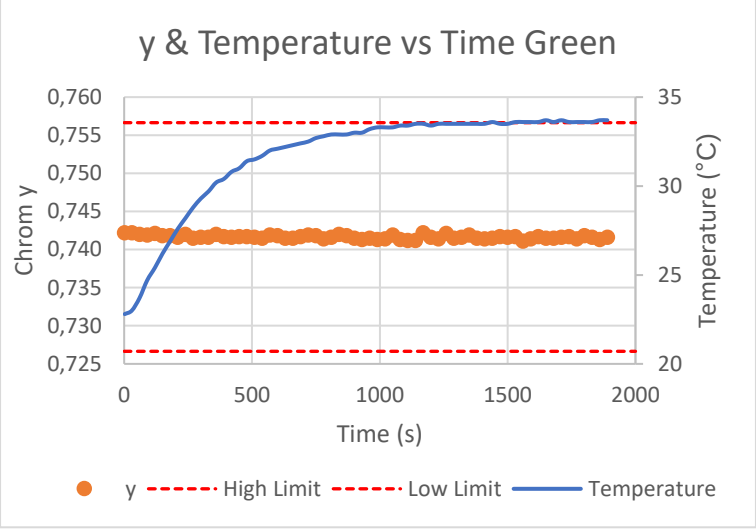
y & Temperature vs Time Green
0,760
0,755
0,750
0,745
0,740
0,735
0,730
0,725
Chrom y
35
30
25
20
Temperature (°C)
0
500
1000
1500
2000
Time (s)
y
High Limit
Low Limit
Temperature

References

[1] R.S. Berns, Billmeyer and Saltzman's Principles of Color Technology, Wiley (2019).

[2] Light and Color Measurement Radiant Webinar

[3] B.G. Grant, Field Guide to Radiometry, SPIE (2017).

[4] T. Tsujimura, OLED display Fundamentals and Applications, Wiley (2017).

[5] M. Koden, OLED Display and Lighting, Wiley-IEEE(2017).

[6] E1.4.1, Requirements for LCD/OLED Display Test and Adjustment, Factory of Future – Smart Manufacturing Project, Bosch-UMinho Partnership (2020).

[7] E2.4.1, Critical Knowledge for Calibration and Alignment Processes of Displays (LCD and OLED), Factory of Future – Smart Manufacturing Project, Bosch-UMinho Partnership (2020).

[8] E3.4.1, Technical Specification and Definition of Calibration and Alignment Processes for LCD/OLED Displays, Factory of Future – Smart Manufacturing Project, Bosch-UMinho Partnership (2021).

[9] Society for Information Display ,Information Display Measurement Standard. IDMS, Version 1.03 (2012).

[10] C. Poynton, Digital Video and HD, Algorithms and Interfaces, 2ndEd., Margan Kaufmann (2012).

[11] https://www.cambridgeincolour.com/tutorials/gamma-correction.htm

[12] Flicker measurement display & lighting measurement, Technical note, Admesy.

[13] Hyperion colorimeter, Operating manual, Admesy.

[14] Iliad software application 1.9.9, Operating manual, Admesy.

[15] htps://en.wikipedia.org/wiki/Gamma_correction

[16] https://en.wikipedia.org/wiki/Scotopic_vision

[17] A. Stockman, Cone fundamentals and CIE standards, Vision Research 30 (2019).

DOI: 10.1016/j.cobeha.2019.06.005

[18] T. Mironova, A. Ktaiski, How to Use a Digital Camera as a Metering Device, SPIE (2016).

[19] Quality Management in the Bosch Group, Technical Statistics, Booklet 10. Capability of Measurement and Test Processes, Edition 05.2010, Robert Bosch GmbH.

[20] J-H. Lee, D.N. Liu, S-T. Wu, Introduction to Flat Panel Displays, Wiley (2008).

[21] R. Mertens, OLED Handbook, Paperback (2017).

[22] V.K. Khanna, Fundamentals of solid-state lightning, CRC Press (2014).

[23] D.J. Gaspar, E. Polikarpov, OLED Fundamentals, CRC Press (2015).

[24] A. Buckley Organic Light-Emitting Diodes, Materials, Devices and Applications, Woodhead Publishing (2013)

[25] German Automotive OEM Work Group Displays, "Uniformity Measurement Standard for Displays V1.30," 2018.

[26] I. Amidror, The Theory of the Moiré Phenomenon, Springer Science+Business Media (2000)

[27] https://asia.nikkei.com/Business/Technology/Samsung-postpones-LCD-exit-to-2022-on-pandemic-demand

[28] https://www.flatpanelshd.com/news.php?subaction=showfull&id=1578476838

[29] OLED Display specification for Automotive Applications V1.1

[30] Radiant Vision Systems | A Konica Minolta Company, “Principles and Applications of Light and Color Measurement” Webinar

[31] I. Rotscholl, U. Kruger, Short distance Uniformity and BlackMURA Measurements, SID, volume 29, Issue 5 (2021)

https://doi.org/10.1002/jsid.1023

[32] J.Ke, L. Deng , L. Zhen, Q. Wu, C. Liao, H. Luo, S. Huang, An AMOLED Pixel Circuit Based on LTPS Thin-film Transistors with Mono-Type Scanning Driving, Electronics 9(4):574, (2020)

https://doi.org/10.3390/electronics9040574

[33] X. Jiang, Modeling of OLED Degradation for Prediction and Compensation of AMOLED Aging Artifacts, Saarbrücken (2018)

[34] B.Patel, M. Prajapati, OLED: A Modern Display Technology, International Journal of Scientific and Research Publications, Volume 4, Issue 6 (2014)

[35] D. Shin, J. Woo, Y. Hong, K.Kim, B. Kim,S. Kim, Quantitative evaluation of image sticking on displays with different gradual luminous variation, Journal of the SID, 18(3), (2010)

DOI:10.1889/JSID18.3.228